UNIVERSITY OF CALIFORNIA SAN DIEGO

Coupled Oscillator Systems

A dissertation submitted in partial satisfaction of the
requirements for the degree
Doctor of Philosophy

in

Music

by

David DeFilippo

Committee in charge:

Professor Miller Puckette, Chair
Professor David Borgo
Professor Shlomo Dubnov
Professor David Kirsh
Professor Shahrokh Yadegari

2023

The dissertation of David DeFilippo is approved, and it is acceptable in quality and form for publication on microfilm and electronically.

University of California San Diego

2023

EPIGRAPH

What the coronal suture yields upon replay is a primal sound without a name, a music without notation, a sound even more strange than any incantation for the dead for which the skull could have been used. Deprived of its shellac, the duped needle produces sounds that "are not the result of a graphic transposition of a note" but are the absolute transfer, that is, a metaphor. A writer thus celebrates the very opposite of his own medium— the white noise no writing can store.

—Friedrich A. Kittler

TABLE OF CONTENTS

LIST OF FIGURES

LIST OF TABLES

VITA

2013	B.A. in Technocultural Studies, University of California Davis
2013-2014	Research Specialist, CNMAT, University of California Berkeley
2016-2023	Teaching Assistant, University of California San Diego
2018	M.A. in Music, University of California San Diego
2023	Ph.D. in Music, University of California San Diego

PUBLICATIONS

David DeFilippo, Adrian Freed, David Wessel, "The Internet of Thingimajigs: Scalability Challenges for Device + Service Naming." *Terraswarm Research Center STARnet Phase, Second Annual Conference [Poster Session]*, 2013.

Adrian Freed, David DeFilippo, Rama Gottfried, John MacCallum, Jeff Lubow, Derek Razo, and David Wessel, "o. io: a Unified Communications Framework for Music, Intermedia and Cloud Interaction." *In ICMC*, 2014.

David DeFilippo, "Implicational Morphologies for Improvised Computer Music." *University of California San Diego [Master's Thesis]*, 2018.

David DeFilippo, "An Investigation of Phase-Coupled Oscillators." *In ICMC*, 2021.

David DeFilippo, "Laterally Coupled Oscillator Systems." *In ICMC*, 2022.

David DeFilippo, "Towards Brain Controlled Sound Sampling." *In Evo* arXiv:2208.0555*, 2022.

David DeFilippo and Shlomo Dubnov, "Synchronization Analysis of a HyperBrain Network of an Improvised Musical Duet." *IEEE Brain Discovery Neurotechnology Workshop [Poster Session]*, 2022.

David DeFilippo, "Coupled Oscillator Systems for Sound Synthesis with Chaotic Itinerancy." *IEEE Brain Discovery Neurotechnology Workshop [Poster Session]*, 2022.

ABSTRACT OF THE DISSERTATION

Coupled Oscillator Systems

by

David DeFilippo

Doctor of Philosophy in Music

University of California San Diego, 2023

Professor Miller Puckette, Chair

Coupled Oscillator Systems (COS) are presented as a method for sound synthesis and musical instrumentation. Seven systems ranging in size from 3 to 9 oscillators are described with different arrangements all containing a topology of velocity based coupling terms. First, each system is described mathematically. Then, each system is analyzed with recurrence plots and recurrence quantification analysis. The analysis characterizes the non-linear dynamics of the output signals and shows why certain ways of structuring COS may be preferable to others. The goal of the COS designs presented is to increase the non-stationarity of the signal, while also increasing the coherence of the phase transistors over an (quasi-) attractor landscape. Varieties of dynamical phenomena are located and quantified, such as drifts, phase transitions and higher

order periodicities. The durations of residence in attractors also reflected higher order temporal proportions. Of key interest, as found by analysis, was the presence of chaotic itinerancy (CI). Orderly CI in neural dynamics corresponds to production of intentional sequences of action and thought. Here cases of synthesis dynamics are located that reflect the quantitative aspects of orderly itinerancy and as a result the production of abstract musical sequences with perceived intentional organization. A theoretical chapter considers novel concepts, such as, extended and embedded intentionality in conjunction with auditory cues to discuss the implications of this tool as an instrument for musical improvisation. Finally, if the phenomena produced by a COS sound musical and are consistent with the phenomenon of CI observed in the brain, can we consider the brain and its dynamics to be a kind of musical phenomenon itself?

Chapter 1

Introduction

Described here is a computer music instrument based on a novel method for systematizing the coupling of multiple oscillators. Musical signals are produced that have deterministic, non-linear temporal structure. The sonic structure generated is primarily on the timescale of musical form. In larger systems, coherent sequences of musical phrases are produced. The instrument also generates sonic structure on the level timbre spanning the range from sinusoidal to white noise. The approach to digital instrument design is related to dynamical systems theory, as well as, computational neuroscience. The resulting musical tool is theoretically an extension of the mind because it can produce a class of dynamics similar to what has been observed in recent neuroimaging studies. As such, it can entrain the performer into regimes of dynamical activity that are somewhat unpredictable. A performer interacts with the instrument by changing its parameters in real-time using their perception to tune the dynamics.

Applications of nonlinear dynamics and synchronization models have been researched in the field of computer music for quite some time. Here are four recent examples that include different computational approaches that include chaotic maps, soft-synchronization, holes in phase space and models for synchronizing large numbers of oscillators:

(1) In terms of chaotic maps, [Rodet, 1993] researched the digitization of the Chua circuit

the for real-time, interactive sound synthesis. The signals produced by the circuit can be used to model the harmonic content of musical instrument timbres and potentially a new family of instrument timbres. The model has three state equations and two control parameters. Many of the values for the two parameters give stable periodic orbits resulting in harmonic spectra. In some cases, the parameter values lead to chaotic signals and result in inharmonic and noisy spectra. Furthermore, the time-delayed Chua circuit was used to the approximate the a collection of timbres like those produced by the clarinet.

(2) In another example of a chaotic map, [Essel, 2006] studied the applications of the circle map to sound synthesis of musical timbre. The circle map is a well researched iterative mapping (from the circle to itself) that produces a range of nonlinear, dynamical phenomena. These phenomena include: mode and phase-locking, period-doubling, subharmonics, quasi-periodicity and routes to chaos. The circle map was examined as an approximation of a sinusoidal oscillator with a fixed phase-angle progression. The coupling strength parameter was then adjusted. When the parameter was below 1 and progressively modified, there was a change in frequency and a deformation of the waveform. The waveform in this case remained periodic. When increasing the coupling strength above 1 the waveform became non-periodic. At values close to 2, the waveform exhibited more complicated quasi-periodicity with potential self-similar structure.

(3) With respect to soft-synchronization and holes in phase space, [Puckette, 2017] developed a method for coupling multiple oscillators to generate unpredictable musical phrases, as a discrete-time digital system. The work analogizes oscillators to a particle moving at a velocity given by a vector field. The vector field defines the flow of the particle in the state space. In some cases, if the oscillators are uncoupled the flow is uniform. Couplings can be introduced between the oscillators. In one instance, if the oscillator pair is soft-synchronized the flow is non-uniform. In the example of a soft-synched oscillator pair (where the oscillators are named A and B), at the moment oscillator A reaches a phase-position of zero, oscillator B begins to move toward zero without necessarily reaching zero. Another approach by Puckette generates quasi-periodicity, not

by making the flow non-uniform via a coupling procedure, but by putting a rectangular wormhole in the phase space. Here the phase space is a torus. Once a particle reaches the edge of the hole it skips directly to the opposite point on the adjacent edge before continuing its trajectory as before. Both the soft-sync and wormhole method can be generalized to dimensions larger than the most basic unit of a pair.

(4) Models for the synchronization (and desynchronization) of large number oscillators were explored by [Lem, 2019]. The Kuramoto Model was digitized with applications to control signals and sound synthesis. The Kuramoto model is used to describe an arbitrary number of oscillators (such as 100) under a coupling strength parameter. The when the coupling strength is a above a critical value (defined by the model) all the oscillator phases align producing a collective synchrony. More specifically, the ensemble oscillators become entrained to the frequency of the oscillator at the center of the distribution. By adding a forcing term to the Kuramoto model, such as a "sawtooth interaction function" the oscillators can be pushed into a regime with non-zero phase locking. The oscillators in this instance will lock but with an array of phase offsets. Another method for inducing incoherence, or complex behavior is to have the coupling strength take on different values for different sub-ensembles. Lem used the model and its augmentation for additive synthesis and for modeling modern procedural compositions, such as Ligeti's *Poeme Symphonic* for 100 metronomes. Here the method for modeling Ligeti was to use the wrap point of each oscillator's phase to trigger the onset of a percussive sound sample.

The instrument described in the Dissertation comprises a new class of synthesis algorithms denoted Coupled Oscillator Systems (COS). The notation 3-COS, will denote a system of 3 oscillators and a 3x2-COS will refer to systems with two groupings of 3 oscillators. Systems 3-COS, 3x2-COS, 3x3-COS, 4-COS, 5-COS and 6-COS will be described and analyzed mathematically. Of the examples of digital technologies just listed, the COS is most similar to methods of soft-synchronization. However, in a COS oscillators move toward or away from other oscillators instead of a phase position of zero. It is also an iterated function, like that of

the circle map or chua circuit. A COS is not explicitly designed for the synchronization of many oscillators as in the Kuramoto Model, as the coupling terms and mappings among subsystems produce intermittency between synchronization and desynchronization. Versions of the COS will also produce a phase space with multiple basins of attraction. The chapters to follow will describe the many system designs and phenomena produced.

Chapter 2 gives mathematical definitions for the systems listed. Each system is memory-less loop containing a topology of velocity-based coupling terms. The topology for all the systems presented here contain overlapping subsystems of oscillators. Subsystems are linked together with coupling terms that are algebraic functions containing dynamic, time-varying descriptions based on phase-positions. For instance, in the 6-COS, subsystems of 3 oscillators are formed from all the possible permutational combinations of 3 out of 6, giving 20 subsystems. Due to the overlap of the subsystems there are extra orders of causality between subsystems creating a foundation for the complex regime dynamics of the resulting signals.

To analyze the dynamics of the resulting signals, chapter 3 will describe the methodology of recurrence plots and recurrence quantification analysis (RQA), along with a theory of dynamics known as chaotic itinerancy (CI) [Kaneko, 1990]. The analysis, in chapter 4, shows that the COS produces many dynamical phenomena, including, but not limited to, phase-transitions, attractor formation, drift and higher-order periodicities. For larger systems (3x3-COS, 5-COS and 6-COS) there is evidence for CI which is observed as a electrical neurological phenomenon associated with active intentional states of consciousness [Freeman, 2006] [Freeman and Zhai, 2009].

Of particular theoretical interest to musical performance is the interactive synthesis (where the a human in the loop changes the parameters of the system in real-time) of musical sequences that imitate a sense of intentional organization. Borrowing from extended mind theory [Clark and Chalmers, 1998], chapter 5 discussions a theory of "extended intentionality" based on parity between CI in neural dynamics and CI in the dynamics of the COS. Finally, the interaction will be viewed theoretically from a perspective of embedded cognition and stigmergy showing how RQA

based sonic cues play a causal role in the co-creation of the musical dynamics in the tradition of experimental electronic music.

Moving forward with chapter 1, more historical examples of analog technologies are presented to situate the work, along with preliminary definitions of the key concepts used throughout the Dissertation. Moreover, COS will be further situated in terms of comparison to the circuit design, interface design and interactivity of four preceding devices: The Crackle Box, Booper, Theremin and Buchla. More generally and derived from the history of the Theremin and phonograph, the COS will be considered a form of automatic time axis manipulation operating on a feedback principle. Concepts including CI, monotonicity, linearity, intentionality, brown noise, black noise and dark energy are introduced.

(1) The Crackle box is a portable hand held synthesizer built at STEIM in 1975 by Michel Waisvisz. Its bent circuitry and touch capacitive interface are housed in a wooden case about the size of a hand [Reus, 2011]. The apparatus produces a large state space of unstable oscillations. Op-amps are configured such that the input, output and compensation pins are exposed to metallic touch pads [Fei, 2007]. The physical interface has six lines of metal in parallel rows. Touching the rows bridges different nodes of the circuit creating feedback paths of electrical flow. Routed to the internal speaker, rectangular waves couplings can be mapped and remapped by pentadactyl gestures of different spatial configurations. The resulting sound contains chaotic variation of frequency and pulse width of the rectangular waves. When the hands are set in a certain spatial distribution, pressure and vibrato actions create momentary articulation. The hands alter the connectivity of the circuit forming topologies of the sound generation. The changes in connectivity of the pins are the main generators of dynamic changes and sound structure control.

(2) Another related technology is the Booper, created by David Wills (a.k.a The Weatherman) from the media detournment group Negativland. Based in the San Francisco Bay Area, the group is known for sampling and reconfiguring mass media into compositions of parody and reflexive re-administration of popular cultural messaging. Aside from the mode of culture

jamming performance, alternative modes of synthesis and processing take the stage. The Booper is a small metal box about the size of a guitar pedal. Each box tends to be unique in its circuitry. One such Booper, is called the Super Booper Electronic Oscillator. It has four switches and four knobs. The first switch turns the thing on or off. The first dial is the volume control. The remaining three dials alter the frequencies of oscillators which are coupled together. The oscillators are transistor circuits with the input connected to the output. The second and third switch alter feedback paths of the oscillators. As stated by Wills, all kinds of dynamical regimes occur when these switches and knobs are set in different combinations. Finally the fourth switch operates a synchronization input. When switched on it can cause the Booper to soft sync with an external source, such as a drum machine or another Booper. In this way larger systems can be formed as chains of standalone pedals, synths and Boopers [Wills, 2007]. Like the Cracklebox, coupled and bendable electronics yield unstable oscillatory media. The controls incorporate a remapping of the circuit by switches. The Booper's dials change the intrinsic frequencies of the oscillators via linear potentiation. The relation of the dials to the intrinsic frequencies of the oscillators is monotonic, however the coupling of the oscillators results in a non-monotonic relation between action and resultant sound generation.

(3) Putting the body in the circuit, or leveraging the body's capacitive nature as a control mechanism for musical instruments is attributed to Lev Sergeyevich Termen (a.k.a Leon Theremin). The well known electronic oscillator instrument, self-named as the Theremin has a history of research and development described by [Glinsky, 2000]. In 1919, Termen was appointed to supervise a laboratory run by A.F. Ioffe, called the Physico-Technical Institute. His first assignment from Ioffe was to create a burglar alarm using the human body as an electrical conductor. The body can store electrical charges emitted into the environment from a source. This is the body's capacitance, and when a body is close to an electrical circuit it can interfere with the capacitor in the electrical circuit, affecting the capacitance of the circuit. Termen used an oscillating Audion for the main component of the alarm system. (The audion, an amplifing

vacuum tube, was recently invented by Lee De Forrest in 1906. The later oscillating audion, was a crucial step in creating long-distance radio transmission. Studying de Forest's invention in 1912, Edwin Howard Armstrong found that connecting the output of the audion to the input and boosting the power to its limit generated high frequencies on its own accord. Armstrong called this a *regenerative circuit*, but it later became the *feedback principle*.) Using an oscillating audion, Termen generated a spectrum of high frequencies, filtered for a specific frequency and transmitted a wavefront of about 15 feet (not miles like a radio transmitter). When a person got close enough to the apparatus, the capacitance of the circuit would change, triggering an alarm. He called it the Radio Watchman.

Ioffe then tasked Termen with the development of another experimental device which would lead directly to the musical instrument, the Theremin. The function of this thing was to measure the density and the dielectric constant of various gases under the dynamic environmental conditions of temperature and barometric pressure. Termen built the device, piping the gases into the non-conductive (dielectric) medium between the two parallel conductive plates of the capacitor. A rise in temperature expanded the gas and changed the capacitance of the circuit, registering the fluctuations on a meter. Surprisingly, Termen also found the device highly reactive to the presence of his hand motion which would also register fluctuations on the meter. Termen then added a tuned audion tube to the device in order to listen to the dynamics. He also added a dial to tune in the precise frequency of the gas. The gas with a stationary density yielded a constant fundamental tone and when non-stationary emitted drifting frequencies consistent with fluctuations of density. Sonifying the fundamental properties of gas, Termen moved his hand over the circuit and found an intuitive consistency. The closer his hand was to the circuit the higher the frequency and the further away the lower the frequency. A natural vibrato effect was also produced by oscillating the hand in a fixed frequency position. Being an inactive cellist, consumed in a torrent of wartime research, he was captivated by the touch-free control of electrical flow and began to experiment with melodic forms. The later design would not incorporate gases, but operated on the same

interaction principle for frequency control. A metal pole protruding vertically could be used by one hand to control the frequency and a U-shaped horizontal rod controlled the amplitude. Like the dial, these metal rods operated on a principle of linear potentiation, to tune into frequencies of interest: a touch-free gestural controller over a stable oscillation to produce expressive melodic sequences.

(4) Buchla was an engineer of commercial modular synthesizers working out of Berkeley, CA, emerging into prominence during the 1960's period of psychedelic, radical culture. As the story goes, in 1965 Morton Subotnick and Ramon Sender at the San Fransisco Tape Music Center (SFTMC) were searching for an engineer to build systems capable of creating electronic music. At the time SFTMC had only a few oscillators, filters and tape machines. Like Robert Moog, Buchla saw the importance of the application of control voltages in creating a modular synthesis system. However, the Moog synthesizer was primarily envisaged as a studio tool for adding effects to recordings of popular music. In contrast to Moog, Buchla was a musician, and when working with Subotnick and Sender saw the potential of the modular synthesizer as a solo instrument for stage performance [Holmes, 2012]. The Buchla synthesizer networks source generators, envelope generators and filters together with patch cables transmitting a common language of control voltages. Dials control parameters such as frequency and magnitude. Switches alter the topology of the underlying circuit. A module of interest to the discussion here is the Programmable Complex Waveform Generator Model 259. This module generates two operator frequency modulation with phase locking. In two operator frequency modulation without phase-locking, one of the two oscillators called the modulation oscillator (in Buchla's design the modulation oscillator has a waveform type selector) drives the frequency of the carrier oscillator. The magnitude of the modulation oscillator can be increased or decreased by a modulation index dial. The value of the modulation index also determines the spectral envelope in a non-linear way given by Bessel functions. Also, the frequency of the modulation oscillator gives the spacing of the sidebands in the generated spectrum [Chowning, 1973]. In Buchla's design, the carrier

oscillator can also be phase locked to the modulation oscillator. Soft-sync and hard-sync are two general methods for phase synchronization. With soft-sync, once the modulation oscillator reaches a phase-position of zero, the carrier oscillator moves toward zero continuously without necessarily reaching zero [Puckette, 2017]. With hard-sync, once the modulation oscillator reaches a phase-position of zero, the carrier oscillator is set to immediately to a phase-position of zero. With phase synchronization methods, the oscillators are coupled by phase-position, which affects the frequency spectrum of the carrier oscillator. The modalities of FM synthesis, waveshape selection and phase-locking produce a wide range of timbres. The module can be driven by a number of external control voltage sources to produce time-varying spectral envelopes.

With the Cracklebox, Booper, Theremin and Buchla, we see a number of control strategies for synthesizers. First a few terms need to be defined as combinations of linear and non-linear with monotonic and non-monotonic. Linear is simply a straight line with constant slope. A straight line is also monotonic because moving along it there is always an increase or decrease in value, depending on the direction of motion up or down the slope. Linearity will always be monotonic, while non-linearity can either be monotonic or non-monotonic. A logarithmic curve is an example of non-linear monotonicity because moving up the slope the value always increases. Logarithmic transfer functions are commonly used on dials or sliders, so even though the gestural motion is linear in the case of a slider, the transfer function causes the effect to be non-linear and monotonic. The timeseries output from a COS and usually coupled oscillators in general are non-linear and non-monotonic because the generated trace continuously changes direction; moving across the trace with a linear time axis gives values that increase and decrease over time. A monotonic or non-monotonic relation can be used to describe the relation between two time series or two functions. For purposes discussed here, there can be either a monotonic or non-monotonic relation between the timeseries data of parameter changes (i.e. operating a dial) and the timeseries of generated sound output. The interaction between the two is the relation and is considered to be a monotonic interaction or non-monotonic interaction.

The Cracklebox and the Theremin both leverage the body's capacitance. The Theremin is touchless and operates over a sinusoidal sound source (a monotonic interaction), while the Cracklebox requires haptic control over non-linear, non-monotonic synthesis sources (a non-monotonic interaction). The Cracklebox also borrows metaphors of modularity between sources like the Buchla synth, however the Buchla uses patch cables to creates the linkages. Both the Booper and the Buchla have an interface of dials and switches. The dials monotonically augment the magnitudes of various parameters, and switches create topology changes to the underlying circuit. The haptic control of the Cracklebox and the switches of the Booper serve the same function of remapping feedback paths between sources. The Cracklebox like the Theremin, also affords vibrato gestures for immediate musical articulations. However, the Theremin and the Buchla Model 259 (unless certain external factors prevail) both provide monotonic control over stable oscillatory media (a monotonic interaction). The Booper and the Cracklebox provide monotonic control control but over unstable oscillatory media (a non-monotonic interaction).

Overall, we are left with a few considerations about a synthesis model and its musical control. The linearity and monotonicity of the control parameters are not always consistent with the linearity and monotonicity of the source circuit. In these cases we see both monotonic and non-monotonic interaction. There is also the control over the circuit topology or the mappings between the elements of sound generation. The COS presented here, has monotonic, linear control (by using dials and sliders) over non-stationary oscillatory media, resulting in a non-monotonic interaction. In these systems, the engineering objective is not only to move from stationarity to increasing forms of non-stationary, but also to increase the coherence among state to state transitions in the non-stationarity.

A dial, as a kind of linear potentiation element is the main control implement for the current configurations of COS. Before the dial's instrumentality became fused to synthesis control paradigms, a few historical antecedents of the dial itself illuminate its deep psychology as a cultural tool.

(1) The sundial is the well known ancient time measuring apparatus. Its earliest known configurations appear in the historical record in 1500 BC Egypt. A Gnomon, or pointer, is set up to cast a shadow over a reference grid in order to gauge time lapses as measurable intervals. An early gnomon is the obelisk which casts a changing shadow as the earth rotates. The shadows, like those cast by trees, get longer, later in the day. The measuring of time lead to the study time, the development of calendars and schedules of prediction of astronomical cycles [Rohr, 2012].

(2) Early forms of the safe used non-electric dials for combination locks. Safes are used to lock others out of things owned. The safe combination dial is notched, like the reference grid on a sundial. The dial embodies the precision necessary for forms of security whether temporal or coded substitutions. Similar to the statement by David Wills about operating the Booper as combinations of dial notches, opening a safe is an act of dialing in a combination. Dialing parameter combinations elicit the self-organization of unstable oscillations; dial in the substitutions and break into the grooves.

(3) The radio dial tunes in and locks into broadcasts of electromagnetic carrier waves. The axis over the spectrum of frequencies can be scanned and selected. The radio dial is used as a method of search for programs of interest via the manipulation of an axis.

The dial as an instrument tunes in, locks out, searches, secures, codes and measures time. Its circularity affords recurrent motion, whether it be the consistency of certain events within lapses of time or returning to a radio program after a commercial break. A linear axis can be manipulated, its grooves retraced. In the control of a COS, the dial changes the intrinsic frequency of each coupled oscillator. In learning to play dynamical systems as a musical synthesizer, it is possible the performer can learn how different displacements of the dial result in temporal effects of self-organization. The frequency of an oscillator is either increased or decreased, where the temporal change causes a cascade of perturbation altering the regime dynamics.

Back to 1919, the year Termen was devising the etherphone, the poet Rainer Maria Rilke was creating his next work, *Primal Sound*. The phonograph had locked transient utterances into a

medium, engraving its traces into a wax cylinder. Given his belief that the task of the poet was to transfer into writing the data of the inner world space, he turned to his attention to the grooves of the coronal suture of a skull. In a sublime analogy to the prevailing phrenological sciences of the time, he situated the phonograph needle to play the groove of the coronal suture. The result was grainy white noise from a trace that had never been uttered, rendering a metaphor [Kittler,1999]. A sound not encoded by a human action of any kind, rather a groove present by the mere effects of biological self-organization. Kittler writes also of Jean-Marie Guyay, a philosopher captivated by the phonograph. In *La Memoire et le Phonographe* (1880), Guyay analogizes the human brain to an infinitely perfected conscious phonograph, where the phonograph itself is not conscious because it does not listen to itself. Lived experience engraves traces in the neural fibers of the mind. Like the time axis manipulation (TAM) possible via a wax cylinder or a petroleum disk, the mind remembers by retracing the grooves of these engravings at varying velocities. Attention (or self-listening) operates in the same manner as TAM [Kittler, 1999].

The Coupled Oscillator Systems presented here can be considered a form of automatic time axis manipulation. Oscillators are coupled together by descriptions of phase-positions which in turn alter the frequencies of the oscillators in the system. The coupling terms cause varieties of directional motion over the time axis of the phasors; speeding up or slowing down, toward or away a phase-position of zero. The phasors are generally set to low frequencies between 0.0 and 10 HZ and situated in a topology of velocity based coupling terms. Unlike the Buchla, Booper and Cracklebox, this underlying topology is static. Groups or *subsystems* of *modifier* oscillators affect other subsystems of *modified* oscillators. While the mapping from modifier to modified is static, the *description* of the modifier subsystem changes the relation or coupling term of the mapping. Given the topology arranged here, the modifier oscillators are also modified by other subsystems, creating deeper, cascading levels of causality.

The COS is a form of dynamical system operating on a feedback principle. Containing no stochastic elements, these systems produce non-linear, deterministic output. Rather than stationary

oscillation, the coupling topology generates sequences of interrelated frequency envelopes at slow, form-level velocities. These envelopes on the timescale of musical form are used as phase angles and are multiplied into auditory range for listening. As mentioned earlier the engineering and artistic motivation of these systems is to increase the non-stationarity of synthesized oscillation, while also increasing the coherence of phase-transitions in phase space. A way to reflect on and gauge this relation is to use recurrence plots (RP) and recurrence quantification analysis (RQA). In systems of higher order (3x3-COS, 5-COS and 6-COS), RP and RQA will show evidence for the dynamical phenomenon known as CI.

CI characterizes the dynamics of a closed-loop trajectory over a landscape of quasi-attractors that comprise a mix of convergent and divergent flows. When the quasi-attractors are considered states in a state space, the closed-loop trajectory that ranges over these states forms a sequence of states. Each escape from a quasi-attractor over the trajectory is a descent into chaos, functioning as a chaotic search among states.

In terms of the coherence of these state to state transitions, the net activity of generated sound in the variety of CI ranges over the statistical characterization of brown and black noise. Both these distributions are described by the $1/f^n$ distribution, where n ranges from 2 to 4. When the resulting slope of the curve is less than -2 it is black noise and when it is at or nearly above -2 it is brown noise [Manaris, Romero, Machado, Krehbiel, Hirzel, Pharr and Davis, 2005]. These noise types characterize the frequency of measured events to have a distribution of a logarithmically decaying slope. Brown noise in the COS is associated with itinerant sequences with discontinuous stationarity an the edges of quasi-attractors. Black noise occurs when rare states predominate the landscape, less drift is seen in the measurement of recurrences and continuous stationarity flows revolve at the edges the of quasi-attractors. While both kinds of sequences are directed, brown noise is less coherent than the efficiency and stability of a black noise sequence. Black noise sequences are scientifically associated with active intentional states of mind [Freeman and Zhai, 2009], rather than the more offline and abstract planning states of

mind associated with more disorderly types, such as brown noise.

From a functionalist perspective, the brain regions responsible for CI in intentional states are a kind of background activity. Though detectable, this activity evades complete functionalist descriptions of foreground activity, being a kind of dark energy [Raichle, 2006], consuming enormous metabolic resources: up to 160 times more than evoked activity. While the connection between dark energy and sound synthesized to produce intentional sonic sequences may seem tenuous, please consider the following:

Initially, considering intentionality from the perspective of philosophy of mind, mental states as abstract representations, observed by scientific tools, are said to have *contents*. The observed electrical dynamics in the brain stored digitally as traces are not mere chaotic fluctuations, but encode a phenomenology of experience. The contents of experience include thoughts, sensory imagery, beliefs, hopes, fears and expectations. The means is not known, however the mind that has these contents is conscious of these contents. In the case of the COS, that has a capacity for stabilized chaotic itinerancy, it is not a self-listening phonograph, so to speak. The quasi-attractors do not contain contents without the aid of human perception. A conscious person in the loop makes observations about the COS signal and creates a mental representation of it. Recurrences during the observation may take on significations, as well as, anomalies or breaks with consistency. Transitions and the successions of transitions, may imply something to a perceiver. The mental states of the perceiver are directed toward the COS signal forming memory traces and cascades of mental coordination, where mental states may generally be a form of chaotic itinerancy itself. Here the COS signal and the mind of the perceiver share common dynamics, not on the level of contents, but on the level of dynamics with the capacity to represent to contents. The COS may seem to point back at the perceiver, as a chiastic mirror or in terms of Extended Mind Theory (EMT) [Clark and Chalmers, 1998] a functional isomorphism. EMT will be revisited chapter 5.

Language, the usual suspect in the study of intentionality, is a mixture of references to an imaginary space and real things to account for a state of affairs [Whorf, 1997]. An utterance

is dually directed toward metaphors and actualities. In other words, the imaginary space has metaphors or analogies to describe the function and dynamics of real things. If speaking is considered intentional as evidenced by the appearance of CI in the mind when speaking, then musicking may also be of the same kind of mixed referentiality. Metaphors elicit predictions about the future implications of certain occurrences or what will be present, along with imagination about what is absent. To borrow from Derrida, absence becomes a presence when the lack is realized by its negation and can become an abstract directive. Here the metaphor can stand in for the real thing, in terms of a directing force for intentional playing.

The culture jamming work of Negativland samples pop culture arranging a pastiche of elements to create an abstract context that can reveal an invisible or unheard real context. While recent work from Negativland has transitioned from sampling to abstract synthesis with the Booper networks, the culture jamming carries over, where that negation of reference is a reference in its own right. A sample has contents because it has a context. It was an expression (content) recorded by a certain artist with certain history during a certain socio-political moment (context). Even in the case where the sample is an abstract synthesized sound like what is generated by a COS, Cracklebox, Booper or Buchla, its context makes it a content to a perceiver. For a sound to become a content on the level of a cultural reference, it simply must be sounded, perceived and comprehended for context.

The discussion of intentionally will be picked up again during the concluding chapter. But at least here, the generation of intentional sequences of musical organization is about the directed perception of the generated itinerancy, creating an embedded and extended relation of intentionality during interactive performance. Intentionality is co-created in the interaction. While the sequence of quasi-attractors sound abstract, the dynamics of the stabilized trajectory embody a mode of directivity, (quantitatively) consistent with embodied people performing intentional acts.

Chapter 2

Coupled Oscillator Systems: A Mathematical Description

The coupled oscillator systems (COS) described here are systematized in such a way that no oscillator runs freely. Unidirectional constructions will not be described here, where one oscillator modulates the intrinsic frequency of another oscillator. Typically this is known as a driving and a driven oscillator. The driven oscillator has no effect on the frequency of the driving oscillator, making it a top-down organization. A two oscillator system is coupled bidirectionally when both oscillations are effectuated by the speed of itself and the other oscillator. In systems with larger numbers of oscillators, the causality of the loop is such that the state of any oscillator at any sample depends on the position of other oscillators. These rows of coupled oscillators will be referred to as systems rather than networks. The word network implies both horizontal and vertical dependency. Here the organization is essentially horizontal, not a lattice configuration. The COS are designed for real-time interactivity with parameters for intrinsic oscillator frequencies and coupling strength. A three oscillator system (3-COS), for instance, has four parameters, one for the frequency of each oscillator and a coupling strength that affects every oscillator.

The focus of this technique is less concerned with timbre transformation, than it is with the synthesis of long-term sonic behaviors. Though there are forms of waveshaping and ring modulation that arise from this technique, the prominent feature involves the appearance of frequency envelopes that, in some cases, continuously vary without repetition. The coupling in COS is a bottom-up generative structure. Observed in the COS are the appearance of higher-level phenomena given certain structural organizations of dependency. One particular system of organization will be described here. Systems of three or more oscillators are partitioned into overlapping subsystems. For instance, when the description of the state of a subsystem of two oscillators is used to modify the phase-increment of an oscillator outside the subsystem, a situation ensues where each oscillator in a subsystem is modified by two other oscillators. Then what is a modifier is also being modified. This case of a three oscillator system will examined in detail later on. But the 3-COS is organization where oscillators 1 and 2 modify 3, 2 and 3 modify 1 and 1 and 3 modify 2. This leads to an extra order of causality, as opposed to a circular chain-like organization where, 1 modifies 2, 2 modifies 3 and 3 modifies 1.

Generalities exist about all the oscillators systems presented here. The equation below reflects a phase-position for each oscillator updated with each sample of digital.

$$\theta_i[t+1] = mod1(L_i^*[t] \cdot (\omega_i/R) + \theta_i[t]) \tag{2.1}$$

Each oscillator in the system can be written as:

$$x_i[t] = cos(2\pi \cdot \theta_i[t] \cdot S) \tag{2.2}$$

The variable, i, is an index number for each oscillator. It is a unique identifier that names it so it can be referred to. The variable n is the time step at sample rate, R. $\omega(i)$ is the intrinsic frequency of the oscillator. In this application, $\omega(i)$ typcially ranges between 0-10 HZ. However, this range can vary because larger numbers of oscillators tend to increase the average frequency

of the system. $L_i^*[t]$ is a time-varying coupling term. There are many possible terms that will be described shortly. The variable $\theta_i[t]$ is the phase-position of the oscillator, between 0 and 1. S is a static base frequency that scales the dynamics into the audible range, where $S \cdot \omega$ becomes the highest possible fundamental frequency of an individual oscillator in the system.

The time varying coupling terms $L_i^*[t]$ involve the measurement of phase differences between oscillators. The phase-positions, $\theta_i[t]$, of all the oscillators are considered the state variables of the systems. Creating abstractions of those state variables via measurement, such as, relative distances are the descriptions of the system. The sign of the distances is a part of a description that helps determine the ordering of phases on a line. These descriptions are embedded in the coupling terms and tend to be the main component that varies the strength of that term over time. Below is an example of varying the coupling term, $L_3[t]$, for oscillator 3 given the descriptions of oscillators 1 and 2.

$$L_3^*[t] = \begin{cases} -L_{\delta\{1,2\}} & \text{if } \theta_1[t] >= \theta_2[t] \\ 1/L_{\delta\{1,2\}} & otherwise \end{cases} \tag{2.3}$$

When phase differences are represented on the edge of a circle, there are two distances between two $\theta_i[t]$. For instance, the distances from $\theta_1[t]$ to $\theta_2[t]$ and then from $\theta_2[t]$ to $\theta_1[t]$. These can be called δ and δ'.

$$\delta = \theta_1[t] - \theta_2[t] \tag{2.4}$$

$$\delta' = 1 - |\delta| \tag{2.5}$$

When the circle has a base point, the ordering of the phase-positions can be determined relative to that base point. Without a base point, the absolute ordering of phase-positions, can change to a metric interpretation, where ordering is the relative distance from $\theta_i[t]$ given the

ascending order of proximities of other $\theta_i[t]$. A circle with a base point is equivalent to a line over the unit interval with a maximal discontinuity or the point where the line wraps from 1 to 0, or 0 to1 depending on the direction of motion. Both representations will be used in the examples of oscillator systems to follow. Here are a few coupling terms, $L_i^*[t]$, that can be used for position on a line. $L_i^*[t]$ is the generic case that refers to all or multiple time-varying coupling terms at once. The term $L_i[t]$ is defined below:

$$L_i[t] = 1 + (\lambda \cdot |\delta|) \tag{2.6}$$

Alterations of the the term $L_i[t]$ are possible where $-L_i[t]$, $1/L_i[t]$ and $-1/L_i[t]$ mean $-1+(\lambda \cdot -|\delta|)$, $1/(1+(\lambda \cdot |\delta|))$ and $-1/(1+(\lambda \cdot |\delta|))$. When one-dimensional positions are on a circle with a base point, only $|\delta|$ is used. The parameter λ is a scalar that increases the magnitude or strength of the term. The first two examples of $L_i^*[t]$ above are linear and in general increase speed as a function of increased λ and distance.The $L_i[t]$ refers to a term that increases the size of the phase increment, or speed, per time step. The speed decreases as distance decreases.

$-L_i^*[t]$ is the same as $L_i^*[t]$, however the term changes the direction of motion. The next two examples of $L_i^*[t]$ are the inverse and in general decrease speed with an increase of λ and of distance. $1/L_i^*[t]$ decreases speed as distances increases. With $-1/L_i[t]$ a negative is applied to the term to change the direction of motion. A negative direction reverses to positive and positive changes to negative. The, i, in $L_i^*[t]$ denotes the oscillator subject to modification via the coupling term. The δ or δ' is a pair of oscillators whose description affects $\theta_i[t]$. More than one δ variable will be used later in oscillator systems of higher dimension. The four $L_i^*[t]$ just described are meant to parlay a sense of the possibilities for coupling terms.

When phase-positions are moving on a line rather than the edge of a circle without a base point, the coupling terms and intrinsic frequencies are not the only factors that determine the

frequency envelopes of the oscillator systems. The discontinuity of the space alters the ordering of phase-positions once per cycle. When each oscillator reaches the base point it switches immediately from the highest position to the lowest position.

In an uncoupled three oscillator system the ordering of phase-magnitudes is observed to repeat in short durations when each intrinsic frequency is an integer. This is also true if each intrinsic frequency is an integer multiplied by the same floating point number. However, if one or more of the intrinsic frequencies is a float and the rest are integers (or all are floats not divisible to integers by the same float) then irregular long term frequency-dependent cycles emerge. One way to see this difference is to plot the ordering of the phase-positions given different sets of frequencies. An irregular pattern is observed in the case where intrinsic frequencies are $\omega_1 = 2.3$, $\omega_2 = 5.4$, $\omega_3 = 4.1$. A regular pattern is observed in the case where intrinsic frequencies are $\omega_1 = 6$, $\omega_2 = 3$, $\omega_3 = 4$. Both plots below show how the six possible orderings of three oscillators change over time.

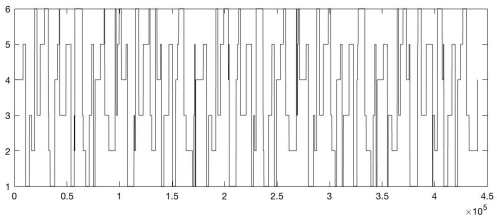

Figure 2.1: The ordering of three uncoupled oscillators moving with static frequencies on a line. The six ordering of three are numbered 1-6. The frequencies of each oscillator are $\omega_1 = 2.3$, $\omega_2 = 5.4$, $\omega_3 = 4.1$. The duration is 10 seconds.

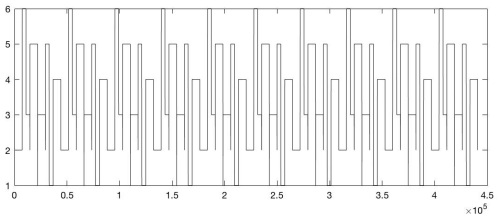

Figure 2.2: The ordering of three uncoupled oscillators moving with static frequencies on a line. The six ordering of three are numbered 1-6. The frequencies of each oscillator are $\omega_1 = 6$, $\omega_2 = 3$, $\omega_3 = 4$. The duration is 10 seconds..

Overall, state variables are used to make descriptions. Descriptions are used as a means to vary coupling terms, as well as, conditions to determine which oscillator is affected by which of the other oscillators at what time. These descriptions can include distances between phase-positions that vary coupling terms. The ordering of positions relative to a base point on a circle or relative to a reference oscillator on a circle without a base point determine conditions of transformation. With these concepts and variables introduced, we can move toward examining specific Coupled Oscillator Systems in the following section.

2.1 A Three Oscillator System (3-COS)

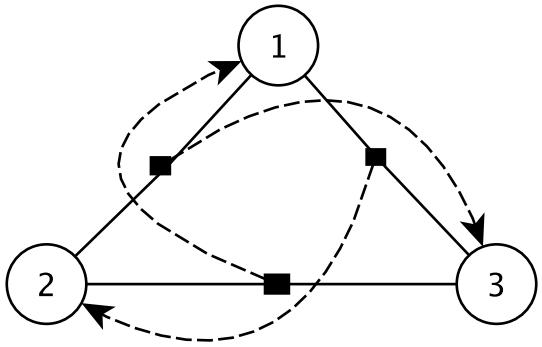

Figure 2.3: The structure of a three oscillator system. Numbered circles represent each oscillator. The solid line with a black box in the middle indicate a pair of oscillators is a subsystem. The hashed line shows which oscillator each subsystem is coupled to.

In the preceding section the idea of coupled oscillators was discussed as a system where interactions of varying order exist between all oscillators. Here a three oscillator system is presented in detail. The structure of this three oscillator system first involves creating overlapping subsystems of pairs. These pairs are then coupled to the remaining oscillator outside the subsystem. Oscillators $\{1,2\}$ affect 3, $\{2,3\}$ affect 1, and $\{1,3\}$ affect 2. As mentioned, this creates something like an extra order of causality. Each member of a subsystem is affected by the distance between two oscillators. A different coupling term affects the targeted oscillator given the order of the

pair, which is also part of a subsystem that targets another oscillator. The phase-positions are represented on a circle with a base point. A loss of monotonicity, then, occurs once per cycle that interrupts the phase ordering and the distance metric. The distance metric is in the form of $\delta = \theta_i - \theta_{i+j}$.

The state of each oscillator shown in equation 1.1 as $\theta_i[t+1] = mod1((L_i^*[t](\omega(i)/R) + \theta_i[t]))$ is updated every sample. The equations below show the details of the cases that update the coupling term, which is the main time-varying component of the phase increment generation. The i, from, $L_i^*[t]$, is the target oscillator. A different $L_i^*[t]$ is given based on the ordering, which is the difference of the magnitudes of the phases. Each $L_i^*[t]$ requires a distance between two oscillators. Denoted here, for instance, $L_{\delta\{1,2\}}$ means the speed of the target oscillator is increased with the distance between $\theta_1[t]$ and $\theta_2[t]$.

$$L_3^*[t] = \begin{cases} L_{\delta\{1,2\}} & \text{if } \theta_1[t] >= \theta_2[t] \\ -1/L_{\delta\{1,2\}} & otherwise \end{cases} \tag{2.7}$$

$$L_2^*[t] = \begin{cases} L_{\delta\{1,3\}} & \text{if } \theta_1[t] >= \theta_3[t] \\ -1/L_{\delta\{1,3\}} & otherwise \end{cases} \tag{2.8}$$

$$L_1^*[t] = \begin{cases} L_{\delta\{2,3\}} & \text{if } \theta_2[t] >= \theta_3[t] \\ -1/L_{\delta\{2,3\}} & otherwise \end{cases} \tag{2.9}$$

The structure of this three oscillator system presented will be abstracted in two more ways before moving on to oscillator structures that involve a basis of 4, 5 or 6 oscillators. The first way is to consider each phase-position in the system as comprised of two oscillators. The second way is to consider each phase-position in the system to be the three oscillator system just explained. Pairs of three oscillators systems rotate a target three oscillator system, creating a nested structure of 9 oscillators.

2.2 A Three by Two Oscillator System (3x2-COS)

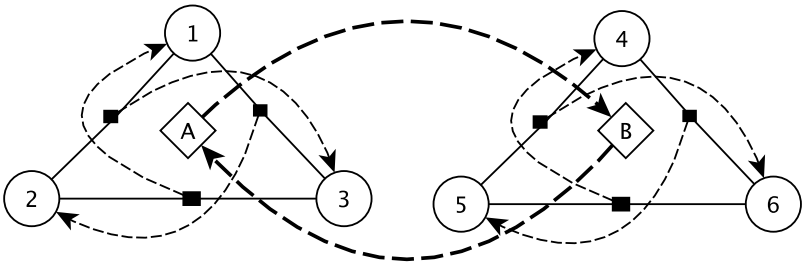

Figure 2.4: The structure of a 3 by 2 oscillator system. Numbered circles represent each oscillator. The solid lines with a black box in the middle indicate a group of 2 oscillators is a subsystem. The hashed line shows which oscillator each subsystem is coupled to. System A is coupled to system B shown with the bold hashed arrow lines.

The three by two oscillator system presented here treats a pair of oscillators as orthogonal, creating a 2-dimensional coordinate for each node. Similar to three oscillator system, there are three of these nodes as ($\theta_1[t]$, $\theta_2[t]$), ($\theta_3[t]$,$\theta_4[t]$) and ($\theta_5[t]$,$\theta_6[t]$). Using an L-2 norm a set of distances are calculated at each time step.

$$\delta_{\{1,2\}} = |\theta_3[t] - \theta_5[t]| + |\theta_4[t] - \theta_6[t]| \tag{2.10}$$

$$\delta_{\{3,4\}} = |\theta_1[t] - \theta_5[t]| + |\theta_2[t] - \theta_6[t]| \tag{2.11}$$

$$\delta_{\{5,6\}} = |\theta_1[t] - \theta_3[t]| + |\theta_2[t] - \theta_4[t]| \tag{2.12}$$

The $\delta_{\{x,y\}}$ notation specifies which oscillators are the target of the two nodes in the outside subsystem. The nodes ($\theta_3[t]$,$\theta_4[t]$) and ($\theta_5[t]$,$\theta_6[t]$) affect ($\theta_1[t]$, $\theta_2[t]$), et cetera. The function to effect ($\theta_1[t]$, $\theta_2[t]$), is based on which of the two nodes in the affecting subsystem is closer to the origin.

$$L^*_{\{1,2\}}[t] = \begin{cases} (-1/L_{\delta\{1,2\}}, -1/L_{\delta\{1,2\}}) & \text{if } \theta_3 + \theta_4 >= \theta_5 + \theta_6 \\ (L_{\delta\{1,2\}}, L_{\delta\{1,2\}}) & otherwise \end{cases} \tag{2.13}$$

The same logic is used to affect the other two nodes to construct the appropriate $L^*_{\{3,4\}}[t]$ and $L^*_{\{5,6\}}[t]$ terms, creating the entangled causality, described earlier.

2.3 A Three by Three Oscillator System (3x3-COS)

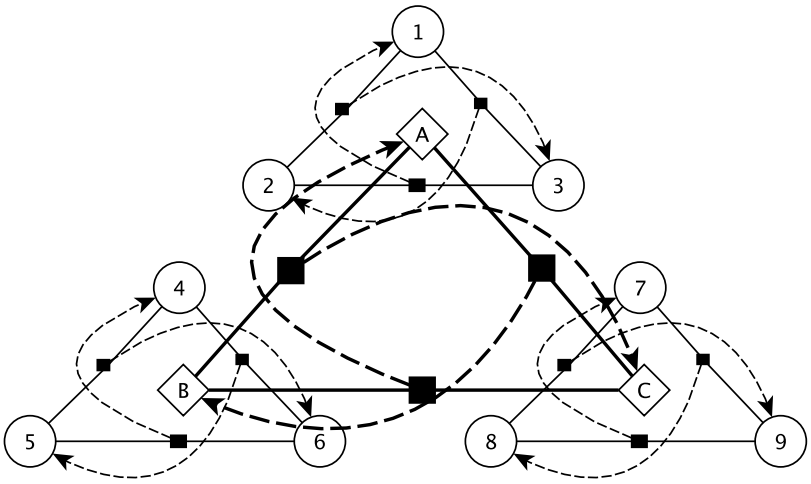

Figure 2.5: The structure of a 3 by 3 oscillator system. Numbered circles represent each oscillator. The solid lines with a black box in the middle indicate a group of 2 oscillators is a subsystem. The hashed line shows which oscillator each subsystem is coupled to. The bold hashed arrow lines show how systems A,B,C are coupled together.

Where the three by two oscillator system considered each node in the system to comprise two oscillators, the three by three oscillator system considers each node to comprise a three oscillator system. Here a total of nine oscillators are arranged in nodes. Node 1 contains oscillators $\{1,2,3\}$. Node 2 contains oscillators $\{4,5,6\}$. Node 3 contains oscillators $\{7,8,9\}$. In the system described here nodes 1 and 2 affect 3, nodes 2 and 3 affect 1, nodes1 and 3 affect 2. This could be considered a self-similar, fractal-like organization of the three oscillator system. Since internal

dynamics of each node comprised of a 3-COS have already been described, we will focus on the dynamics between nodes. Each node of 3 oscillators moves along the edge of a circle with a base point discontinuity.

First we need to compute of a set of nine distances, in the form of $\delta = \theta_i - \theta_{i+j}$. This will yield the following distances: $\delta_{\{1,2\}}[t]$, $\delta_{\{2,3\}}[t]$, $\delta_{\{1,3\}}[t]$, $\delta_{\{4,5\}}[t]$, $\delta_{\{5,6\}}[t]$, $\delta_{\{4,6\}}[t]$, $\delta_{\{7,8\}}[t]$, $\delta_{\{8,9\}}[t]$, and $\delta_{\{7,9\}}[t]$. These differences listed can be negative or positive based on the ordering on the line. From the order just listed, each successive set of three $\delta_{\{i,i+j\}}$ forms a node. For each node a set of $L_i^*[t]$ is constructed as in equations (2.7), (2.8) and (2.9). With this we have three uncoupled three oscillator systems.

To start to couple the nodes together, recall that in the three oscillator system a $L_i^*[t]$ is selected based on the ordering of two phase-positions, $\theta_i[t]$. To determine the relative order of two nodes on a line we use the following expressions to obtain sums that reflect a negative or positive distance, as $\Delta_i[t]$.

$$\Delta_{\{1,2\}}[t] = (\theta_1[t] - \theta_4[t]) + (\theta_2[t] - \theta_5[t]) + (\theta_3[t] - \theta_6[t]) \tag{2.14}$$

$$\Delta_{\{1,3\}}[t] = (\theta_1[t] - \theta_7[t]) + (\theta_2[t] - \theta_8[t]) + (\theta_3[t] - \theta_9[t]) \tag{2.15}$$

$$\Delta_{\{2,3\}}[t] = (\theta_4[t] - \theta_7[t]) + (\theta_5[t] - \theta_8[t]) + (\theta_6[t] - \theta_9[t]) \tag{2.16}$$

We then write a set of conditions to generate a coupling term to affect the node outside the subsystem of nodes. Since each node is internally coupled by terms named $L_i^*[t]$, we use $M_i^*[t]$ to denote a secondary coupling term for coupling nodes together.

$$M^*_{\{7,8,9\}}[t] = \begin{cases} (-1/M_{\delta\{1,4\}}, -1/M_{\delta\{2,5\}}, -1/M_{\delta(3,6)}) & \text{if } \Delta_{\{1,2\}}[t] >= 0 \\ (M_{\delta\{1,5\}}, M_{\delta\{2,5\}}, M_{\delta\{3,6\}}) & otherwise \end{cases} \tag{2.17}$$

$$M^*_{\{4,5,6\}}[t] = \begin{cases} (-1/M_{\delta\{1,7\}}, -1/M_{\delta\{2,8\}}, -1/M_{\delta\{3,9\}}) & \text{if } \Delta_{\{1,3\}}[t] >= 0 \\ (M_{\delta\{1,7\}}, M_{\delta\{2,8\}}, M_{\delta\{3,9\}}) & otherwise \end{cases} \tag{2.18}$$

$$M^*_{\{1,2,3\}}[t] = \begin{cases} (-1/M_{\delta\{4,7\}}, -1/M_{\delta\{5,8\}}, -1/M_{\delta\{6,9\}}) & \text{if } \Delta_{\{2,3\}}[t] >= 0 \\ (M_{\delta\{4,7\}}, M_{\delta\{5,8\}}, M_{\delta\{6,9\}}) & otherwise \end{cases} \tag{2.19}$$

Recall the phase-position of each oscillator is generally updated as $\theta_i[t+1] = mod1(L^*_i[t] \cdot (\omega_i/R) + \theta_i[t])$. However, in this case each oscillator contains a product of two coupling terms, each with the same coupling strength λ, as $L_i[t] \cdot M_i[t]$. This leads explicitly to a basic ring modulation effect for each oscillator.

2.4 A Four Oscillator System (4-COS)

The four oscillator system presented here has a similar organization to the three oscillator system. A key difference is that the phase-positions are represented on a circle without a base point. With no base point defined in the circular space, descriptions are based on relative distances. The subsystems are overlapping groupings of three oscillators as, {1,2,3}, {1,2,4}, {1,3,4}, and {2,3,4}. The subsystem has a description which is used to affect an oscillator outside the subsystem. For instance, the description of the subsystem {2,3,4} affects oscillator 1. The description of each subsystem is not the possible orderings of the positions, as in the three oscillator system. Instead, each subsystem is described as having a selected oscillator as positioned in the center or not. This yields two conditions for the alteration of the targeted oscillator.

The description of the center oscillator is based on a metrical procedure. To start off, we need a representation of each phase-position, $\theta_i[t]$, as if it is moving on a circle without base

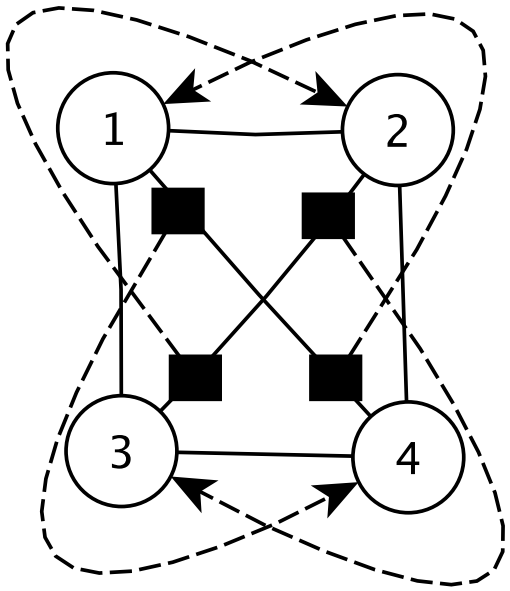

Figure 2.6: The structure of a four oscillator system. Numbered circles represent each oscillator. The solid lines with a black box in the middle indicate a group of 3 oscillators is a subsystem. The hashed line shows which oscillator each subsystem is coupled to.

point, or in other words without a discontinuity. In this case, a pair of phase-positions has two distances to consider, one of which is the minimum distance between the phase-positions. If at each timestep, n, the minimum distance between all phase-positions is updated to effect the coupling term, then the phase-positions are interacting as if on a circle. Below is an example of an if-statement to find the minimum distance, whether it is $|\delta|$ or δ' (see equation (2.4)), between $\theta_1[t]$ and $\theta_2[t]$.

$$\delta^{\mu}_{\{1,2\}} = \begin{cases} |\delta_{\{1,2\}}| & \text{if } |\delta_{\{1,2\}}| <= \delta'_{\{1,2\}} \\ \delta'_{\{1,2\}} & \text{otherwise} \end{cases} \tag{2.20}$$

After finding the minimum distance between all the pairs. The center of the subsystem is defined as the oscillator that has the least sum of minimum distances from the other two. To see if $\theta_1[t]$ or rather oscillator 1 is in the center of the subsystem $\{1,2,3\}$ the following the block is used

to gather the sums. The remaining three subsystems are also checked with this method.

$$\Sigma_1\{1,2,3\} = \delta^{\mu}_{\{1,2\}} + \delta^{\mu}_{\{1,3\}} \tag{2.21}$$

$$\Sigma_2\{1,2,3\} = \delta^{\mu}_{\{1,2\}} + \delta^{\mu}_{\{2,3\}} \tag{2.22}$$

$$\Sigma_3\{1,2,3\} = \delta^{\mu}_{\{2,3\}} + \delta^{\mu}_{\{1,3\}} \tag{2.23}$$

Next, we find the minimum of the 3 sums to check if the center, C, of subsystem $\{1,2,3\}$ is oscillator 1.

$$C\{1,2,3\} = \begin{cases} 1 & \text{if } \min([\Sigma_1, \Sigma_2, \Sigma_3] == \Sigma_1) \\ 0 & otherwise \end{cases} \tag{2.24}$$

The center is found for each subsystem using the procedure above. However, a different oscillator is selected for the center position in each subsystem to give a unique δ^{μ} to alter the targeted oscillator's course. For C$\{1,2,3\}$ it is oscillator 1, yielding $\delta^{\mu}_{\{2,3\}}$. For C$\{2,3,4\}$ it is oscillator 2, yielding $\delta^{\mu}_{\{3,4\}}$. For C$\{1,3,4\}$ it is oscillator 3, yielding $\delta^{\mu}_{\{1,4\}}$. For C$\{1,2,4\}$ it is oscillator 4, yielding $\delta^{\mu}_{\{1,2\}}$. With two results from each subsystem, a coupling term based on L_n or $-1/L_n$ is used to affect the target oscillator.

$$L^*_4[t] = \begin{cases} L_{\delta^{\mu}\{2,3\}} & \text{if C}\{1,2,3\} == 1 \\ -1/L_{\delta^{\mu}\{2,3\}} & otherwise \end{cases} \tag{2.25}$$

$$L^*_1[t] = \begin{cases} L_{\delta^{\mu}\{3,4\}} & \text{if C}\{2,3,4\} == 2 \\ -1/L_{\delta^{\mu}\{3,4\}} & otherwise \end{cases} \tag{2.26}$$

$$L_2^*[t] = \begin{cases} L_{\delta^\mu\{1,4\}} & \text{if C}\{1,3,4\} == 3 \\ -1/L_{\delta^\mu\{1,4\}} & otherwise \end{cases} \tag{2.27}$$

$$L_3^*[t] = \begin{cases} L_{\delta^\mu\{1,2\}} & \text{if C}\{1,2,4\} == 4 \\ -1/L_{\delta^\mu\{1,2\}} & otherwise \end{cases} \tag{2.28}$$

2.5 A Five Oscillator System (5-COS)

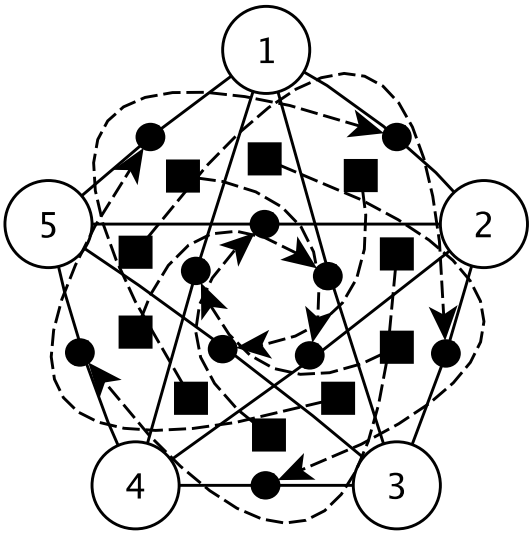

Figure 2.7: The structure of a five oscillator system. Numbered circles represent each oscillator. The solid lines with a black box in the middle indicate a group of 3 oscillators is a subsystem. The hashed line points to a circle on an edge that demarcates the affected subsystem of 2 oscillators.

Comparing the figures representing the four and five oscillator systems there is a visible a jump in the complexity of the causality. This is partly due to combinatorial expansion. Here there are ten subsystems of three that affect their compliment as ten subsystems of two. Not visible in the diagram are the downstream effects of affecting complement sets with more than one oscillator. As a result there will be four coupling terms, whose product updates the phase

increment for each oscillator with every timestep. The product of the coupling terms is denoted, $L_i^*[t] \cdot M_i^*[t] \cdot N_i^*[t] \cdot \emptyset_i^*[t]$. The phase of each of oscillator in the five oscillator system is then:

$$\theta_i[t+1] = mod1(L_i^*[t]M_i^*[t]N_i^*[t]\emptyset_i^*[t](\omega_i/R) + \theta_i[t])) \tag{2.29}$$

The system also introduces two more variations of structure not present in previous instances. One is that each subsystem of three oscillators generates six conditions from its ordering to initiate some form of coupling term, $L_i^*[t]$. The other is a coupling term that contains a linear combination of multiple δ. Now let's move toward a more detailed explanation of the algorithm.

To start off, we take the familiar step of computing a set of distances, in the form of $\delta = \theta_i[t] - \theta_{i+j}[t]$. Here there will be ten distances, necessary for determining the ordering of three oscillators on a line: $\delta_{\{1,2\}}[t]$, $\delta_{\{1,3\}}[t]$, $\delta_{\{1,4\}}[t]$, $\delta_{\{1,5\}}[t]$, $\delta_{\{2,3\}}[t]$, $\delta_{\{2,4\}}[t]$, $\delta_{\{2,5\}}[t]$, $\delta_{\{3,4\}}[t]$, $\delta_{\{3,5\}}[t]$, and $\delta_{\{4,5\}}[t]$. Next, the ordering these pairs on a line is determined by checking if the difference of the phase magnitudes is positive or negative. The following is an example of checking the ordering between $\theta_1[t]$ and $\theta_2[t]$.

$$\Theta_{\{1,2\}}[t] = \begin{cases} (1,2) & \text{if } \delta_{\{1,2\}}[t] >= 0 \\ (2,1) & \text{otherwise} \end{cases} \tag{2.30}$$

The same procedure is used to check the order of all ten pairs. Θ is used to refer to the possible orders of multiple $\theta_i[t]$. Next the ordering of a subsystem of three is determined. These include: $\Theta_{\{1,2,3\}}[t]$, $\Theta_{\{1,2,4\}}[t]$, $\Theta_{(1,2,5)}[t]$, $\Theta_{\{1,3,4\}}[t]$, $\Theta_{\{1,3,5\}}[t]$, $\Theta_{\{1,4,5\}}[t]$, $\Theta_{\{2,3,4\}}[t]$, $\Theta_{\{2,3,5\}}[t]$, $\Theta_{\{2,4,5\}}[t]$, and $\Theta_{\{3,4,5\}}[t]$. The expressions for the possible orderings of $\Theta_{\{1,2,3\}}[t]$ are below.

$$\Theta_{\{1,2,3\}}[t] = \begin{cases} (1,2,3) & \text{if } \Theta_{\{1,2\}}[t] == (1,2) \;\&\&\; \Theta_{\{2,3\}}[t] == (2,3) \\ (1,3,2) & \text{if } \Theta_{\{1,3\}}[t] == (1,3) \;\&\&\; \Theta_{\{2,3\}}[t] == (3,2) \\ (2,1,3) & \text{if } \Theta_{\{1,2\}}[t] == (2,1) \;\&\&\; \Theta_{\{1,3\}}[t] == (1,3) \\ (2,3,1) & \text{if } \Theta_{\{2,3\}}[t] == (2,3) \;\&\&\; \Theta_{\{1,3\}}[t] == (3,1) \\ (3,1,2) & \text{if } \Theta_{\{1,3\}}[t] == (3,1) \;\&\&\; \Theta_{\{1,2\}}[t] == (1,2) \\ (3,2,1) & \text{if } \Theta_{\{2,3\}}[t] == (3,2) \;\&\&\; \Theta_{\{1,2\}}[t] == (2,1) \end{cases} \tag{2.31}$$

The orders of $\{1,2,3\}$ modify a pair of oscillators outside the subsystem. In this case, the phase-positions of $\theta_4[t]$ and $\theta_5[t]$ are modified. With the occurrence of each ordering two coupling terms are computed to effect those phase-positions. Here are the $L^*_{\{4,5\}}[t]$ produced as a result. In code, this block below would be consolidated with the block above.

$$L^*_{\{4,5\}}[t] = \begin{cases} L_4[t] = ((\delta_{\{1,3\}} + \delta_{\{2,4\}}) \cdot \delta_{\{1,3\}} \cdot \lambda) + 1 & (1,2,3) \\ L_5[t] = ((\delta_{\{1,3\}} + \delta_{\{2,5\}}) \cdot \delta_{\{1,3\}} \cdot \lambda) + 1 & \\ L_4[t] = ((\delta_{\{1,2\}} + \delta_{\{3,4\}}) \cdot \delta_{\{1,2\}} \cdot \lambda) + 1 & (1,3,2) \\ L_5[t] = ((\delta_{\{1,2\}} + \delta_{\{3,5\}}) \cdot \delta_{\{1,2\}} \cdot \lambda) + 1 & \\ L_4[t] = ((\delta_{\{2,3\}} + \delta_{\{1,4\}}) \cdot \delta_{\{2,3\}} \cdot \lambda) + 1 & (2,1,3) \\ L_5[t] = ((\delta_{\{2,3\}} + \delta_{\{1,5\}}) \cdot \delta_{\{2,3\}} \cdot \lambda) + 1 & \\ \tilde{L}_4[t] = ((\delta_{\{2,3\}} + \delta_{\{1,4\}}) \cdot \delta_{\{2,3\}} \cdot \lambda) - 1 & (3,1,2) \\ \tilde{L}_5[t] = ((\delta_{\{2,3\}} + \delta_{\{1,5\}}) \cdot \delta_{\{2,3\}} \cdot \lambda) - 1 & \\ \tilde{L}_4[t] = ((\delta_{\{1,2\}} + \delta_{\{3,4\}}) \cdot \delta_{\{1,2\}} \cdot \lambda) - 1 & (2,3,1) \\ \tilde{L}_5[t] = ((\delta_{\{1,2\}} + \delta_{\{3,5\}}) \cdot \delta_{\{1,2\}} \cdot \lambda) - 1 & \\ \tilde{L}_4[t] = ((\delta_{\{1,3\}} + \delta_{\{2,4\}}) \cdot \delta_{\{1,3\}} \cdot \lambda) - 1 & (3,2,1) \\ \tilde{L}_5[t] = ((\delta_{\{1,3\}} + \delta_{\{2,5\}}) \cdot \delta_{\{1,3\}} \cdot \lambda) - 1 & \end{cases} \tag{2.32}$$

To describe this function a bit more clearly as it appears in 60 different permutations for the five oscillator system. Assign the letters a thru c to denote the position in the ordering of the subsystem and the expression becomes: $L_i[t] = ((\delta_{\{a,c\}}[t] + \delta_{\{b,i\}}[t]) \cdot \lambda) + 1$ or $\tilde{L}_i[t] = ((\delta_{\{a,c\}}[t] + \delta_{\{b,i\}}[t]) \cdot \lambda) - 1$.

The coupling terms, $L^*_{\{4,5\}}[t]$, are structured such that when (1,2,3) modifies oscillator 4, the function is never greater than the outer pair $\delta_{\{1,3\}}[t] \cdot \lambda + 1$. The center of the subsystem (1,2,3) is measured against oscillator 4 as $\delta_{\{2,4\}}[t]$ and used to modulate the function within that range. Since we know the ordering, we know that δ is a positive value in this case. Meaning that the category for this coupling term is $L_i[t]$ or is generally positive in direction and increasing in speed with distance. For (3,2,1) the formula yields the same set of δ, except the output is never greater than $\delta_{\{1,3\}}[t] \cdot \lambda - 1$, where $\delta_{\{1,3\}}[t]$ is a negative value. The output of the function

$\tilde{L}_4[t]$ then switches intermittently between a positive and negative direction, further modulated by $\delta_{\{2,4\}}[t]$ or $\delta_{\{2,5\}}[t]$ depending on the reference. The aggregate effect of all these terms mostly becomes oscillators that move in a positive direction. Negative direction is much less likely. With direction changes musically useful results occur with an imbalance of direction changes skewed more to one way than the other.

Each of the five oscillators will be assigned a product of 4 coupling terms as mentioned earlier. This happens because of the overlap of subsystems. For instance, $\Theta_{\{1,2,3\}}[t]$, $\Theta_{\{1,2,4\}}[t]$, $\Theta_{\{1,3,4\}}[t]$, $\Theta_{\{2,3,4\}}[t]$ all yield terms that modify oscillator 5. Ring modulation affects the timbre of each oscillator resulting from the product of coupling terms and the fact that each coupling term contains products of $\delta_{\{sort(i,i)\}}[t]$.

2.6 A Six Oscillator System (6-COS)

This implementation of a six oscillator system maps subsystems of three oscillators to modify its complement of three oscillators. The same principle used in previous examples is used here. A subsystem modifies the set of oscillators that it has no overlap with via coupling terms. Each modifier subsystem overlaps with all other modifier subsystems by one or two oscillators. Given six oscillators there are 20 possible subsystems of three. The modification of oscillator phase is arranged such that each oscillator contains a product of five coupling terms: $L_i^*[t] \cdot M_i^*[t] \cdot N_i^*[t] \cdot \emptyset_i^*[t] \cdot P_i^*[t]$. Splitting the subsystems of three oscillators into two groupings of ten means that each grouping of ten subsystems contains five of each oscillator. Table 2.1 below details the solution.

Table 2.1: The organization of subsystems of oscillators in the six oscillator system. The subsystems are organized such that each column, the modifier and the modified, contain the same distribution of digits for oscillator indices.

Modifer	Modified
{1,2,5}	{3,4,6}
{1,2,6}	{3,4,5}
{1,3,4}	{2,5,6}
{1,3,6}	{2,4,5}
{1,4,5}	{2,3,6}
{2,3,4}	{1,5,6}
{2,3,5}	{1,4,6}
{2,4,6}	{1,3,5}
{3,5,6}	{1,2,4}
{4,5,6}	{1,2,3}

The process from here is similar to the five oscillator system in the previous section. The state variables $\theta_i[t]$ are described by the function $\delta_{\{sort(i,i)\}}[t]$ as having a positive or negative phase difference. Equations (2.30) and (2.31) show how subsystems of three, in this case, the modifier oscillators are determined to have a descending ordering of phase magnitudes. Given on of the six orderings for each subsystem of three oscillators, a different group of three coupling terms are mapped to the modified oscillators. As an aggregate each oscillator will be influenced by five such coupling terms from five modifier subsystems at each timestep, n. This produces a series of frequency envelopes with long-term variation coextensive with timbre alterations from resultant ring modulation effects. Before writing a long form conditional expression for one mapping of modifier oscillators to modified oscillators, below is a condensed description that shows how the $\tilde{L}_x[t]$ are constructed with a pattern of phasors. $L^*_{\{x,y,z\}}[t]$ are unordered modified oscillators. $\Theta_{(a,b,c)}[t]$ is the modifier set representing the permutations. $\tilde{L}_i[t]$ is an undirected coupling term representing one term of the modified subsystem. Each $L^*_{\{x,y,z\}}[t]$ of which there are six contains a different offset designations. The sort() function is used to name the δ function with phasor indices in descending order.

$$L^{*}_{\{x,y,z\}}[t] = \begin{cases} \tilde{L}_x[t] = (\delta_{\{sort(a,c)\}} \cdot \delta_{\{x,z\}} \cdot \lambda) & \Theta_{(a,b,c)}[t] \\ \tilde{L}_y[t] = (\delta_{\{sort(a,c)\}} \cdot \delta_{\{y,z\}} \cdot \lambda) & \\ \tilde{L}_z[t] = (\delta_{\{sort(a,c)\}} \cdot \delta_{\{sort(c,z)\}} \cdot \lambda) & \end{cases} \tag{2.33}$$

Below is a conditional expression that shows how oscillators $\{1,2,5\}$ modify oscillators $\{3,4,6\}$ given the occurrence of descriptions of orderings.

$$
L^{*}_{\{3,4,6\}}[t] = \begin{cases}
\tilde{L}_3[t] = (\delta_{\{1,5\}} \cdot \delta_{\{3,6\}} \cdot \lambda) + 1 & (1,2,5) \\
\tilde{L}_4[t] = (\delta_{\{1,5\}} \cdot \delta_{\{4,6\}} \cdot \lambda) + 1 & \\
\tilde{L}_6[t] = (\delta_{\{1,5\}} \cdot \delta_{\{5,6\}} \cdot \lambda) + 1 & \\
\tilde{L}_3[t] = (\delta_{\{1,2\}} \cdot \delta_{\{3,6\}} \cdot \lambda) - 1 & (1,5,2) \\
\tilde{L}_4[t] = (\delta_{\{1,2\}} \cdot \delta_{\{4,6\}} \cdot \lambda) - 1 & \\
\tilde{L}_6[t] = (\delta_{\{1,2\}} \cdot \delta_{\{5,6\}} \cdot \lambda) - 1 & \\
\tilde{L}_3[t] = -1 \cdot (\delta_{\{2,5\}} \cdot \delta_{\{3,6\}} \cdot \lambda) + 1 & (2,1,5) \\
\tilde{L}_4[t] = -1 \cdot (\delta_{\{2,5\}} \cdot \delta_{\{4,6\}} \cdot \lambda) + 1 & \\
\tilde{L}_6[t] = -1 \cdot (\delta_{\{2,5\}} \cdot \delta_{\{5,6\}} \cdot \lambda) + 1 & \\
\tilde{L}_3[t] = -1 \cdot (\delta_{\{1,2\}} \cdot \delta_{\{3,6\}} \cdot \lambda) - 1 & (2,5,1) \\
\tilde{L}_4[t] = -1 \cdot (\delta_{\{1,2\}} \cdot \delta_{\{4,6\}} \cdot \lambda) - 1 & \\
\tilde{L}_6[t] = -1 \cdot (\delta_{\{1,2\}} \cdot \delta_{\{5,6\}} \cdot \lambda) - 1 & \\
\tilde{L}_3[t] = 1 + (\delta_{\{2,5\}} \cdot \delta_{\{3,6\}} \cdot \lambda) + 1 & (5,1,2) \\
\tilde{L}_4[t] = 1 + (\delta_{\{2,5\}} \cdot \delta_{\{4,6\}} \cdot \lambda) + 1 & \\
\tilde{L}_6[t] = 1 + (\delta_{\{2,5\}} \cdot \delta_{\{5,6\}} \cdot \lambda) + 1 & \\
\tilde{L}_3[t] = (\delta_{\{1,5\}} \cdot \delta_{\{3,6\}} \cdot \lambda) & (5,2,1) \\
\tilde{L}_4[t] = (\delta_{\{1,5\}} \cdot \delta_{\{4,6\}} \cdot \lambda) & \\
\tilde{L}_6[t] = (\delta_{\{1,5\}} \cdot \delta_{\{5,6\}} \cdot \lambda) &
\end{cases} \tag{2.34}
$$

The systems presented share common structure and can be mixed into many different configurations by increasing the number of oscillators, changing the kind of descriptions of subsystems and changing the list of coupling terms. With seven COS mathematically defined, focus will shift to the description and analysis of kinds of auditory phenomena, or music generated.

The analysis also shows why certain configurations may be preferable to others. The next chapter will define the methodology of analysis. Then an in-depth analysis of each of the seven COS is presented.

Chapter 3

Analysis Methodology

Evidence for non-linear data output will be presented, along with evidence for synchronization. Then the methodology will be two fold for each system. First phase plots will be described qualitatively to illustrate the kinds of phenomena generated. A phase plot is simply the phase of each oscillator, as time series data at sample rate. Second, recurrence plots (RP) and recurrence quantification analysis (RQA) will be used in conjunction with chaotic itinerancy (CI). First, evidence for COS generation of non-linear timeseries is presented because RP and RQA are used for analysis of non-linear phenomena.

3.1 Evidence of Non-linear Timeseries

When choosing a suitable method for analyzing timeseries, an important early step is to determine whether the process to be quantified is linear or nonlinear. In the mechanisms described in the previous chapter, we have mathematical procedures that define a systematization of feedback. This systemization allows the feedback of the previous state of the system to affect the current state of the system, to put it in general terms. While many mechanisms with feedback topology produce non-linear output, there are still few that won't, such as a loop that produces as cumulative sum as output. Judging the non-linearity of the system on the

basis of the mechanism's structural principles, such as feedback, does not always yield accurate determinations. Furthermore, reasoning from the structure of the mechanism also says nothing about the extent of the nonlinearity of the output. That said, it is best to focus only on the output as a first step, which will yield information about the extent of the nonlinearity. Once it is determined that the COS produces non-linear output, focus can return to the structure of the mechanism. Using non-linear analysis tools to track the output data, parts of the structure can be added, subtracted and modified to determine the contribution of function to the kind of output. In subsequent sections, non-linear analysis will be deployed to show what parts of the structure cause the onset of complexity in the output.

A method for determining the linearity of a timeseries is to fit a straight line to an output series of a certain duration. Different durations can be used to determine if the series is linear at all even over short durations. This has interesting implications for a COS which will be described in the next subsection.

Linear Regression is a way of fitting a straight line to a 2-dimensional time series data. If the data is tightly clustered and tends to distribute in a single direction the line will fit well and the data is regarded as linear. How well the line fits is given by a metric called the least square error (R^2), returning a value from 1 to 0. The 1 indicating a perfect fit. Overall, in the case of a COS the output is shown to be highly nonlinear with R^2 values generally close to 0. Figure 3.1 shows an attempt of the linear regression formalism to fit a line to 2 seconds of output from a pair of oscillators in the 4-COS. $R^2 = 0.0047$ for the time series depicted, meaning the data is very nonlinear. In the next section, line fitting will be used at short time scales. Using a moving window of 1000 samples reveals quasi-periodic rhythms of synchronization between oscillator pairs.

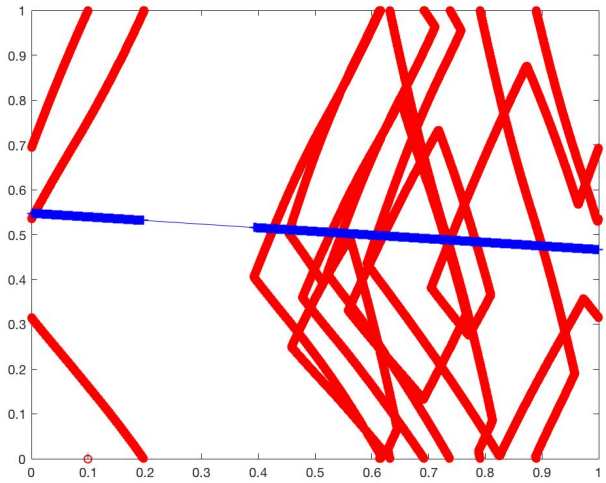

Figure 3.1: Fitting a line to the nonlinear data output from the 4 Oscillator System between oscillators 1 and 4. The duration depicted is 2 seconds. $R^2 = 0.0047$.

3.1.1 Least-square Error of Linear Regression shows Synchronization

The least square error shows the error of fit between two dimensions of data in a linear regression model. When this metric is applied to a COS with a short term moving window, here a 1000 sample duration with containing 20 equidistant sample points, moments of synchronization between pairs can be detected. Synchronization corresponds to $R^2 = 1$, and can be seen to occur at short time scales on the order or 10-100ms in the Three Oscillator system. Viewing figure 3.2 showing the 3-COS over 2 seconds, moments of synchronization emerge with a quasi-periodic structure. At times all pairs of oscillators are synchronized. Over the course of the plot, with the exception of 2 moments in the tens of milliseconds range, at least one pair is always synchronized. The moments of synchronization are always followed by sharp decays that drop the $R^2 = 1$ to $R^2 = 0$ almost immediately. This is likely caused by a crossing of a pair that affects a targeted oscillator, switching its coupling term from $-1/L$ to L or visa versa. Also of note are a number of peaks around $R^2 = 0.3$, potentially related to the development of synchronization that is suppressed before realization. This set of features also has quasi-periodic synchronization.

Listening to the signal of figure 3.2 quasi-periodic rhythms can be heard. These quasi-

periodic alternations of synced pairs correlate to the perception of rhythm. The number of pairs synced at once correlate to the perceived strength of the beat. Rhythmic relations are viewable between the blue and green pairs for example where most times the blue peak contains two green peaks. The location of the split between the green peaks moves relative to the center of the blue, sometimes left of center and at other times right, subtly different with each recurrence, meaning slight timbral differences in the micro-structure of strong beats and is generally similar to the dynamics of acoustic signals that never quite repeat given the same referent action.

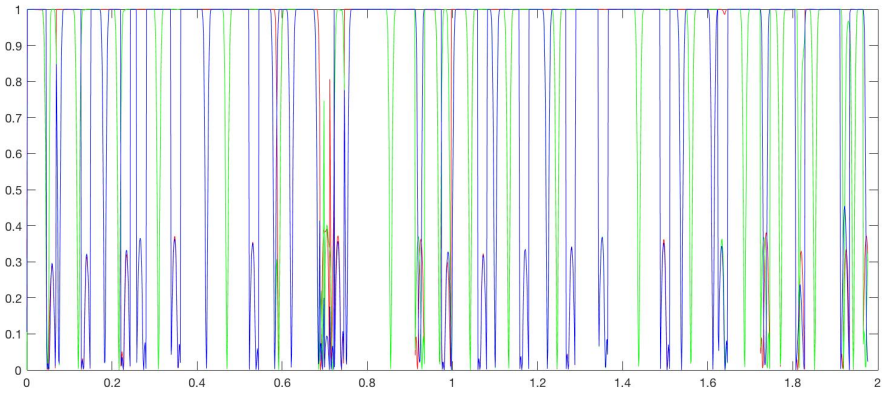

Figure 3.2: A plot of the windowed least square error of three oscillator system. The parameters are $\omega_1 = 7.2$, $\omega_2 = 2$, $\omega_3 = 3.2$, $\lambda = 1.3$ and the duration is 2 seconds. The color mapping indicates the three pairs of three oscillators.

3.2 Recurrence Plots

The Recurrence Plot (RP) is a standard method for the analysis of the phase plot of dynamical systems. It provides a graphical representation of n-dimensional timeseries data that can be analyzed via quantifications or by principled expositions of viewable regularities and irregularities. To construct a recurrence plot, two copies of the timeseries are situated on a vertical and horizontal axis. The dimension is reduced by using a distance metric between the two copies. A square grid of size T^2, (T = the length of the time series in samples), measures the distance

between all possible pairs of points in time, giving a fully extended non-linear comparison of the time series. This way every sample of the timeseries can be compared to every other sample. A threshold distance is a free parameter, if the pair of points have say, a euclidian distance of less than the threshold set, then a black dot is drawn, and if not the point remains white. Once the operation is complete patterns emerge, straight and diagonal lines, for instance are of key interest in most deterministic complex systems. The mathematical definition of a recurrence plot is:

$$R_{i,j} = \Theta(\varepsilon - ||x_i - x_j||), \qquad i, j = 1, ..., T \tag{3.1}$$

Where $\Theta(x)$ is the Heavyside function returning 0 if $x < 0$ or 1 if $x > 1$. ε is the threshold value and $||.||$ indicates the use of a norm for distance to be compared with the threshold. The i, j are indices of the relation between time steps of the series x and $R_{i,j}$ is the set of recurrence points.

Methods of visual inspection of the plots will be described first, followed by a mathematical description of quantification techniques. For visual analysis, there are many patterns that can be observed that carry specific meanings about the phase space of the dynamical system. Here are nine such patterns [Marwan, Romano, Thiel and Kurths, 2007].

(1) Homogeneity refers the uniform distribution of isolated points and means that the process is nonstationary. One such example of homogeneity is white noise. White noise in this context corresponds to maximal fluctuation of process and minimal relaxation time between fluctuations.

(2) Distributions that dissipate in density when approaching the upper left and lower right corners indicate phase spaces that are non-stationary and exhibit the phenomenon of drift.

(3) White bands in the plot, known as disruptions, also indicate non-stationary data. This occurs with the appearance of rare states defined as states that are far from the normal. Focally it indicates that some form of chaos-to-chaos transition may have happened during the measured event. The material might have undergone a phase change of some order.

(4) Periodic or quasi-periodic spacing shows periodicities. Uniform distances between periodic patterns, typically diagonal lines, indicate a stable oscillation of process that does not vary its duration. While non-uniform distances between patterns show quasi-periodic processes.

(5) Single isolated points reveal major fluctuations in the process. In the case when there are only single points in the plot, the process measured is likely uncorrelated or even anti-correlated randomness.

Before moving on to the final four patterns it is important note some general characteristics about recurrence plots. The *LOI* or line of identity is the main diagonal line in the plot spanning the bottom left to top right corner. The plot exhibits a bilateral symmetry about this line. This also explains why horizontal lines are not quantified. Vertical and horizontal lines are in effect mirrored. There are just as many horizontal of lines of the same distribution of lengths as vertical lines. Thus it is only necessary to select the verticals for quantification.

(6) Diagonal lines parallel to the *LOI* of a certain level of occurrence (i.e. many and longer) indicate a deterministic process, it also can mean that the evolution of states is similar at different reference times (epochs) of the process. If these lines are proximal to single isolated points the process might then be chaotic. Now if these lines in question are periodic and interposed with single points then this can mean the presence of unstable periodic points in the chaotic regime.

(7) Diagonal lines orthogonal to the *LOI* indicates similarity in the process at different times, although, with reverse time.

(8) The vertical lines (or horizontals) in the form of lines or clusters an indication of laminar states in the process, these are slowly changing stable states having minimal fluctuation.

(9) Long bowed line structures appear when the ontogenesis of states is similar at different times in the plot but have different velocities. It is potentially an early indication that the dynamics of the system are undergoing significant change.

3.3 Recurrence Quantification Analysis

Recurrence Quantification Analysis (RQA) is mathematical method to quantify many of the nine patterns described in the previous section. These commonly used measures are based on measuring density, diagonal line and vertical lines as statistics [Marwan, Romano, Theil and Kurths, 2007] The density measure used is known as the recurrence rate (*RR*).

$$RR = 1/T^2 \sum_{i,j=1}^{T} R_{i,j} \tag{3.2}$$

There are a few common measures of diagonals. A visual heuristic for interpreting Determinism (*DET*) is the shorter the diagonal lines in the RP, the less predicable the process. *DET* measures the percentage of points in the RP that exist on diagonal lines to estimate predictability or repetitions of areas cross referenced against other epochs. The notation $P(l)$ refers to the histogram gained from the RP that only includes diagonal lines of length l. The average diagonal line length L is a measure that relates to the analytic function of DET. However, L conveys the average amount of time trajectories are within the ε threshold. This is then the average of the prediction time of the system.

$$DET = \sum_{l=l_{min}}^{T} lP(l) \Bigg/ \sum_{l=1}^{T} lP(l) \tag{3.3}$$

$$L = \sum_{l=l_{min}}^{T} lP(l) \Bigg/ \sum_{l=l_{min}}^{T} P(l) \tag{3.4}$$

The the longest diagonal line in P(l), not including the *LOI*, is called the L_{max} its length is given by:

$$L_{max} = max((L_i)_{i=1}^{T}) \tag{3.5}$$

An important measure is the Divergence (*DIV*) and is simply the inverse of the L_{max}.

The *DIV* is proportional to the largest lyapunov exponent [Eckmann, Kamphorst and Ruelle, 1995]. An exponent used in dynamical systems analysis to characterize the average rate at which trajectories in phase space converge or diverge. Shorter diagonal lines in this context relate to how fast trajectories diverge.

$$DIV = 1/L_{max} \tag{3.6}$$

Finally, $RATIO$ is a measure that can show phase transitions in the systems. The average length of diagonal is divided by the density of points over all, yielding a density of diagonal lines. A low ratio will capture a nonstationary system with many single points that signify the occurrence of fluctuations. When proximal to diagonals, single points can mean the onset of a phase transition.

$$RATIO = DET \Big/ RR \tag{3.7}$$

Similar to DET, the Laminarity (LAM) measures the percentage of points of at least v_{min} in length that are organized in vertical lines. This refers to relative static moments recurring at different times that exist in the intermittency between bursts.

$$LAM = \sum_{v=v_{min}}^{T} vP(v) \Big/ \sum_{v=1}^{T} vP(v) \tag{3.8}$$

Simliar to L the Trapping Time (TT) returns the average amount of time the measured output of the system is trapped in a laminar or relatively unchanging state with respect to the threshold, ε.

$$TT = \sum_{v=v_{min}}^{T} vP(v) \Big/ \sum_{v=v_{min}}^{T} P(v) \tag{3.9}$$

RQA will be used to here to uncover important structural components of a COS that lead

to musically relevant nonlinear phenomena. Analyzed here via RQA will be the dynamics of the low frequency phasors of the COSs. These phase traces directly correspond to the nonlinear frequency envelopes. It is convenient to use these envelopes because of perceptual salience as well as the low frequency range of the phasors. These frequencies between 0.01 and 10 Hz allow for a low sampling rate, set here at 100 Hz, preserving much of the structure. Long plots on the order of minutes can be generated at low computational cost as a result.

3.4 Describing Chaotic Itinerancy

The RP and RQA can be used to evaluate a range of properties of a given dynamical regime, including recurrence, stationarity, phase transition, convergence flow and divergent flow. Considering the statistical weight of properties from RQA in conjunction with the temporal or sequential organization of properties shown by an RP enriches the statistics and lends to theoretical frameworks. One such framework that fits the observations of the COS is known as chaotic itinerancy (CI) [Kaneko, 1990].

CI generally describes the transitions in a state-space of any dimension. The states are a kind of attractor, described as a quasi-attractor. A quasi-attractor differs from Milnor's concept of an attractor [Milnor, 1985], in that it is a conglomeration of both convergent and divergent flows that do not allow complete convergence to the attractor. The convergent flows attract and absorb being causally linked to the appearance of order and periodicity in phase space. Divergent flows repel and disperse phase increments generating chaotic and disordered periodicity. The mixture of flows destabilize leaving a ruin and trajectories escape creating succsessive transitory phenomena to other quasi-attractors.

Itinerancy describes transitions among quasi-attractors, where these quasi-attractors form a landscape in phase space. The transitions are a closed-loop trajectory through the landscape. The trajectory through a series of quasi-attractors is thought of as a sequence. With each transition

there is an interval of time between the departure and arrival. In CI, this interval of time is a descent into chaos and dispersion which functions as search in the state space. The departure from quasi-attractors results from its destabilization, leaving a ruin in it original locality. This ruin or attractor ruin [Tsuda and Umemura, 2003], maintains its location and a level of influence in phase space. It can reform or deform again based on the dynamics of surrounding flows, most times with a morphological alteration. In CI, the dynamics surrounding the edges of quasi-attractors are stationary flows [Tsuda and Umemura, 2003]. This neighborhood of stationarity can be seen in an RP by laminar organizations on the horizon of quasi-attractors. Quasi-attractors typically take the form of squares with differing textures sequenced on the main diagonal of the RP.

Some of these laminar organizations are continuous showing largely unbroken vertical and horizontal lines at horizons. While other laminar areas are discontinuous or intermittent, showing broken vertical and horizontal line organization. Here the flows fluctuate rapidly between stationarity and non-stationarity. The laminarity shows segments of slowly changing timeseries and when located on a quasi-attractor horizon bolsters processes of absorption. It is associated with how effective an attractor can trap a particle. Intermittency at horizons allows particles to escape at gaps in stationarity and return to chaotic search.

Certain kinds of noise can characterize the sequence of transitory phenomena. White noise is the uniform distribution. Brown noise or a constrained random walk produces a ponderous, resting and wandering motion. Black noise characterizes the predominance of rare states in a sequence and has been associated from neurological data with the production of intentional actions [Freeman and Zhai, 2009]. Rare, in this case doesn't refer to the generative capacity of a system, rather it refers to how often the state occurs (when coupled to the environment: a state of affairs). So these potential states could be just as common considering the structure and what it can do, but uncommon to appear during measurement of its output. Also important here is that transitory phenomena in dynamical systems are not merely random. These phenomena can statistically resemble stochastic processes, but have deterministic closed-loop trajectories rather

than weighted-random trajectories through state-space.

CI has been applied to areas of neuroscience as a general framework to describe many neurological processes. Orderly itineracy has been shown to reflect intentional states and may also reflect internal representations of experience [Freeman, 2006][Freeman and Zhai, 2009]. The spontaneous activity of the default mode network exhibits closed-loop trajectories [Mason, Norton, Van Horn, Wegner and Grafton, 2007]. Mental idling is characterized by dynamically transitioning mental states that might reflect sensory expectations [Kenet, Bibitchkov, Tsodyks, Grinvald and Arieli, 2003].

Focusing here on the research regarding the neural dynamics of intentionally, [Freeman 2009] disputes the claim by [Elul, 1972] that the background activity of the brain is essentially random noise. For Elul, noise distorts the sinusoidal periodicity of the foreground cortical signal and as a result should be extracted for a proper interpretation of the signal. For Freeman, dynamic modulation of the foreground signal in the cortex beyond its stable set point depends on excitatory activity of the background. Freeman modeled ECoG data taken invasively from rabbits and one person who had the implant for neurosurgical preparation. ECoG is a film attached directly to the skin through an opening in the skull that can deliver and record electrical activity. Afferent pulses were administered and an impulse response was recorded as a power density spectrum during resting (default mode states) and also active (intentional states). Removing the initial transient, the background activity is observed in the foreground are dynamic modifications of the power spectrum slope. The modulations of slope if extracted by comparing with an idealized $1/f^n, n = 2, ..., 4$ distribution, correlate to the distributions of CI in the background activity known as dark energy. In resting the states the resulting slope of activity, conformed to disorderly brown noise distributions and in active states the slope was slightly less than -2, conforming to a black noise distribution. Both distributions are forms of orderly CI, where the black noise is the more orderly of the two.

Dark energy is discussed by [Raichle, 2010] to be related to the activity of the default

mode network (DMN). The impulse response dynamics were then modeled by convolving kernel composed of a sum of two exponential functions with the pulses of a poisson distribution and summing. The dynamics of the cortex in the foreground are typically thought to be the product of interaction between excitatory and inhibitory neurons. Here the assertion is that DMN generates pulse trains during intentional states. The excitatory action of the DMN inhibits and entrains the foreground via the refractory periods of the pulse train. The pulse trains can be modeled by the stochastic means presented, but in reality are deterministic dynamics with a distribution of refractory periods similar to black noise. The DMN is related to imagination and rumination without external stimulus [Mason, Norton, Van Horn, Wegner, Grafton and Macrae, 2007], but plays a role in modulating foreground activity during intentional action. Importantly, it may relate to the internal experience of intentional action, as mental imagery, hypothesized as a cinematographic process [Freeman, 2006].

A focus on engineering systems to promote laminarity could generate kinds of orderly CI sequences perceived as intentional and active, in addition to drifting sequences perceived as imaginative and resting. The dark energy of the DMN is a proto-intentional energy that produces intention-related transitory phenomena in the foreground state-space. Music in the abstract could be the unnamed intentional energy, where states don't carry semantic or pragmatic meaning, but rather are the ruins of these things.

Chapter 4

Analysis of Systems

We now move into the data analysis of each COS presented in chapter 2. Each COS will be presented with two sections of analysis: (1) a more qualitative description of regime dynamics from phase-plots and (2) a more quantitative description of regime dynamics from RPs and RQA.

4.1 3-COS

The volume of a point in state space for the three oscillator system is defined as the product of three lines, which is a cube. Each point is indexed by a parameter setting containing four values, as three intrinsic frequencies and one coupling strength. All the parameter settings can be considered to exist as a point in a four-dimensional cube. We will look at a few points in the state space, given by the parameters, as three dimensional cubes containing phase-traces over short durations.

These points in state-space will be shown in two different representations. Each representation is based on the output of $\theta_i[t+1]$. One representation is a three-dimensional curve in the volume of cube and the other is the set of phase magnitudes plotted over time. Examples are selected to demonstrate salient moments that the system produces via dynamical procedures. Points close in state space tend to sound similar. Moving through the state space with a controller,

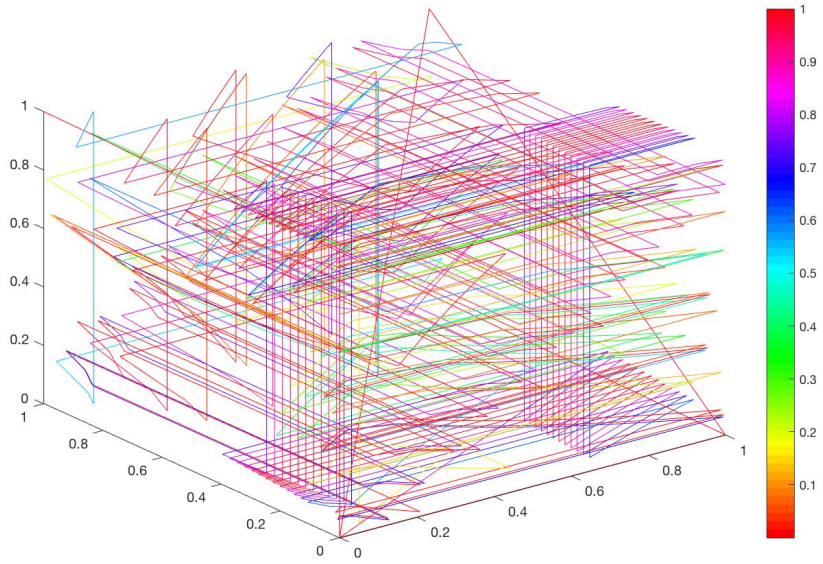

Figure 4.1: A phase plot of the three oscillator system. The parameters are $\omega_1 = 7.2$, $\omega_2 = 2$, $\omega_3 = 3.2$, $\lambda = 1.3$ and the duration is 10 seconds. The color mapping and color bar shows the time progression.

has the intuitive feel of moving across the frequency continuum of an acoustic musical instrument. That being said, each parameter setting tends to generate activity that revolves around a central tendency in the 3-COS, at times there is a phase transitions of minimal order.

It is common to hear sequences emerge that sound similar to whistling in terms of timbre and frequency envelopes. The whistling has melodic contour and vibrato. Variation is constant. It is subtle variation around recurring motifs. The perception of phrases is also perhaps due to recurring accelerandos, as well as, the presence of less audible gaps of sound, in irregular, yet appropriate intervals, surrounding the fragments of the melodic sounds. These gaps seem to intercede and fragment the melodic tendency from a given set of parameters, constantly reframing it. Of importance, there are also audibly distinct moments of self-organization where the three oscillators will entrain in an ascending or descending series of isochronous pulses.

Correspondingly, figures 4.1 and 4.2 show a point in phase space defined as $\omega_1 = 7.2$, $\omega_2 = 2$, $\omega_3 = 3.2$, $\lambda = 1.3$. Figure 4.1 shows the volume of the point and leads to insights about

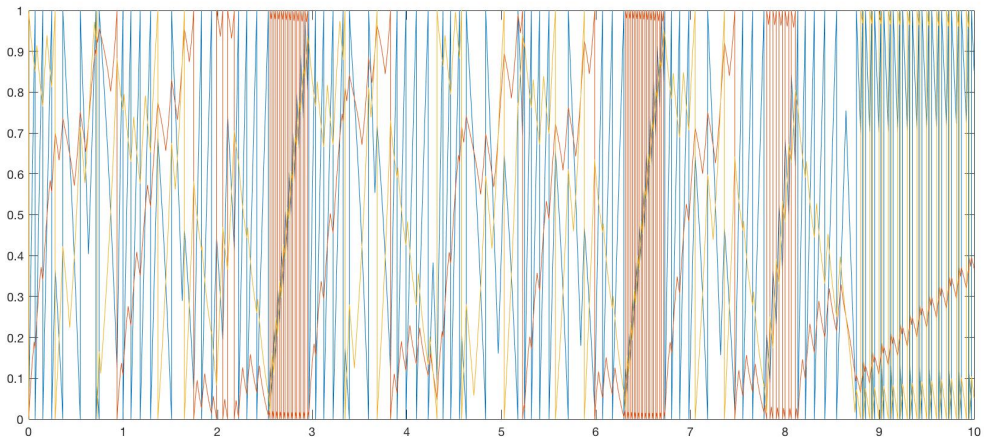

Figure 4.2: A phase plot of the three oscillator system. The parameters are $\omega_1 = 7.2$, $\omega_2 = 2$, $\omega_3 = 3.2$, $\lambda = 1.3$ and the duration is 10 seconds.

the dimensionality of the curve. The figure depicts every sample of phase-position over a duration of 10 seconds. Viewing the horizontal axis from positions 0.0 to approximately 0.5 there are a series of vertical planes in succession orthogonal to the vertical axis and spanning the depth axis. This series represents instances of 2-dimensional motion within the cube. As the phase value increases on horizontal axis, so does the frequency of each oscillator. It is significant that the planes are evenly spaced, leading to sounds that are evenly spaced in frequency. If this feature of the phase plot is heard in real time it is the self-organization behavior eluded to earlier, where the system of three oscillators entrain into a series of ascending or descending isochronous pulses. Viewing the plot in 4.2, this features occurs approximately at 2.5, 6.3, 7.8 and 8.8 seconds. The planes seen in 4.1 are consecutive in time for a few iterations. While one oscillator zig-zags directly between 0 and 1, the other two organize into a staircase that sounds like an ascending row of equally spaced frequencies. The second occurrence of this feature is a near copy of the first. In the two occurrences that follow, the slope of the staircase organization decreases. The first is similar to the preceding two in terms of the role of each oscillator. In the last one depicted, the two oscillators that formed the staircase, now both zig-zag between 0. and 1., while the remaining oscillator forms a frequency staircase.

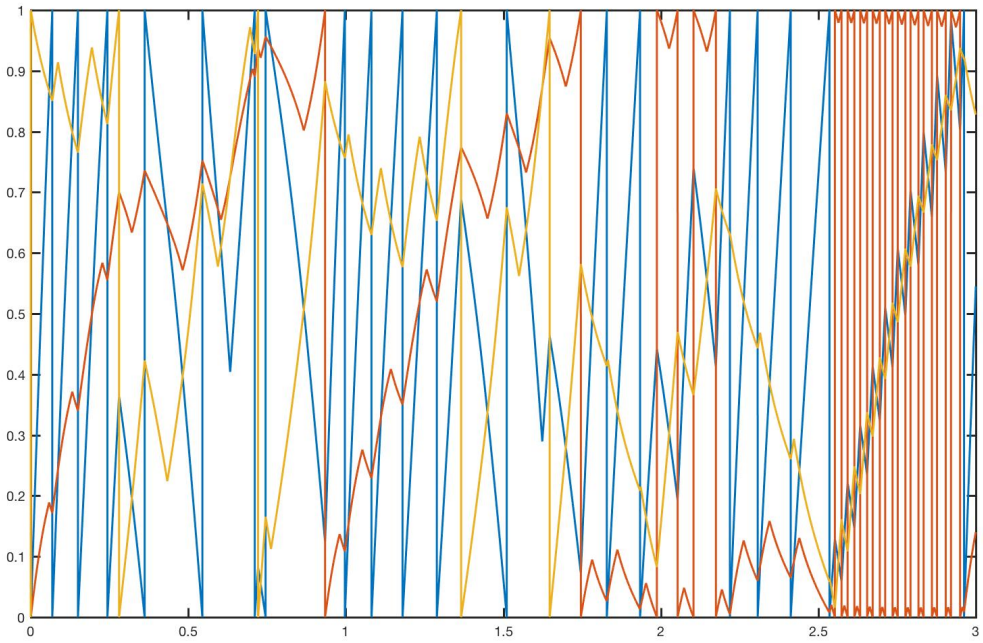

Figure 4.3: A phase plot of the three oscillator system. The parameters are $\omega_1 = 7.2$, $\omega_2 = 2$, $\omega_3 = 3.2$, $\lambda = 1.3$ and the duration is 3 seconds.

At other times seen in 4.1, the curve moves in a way that is less similar to itself as either consecutive moments or moments proximal in position. The trace moves in a more varied way in the 3-dimensional space. These areas of the plot correspond to the melodic whistling tones described. The shapes appear at many times as parallel two-dimension planes with changing areas and distances between planes. If grouped together visually these figure are also skewed in the space. Figure 4.3 shows the same parameter setting being discussed over the first 3 seconds. Of importance, each trace of each phase-position can be said to have a series of local peaks and valleys. The descent or ascent of one of these traces always intersects with the local peak or valley of at least one other trace. So when a trace changes direction it is at many times in the same position as another signal. In the frequency staircase occurrence, near the end of the plot, the entrainment of intersections becomes regularly spaced. What could be said to happen is is the group of signals becomes entrained via intersections when there is a sufficiently high coupling

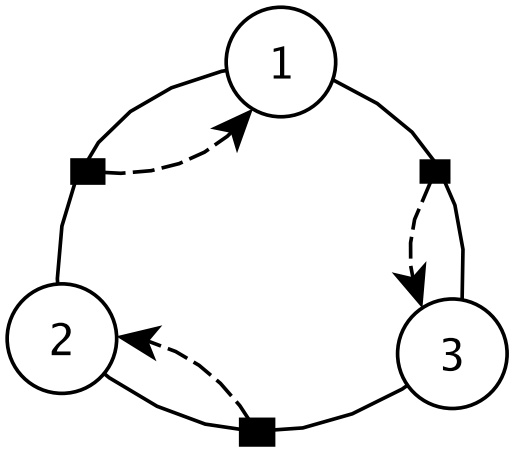

Figure 4.4: Self-affecting subsets within a three oscillator system. The numbered circles are each oscillator. The solid lines between adjacent circles link indicate a subset, as $\{1, 2\}$, $\{1, 3\}$ and $\{2, 3\}$. The black box indicates that the relation between the two in the subset affects the oscillator pointed to with the hashed line. In this case, the coupling is to an oscillator inside of the subset.

coefficient, λ. The set of coupling terms allow for changes in direction and the space the phase-positions are moving in has a discontinuity between 1 and 0. If one the phase-positions begins to oscillate rapidly over the discontinuity due to its dependency on the other phase-positions, this compresses the timescale of the intersections, regularizing those into the rapid succession depicted.

The dependencies among phasors is a factor when considering the causality of the kinds of sonic events just discussed. The way the coupling terms cross link the phase progression of the phasors leads to second-order effects. Figure 4.4 depicts a three oscillator system where subsystems are not cross linked to modify other subsystems. For instance, in the subsystem of oscillators 1 and 3, the distance between the two modifies oscillator 3, not oscillator 2. With this organization the activity becomes vacant, even though the same number of linkages exist. Figure 4.4 shows a 3-dimensional plot of the same point in state-space discussed, that being $\omega_1 = 7.2$, $\omega_2 = 2$, $\omega_3 = 3.2$, $\lambda = 1.3$. The curve becomes a flat 2-dimension plane and the sound is an

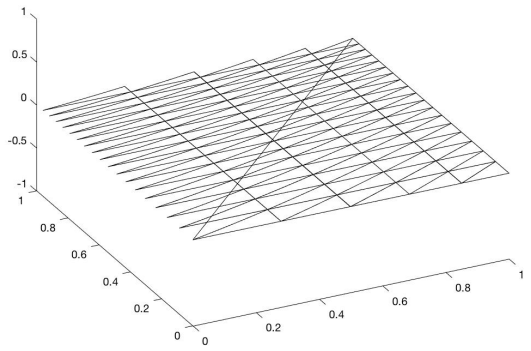

Figure 4.5: A phase plot of self-affecting subsystems within a three oscillator system. The parameters are $\omega_1 = 7.2$, $\omega_2 = 2$, $\omega_3 = 3.2$, $\lambda = 1.3$ and the duration is 10 seconds.

infinitely repeating pattern of pulses.

4.1.1 Quantitative Description

The three oscillator system contains both positive linear and negative inverse coupling terms, as L and $-1/L$. These terms alternate based on the ordering of a subsystem of phasors which in turn affect the velocity of a particular oscillator outside the system. The mapping is two oscillators to one oscillator via the dynamics of a changing description containing information about order and and distance. When the coupling strength is reduced to zero in this arrangement, the coupling terms reduce to values of 1 and -1. For oscillators to sound as independent, or rather as uncoupled sine tones, all the terms need to reduce to 1, when the coupling strength is 0.

In the first part of this section, the impact of different kinds of coupling terms on the output will be assessed using RQA. This will demonstrate the role of inverse and negative terms.

When the terms of this system are changed to L and 1/L and the coupling strength is $\lambda = 0$. The recurrence plot 4.6 shows stable periodic motion given by evenly spaced diagonal lines parallel to the *LOI*. The picture will be the same for any initial phase offset of oscillators. Since the oscillators are uncoupled there is no sensitivity to initial conditions.

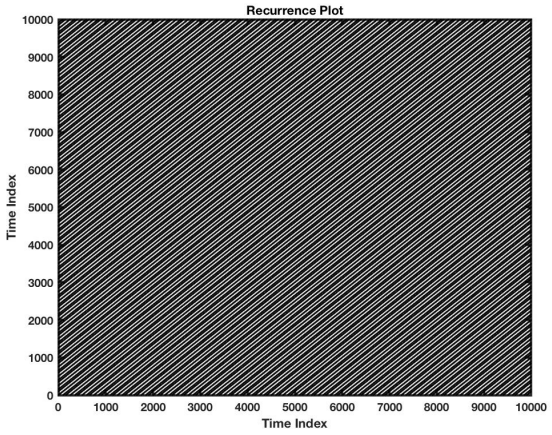

Figure 4.6: A recurrence plot of the three oscillator system. The parameters are $\omega_1 = 7.2$, $\omega_2 = 2$, $\omega_3 = 3.2$, $\lambda = 0.0$ and the duration is 100 seconds. The terms of this system are changed to L and 1/L.

This is not the case given $\lambda = 0$ and coupling terms equally distributed between L and -1/L. The reduction of coupling terms to 1 and -1 preserves a degree of coupling and the initial conditions will distort the recurrence plot. The effect is easiest to see on a shorter time scale depicted in figure 4.7 showing 10 seconds of activity, with phase offsets are 0.4, 0.1, and 0 respectively. Figure 4.8 shows the case with no offset.

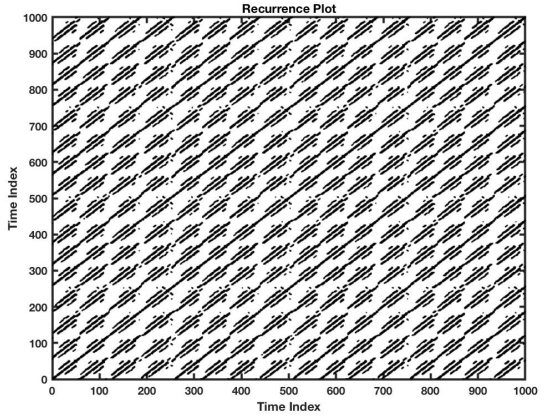

Figure 4.7: A recurrence plot of the Three Oscillator System. The parameters are $\omega_1 = 7.2$, $\omega_2 = 2$, $\omega_3 = 3.2$, $\lambda = 0.0$ and the duration is 10 seconds. The terms of this system are changed to L and -1/L. Phase offsets are 0.4, 0.1, and 0.

When the coupling strength is increased under an equal distribution of L and 1/L. The

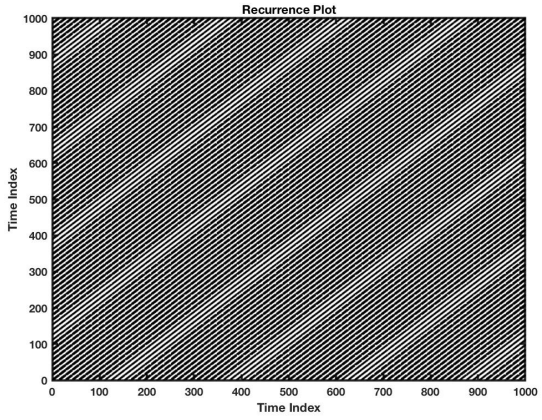

Figure 4.8: A recurrence plot of the three oscillator system. The parameters are $\omega_1 = 7.2$, $\omega_2 = 2$, $\omega_3 = 3.2$, $\lambda = 0.0$ and the duration is 10 seconds. The terms of this system are changed to L and -1/L. Phase offsets are nonexistent at 0., 0., and 0.

resulting generation gives a quasi-periodic repeating pattern. This pattern is seen by the uneven spacing between long diagonals. The long diagonals are interposed with short diagonals showing stable fluctuations of process that contribute to a limiting behavior.

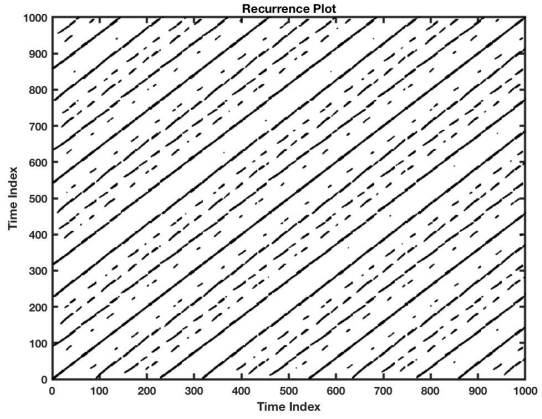

Figure 4.9: A recurrence plot of the Three Oscillator System. The parameters are $\omega_1 = 7.2$, $\omega_2 = 2$, $\omega_3 = 3.2$, $\lambda = 1.03$ and the duration is 10 seconds. The terms of this system are changed to L and 1/L. Phase offsets are nonexistent at 0., 0., and 0.

When the coupling strength is increased under an equal distribution of L and -L terms. The resulting generated RP also shows a quasi-periodic repeating pattern. Again, the long diagonals are interposed with short diagonals showing stable fluctuations of process that contribute to a

limiting behavior.

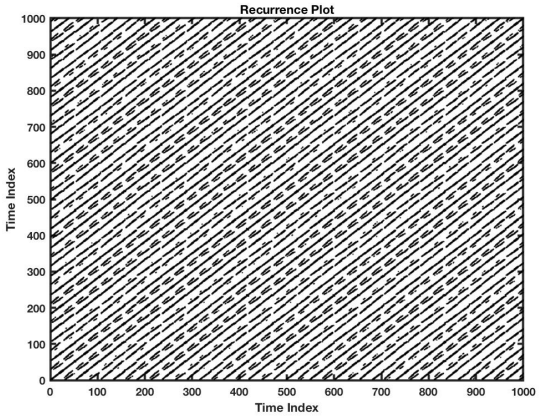

Figure 4.10: A recurrence plot of the three oscillator system. The parameters are $\omega_1 = 7.2$, $\omega_2 = 2$, $\omega_3 = 3.2$, $\lambda = 1.3$ and the duration is 10 seconds. The terms of this system are changed to L and -L. Phase offsets are nonexistent at 0., 0., and 0.

Both the equal distribution of L and -L and the equal distribution of L and 1/L give similar visual results of quasi-periodic oscillation. Notably the laminarity (*LAM*) and trapping time (TT) are both insignificant giving TT of only about 0.006 seconds, meaning stable limit cycles before and without the onset of chaotic intinerancy (CI). Also of note, the L and -L have a DET of 36 percent while the L and $1/L$ has a DET of 57 percent. That being said, the use of negatives alone contributed more to the uncertainty of the system than the use of logarithms. Correspondingly the case with $-L$ has a divergence (DIV) of 1/149 while the case of 1/L is 1/79. This would suggest that the use of a logarithm also produces trajectories that diverge faster comparatively.

Significant laminarity has been seen to occur for certain parameter settings in the 3-COS. A few examples will be demonstrated. High values for *LAM* may indicate CI. In figure 4.11 the *LAM* is 31.14 percent and the TT is brief giving an average time of 0.14 seconds. The DIV is slow at 1/228 and the DET is 36.25 percent. The pattern formation of attractor states can be viewed across the main diagonal, in the form of rectangular structures. In this figure there are two attractor states that occur over the 200 second duration. This indicates the beginning of an transition from State A to state B. Viewing a phase plot for 1000 seconds, state A returns at 600

seconds, then back to state B at 800 seconds. This regime seems to consist of an alternation between two general states. State A sounds like a series of decelerating pulses with a condensed frequency range. While state B maintains this rhythmic structure, the frequencies separate and one of the oscillators moves into a high frequency register with gliding envelopes that at times disrupt the established pattern of the limit cycle. The laminarity in the plot existing in the off diagonal square is the cross-recurrence of attractors A and B. If stationarity motion existed in the horizon neighborhood of the attractors, then orderly CI could be implicated. However, since it is only a laminar cross-recurrence, there is only a correlated stationarity between attractors, speaking to informational similarity, not CI.

Two attractors are informationally similar but not necessarily sonically similar. In this unique case seen in figure 4.11, an auditory illusion emerges, known as a galloping illusion. The narrow-band pulses in A, give way to narrow-band pulses interposed with a high-frequency gliding envelope, which interrupts the perception of metrical structure of a galloping rhythm. In the galloping illusion, three pulsed durations are played in a loop, such as, eighth note, eighth note, quarter note. The middle tone is gradually increased in frequency. Once the note reaches a distinct high frequency relative to the other two pulses, it becomes difficult to perceive the metric location of the high tone. This is explained by a theory of separate perceptual streams and hierarchical gestalts in the auditory cortex. The frequency perception supersedes metrical perception and the interference is irreconcilable leading to an illusion [Deutsch, 1999].

Patterns without laminarity produce interesting musical results in the case of the 3-oscillator system. The regime with parameters $\omega_1 = 7.2$, $\omega_2 = 2$, $\omega_3 = 3.2$, $\lambda = 1.3$, described in detail in the preceding section is one of these examples. A 20 second recurrence plot will be shown in figure 4.12. The shorter duration is selected in this case because it depicts much of what happens in the long-term plots, and the micro-scale of the graphical structure is enlarged.

Graphical differences can be seen in the rectangular structures along the diagonal, although the musical difference seems minimal in terms the level of variation from state A to state B.

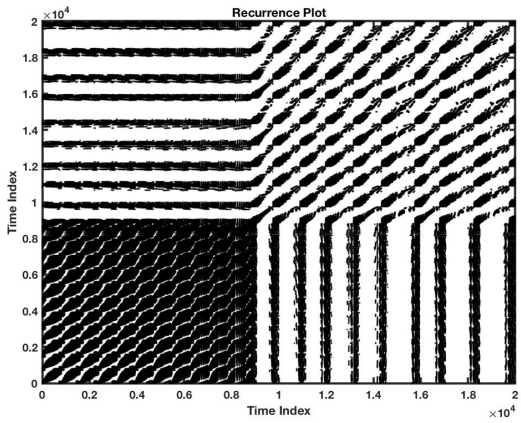

Figure 4.11: A recurrence plot of the three oscillator system. The parameters are $\omega_1 = 0.2$, $\omega_2 = 3.44$, $\omega_3 = 1.3$, $\lambda = 1.3$ and the duration is 200 seconds. The terms of this system to -1/L and L.

The dark black diagonal bar appearing in the center of the plot corresponds to the sequences of high frequency entrainment among phasors discussed earlier, when one phasor alternates rapidly between 0. and 1. and the two other phasors entrain to that wavelength. Wide white areas or extended white bars protrude in a cross from the black diagonal bar. The wide white areas contain bowed line structures. Shorter bowed line structures also appear in groupings in the bottom right corner. The vertical and horizontal white bars show non-stationarity in the process. The bowed line structures within the extended white bars indicate similar structures within the process that have different velocity. Changes in velocity are a possible indication of changes in the future dynamics. There is a minimal change in the rectangle (called state B) succeeding the high velocity black bar. The minimal change in dynamics may be related to low convergence. The lack of convergence in the states is characterized by the relatively high divergence, a *DIV* of 1/79 corresponding to the longest diagonal line. The thick black line structures overall exhibit drift from the LOI, related to high divergence and non-stationarity. Single isolated points and small clusters of points near diagonals and bowed line structures also indicate fluctuations in the process.

Figure 4.13 shows additional example of a regime given from parameter $\omega_1 = 1.47$,

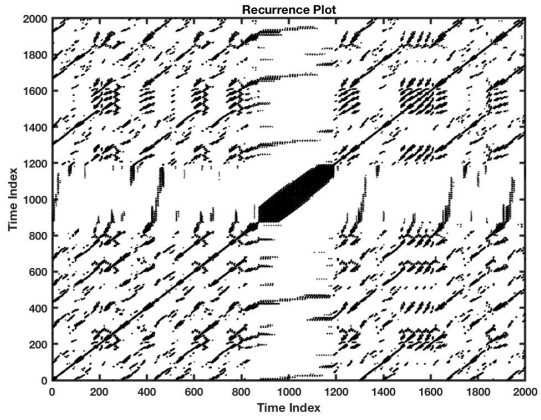

Figure 4.12: A recurrence plot of the three oscillator system. The parameters are $\omega_1 = 7.2$, $\omega_2 = 2$, $\omega_3 = 3.2$, $\lambda = 1.3$ and the duration is 20 seconds. The terms of this system to -1/L and L.

$\omega_2 = 5$, $\omega_3 = 5.7$, $\lambda = 1.3$, that has no laminarity and high divergence. The divergence here is DIV = 1/89. The plot is similar to the statements made about Figure 4.12. Instead of a dense black bar, the high-velocity entrainment feature appears at time index of 500, as a distributed square with a regular tessellation of black and white patches. Extended white bars in the form of a cross protrude from the feature, indicating non-stationarity. When this process is run for a longer duration of 60 seconds, the longest diagonal is still 89. No longer diagonals appear at later time indices indicating dynamics that have changes in divergence or convergence at different epochs. However, given the same set of ω_i and a reduction of the coupling strength to $\lambda = 1.15$ there are changes in the *DIV* measure at difference durations of measurement, meaning longer diagonals at later epochs of the process. With a 30 second window and $\lambda = 1.15$ the $DIV = 1/63$. As seen in Figure 4.14 at a time index of about 3000 (corresponding to 30 seconds of real time) a highly dense black square appears, corresponding to a relatively high-velocity entrainment event and protruding white bars. During this black square a new L_{max} occurs changing the divergence to $DIV = 1/111$. The large square (from diagonal time index 4000 to 6000) succeeding the changes in dynamics sound like a mixed state attractor, where the dynamics from 0 to 30 seconds alternate with moments of high-velocity entrainment every 2 to 3 seconds. After 60 seconds until 160

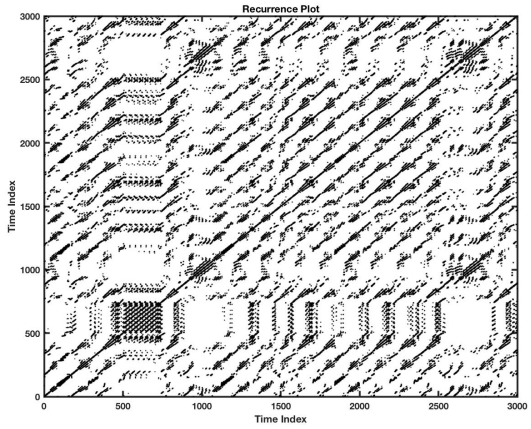

Figure 4.13: A recurrence plot of the three oscillator system. The parameters are $\omega_1 = 1.47$, $\omega_2 = 5$, $\omega_3 = 5.7$, $\lambda = 1.3$ and the duration is 30 seconds. The terms of this system to -1/L and L.

second the divergence remains the same. The established pattern from 0 to 60 compresses to a much shorter timescale recurring at different intervals of duration as seen in Figure 4.15. A final observation is that all the RQA stats from the plots discussed (with parameters $\omega_1 = 1.47$, $\omega_2 = 5$, $\omega_3 = 5.7$), involving variations of the duration and coupling strength maintain a *RR* of about 5 percent and a *DET* of about 30 percent. This was also found to be true for the regime discussed with $\omega_1 = 7.2$, $\omega_2 = 2$, $\omega_3 = 3.2$, $\lambda = 1.3$. This is possibly a region of statistical characterization in the zero laminarity cases of the 3-COS, that leads to sound that is good for use in experimental electronic music as a foreground event with more pronounced variation. The high laminarity regimes in the 3-COS shown have repetitive structures given by the attractor dynamics that have minimal variation and typically assume a functional role in music in the background. Of course, this distinction between the appropriate function for foregrounds and backgrounds, and even the general distinction of having such categories are unstable notions and at times irrelevant in the arts, due to the dynamics of aesthetic processes.

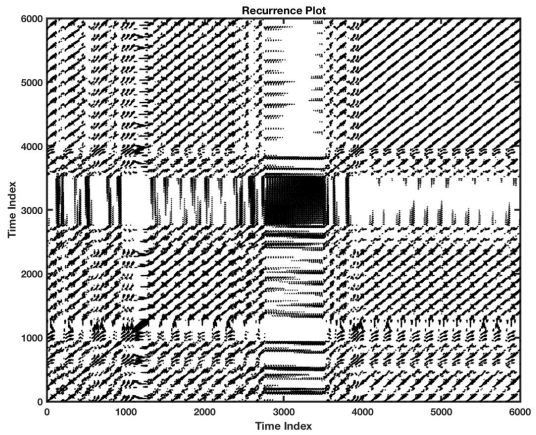

Figure 4.14: A recurrence plot of the three oscillator system. The parameters are $\omega_1 = 1.47$, $\omega_2 = 5$, $\omega_3 = 5.7$, $\lambda = 1.15$ and the duration is 60 seconds. The terms of this system to -1/L and L.

4.2 3x2-COS

The three by two oscillator system has a similar sonic characteristic to the three oscillator system. The three oscillator system tended to revolve around a central tendency related to the initial parameter settings. The central tendency that emerges with this system is longer and more nuanced. It has structure, yet is at first less recognizable in terms of a perceived frequency shape. Ascending and descending melodic lines are presenting, accelerating or decelerating in rhythm. Although, these lines have trajectories that are interrupted and reformed into new trajectories. The model gives the impression of well formed linear trajectories that sound as if being suppressed under the coupling forces of other oscillators. Where the 3-COS gave the impression of variation over time, here the variation is music more distinction. Over longer intervals of time, the rhythm of the sound slows for sections and then increases. The grouping of pulses and frequency envelopes find all sorts of permutation, leading to the perception of a long-term musical structure with sections. Overall there is less distinct repetition and the sense of listening to a directed flux. As seen in 4.16 the color mapping of the phase-position can be seen to have in general moments of high-speed entrainment that interrupt a fairly regular pattern for the

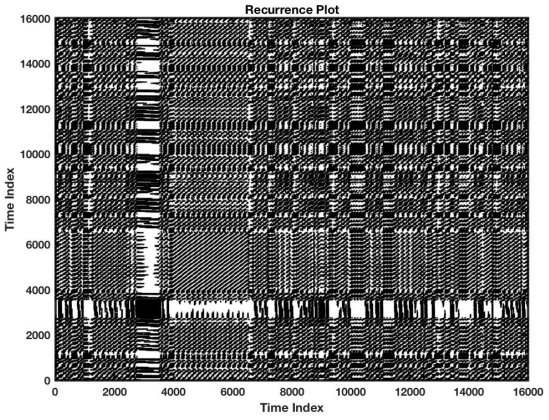

Figure 4.15: A recurrence plot of the Three Oscillator System. The parameters are $\omega_1 = 1.47$, $\omega_2 = 5$, $\omega_3 = 5.7$, $\lambda = 1.15$ and the duration is 160 seconds. The terms of this system to -1/L and L.

phase regime. This phase regime is what has been referred to as the central tendency. Viewing the plot 4.17 there are sections of high-speed entrainment. Although here, the staircase formations of each phase are seen as distinct, all moving in different orientations. This means the hyperplanes have a higher volume relative to the other system.

When high-frequency entrainment occurs in the 3x2-COS, the event is less centrally directed than the similar event observed in the 3-COS. It is distributed significantly in at least four independent directs. At other times, when the regime is not catalyzed as a hyperplane, the color coding demonstrates no distinct motif. Rather, a drifting pattern with sections of rhythmic expansion and compression over time. The values of ω_i for figure 4.17 are smaller, reduced at least 50 percent. This has been observed as a property of these systems, that with more oscillators the average speed of the frequency envelopes increase. Possibly due to synergistic effects of perturbation between more moving bodies.

4.2.1 Quantitative Description

In the 3x2-COS the recurrence plots demonstrate disrupted drift. The drift is characterized by the fading to the upper left and bottom right corners. In addition, distinct white bands

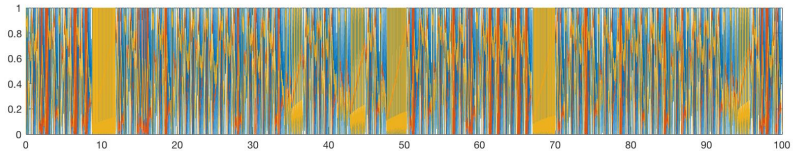

Figure 4.16: A phase plot of the three oscillator system. The parameters are $\omega_1 = 7.2$, $\omega_2 = 2$, $\omega_3 = 3.2$, $\lambda = 1.3$ and the duration is 100 seconds. The color mapping is the phase of each oscillator, meant to give a sense of long-term structure.

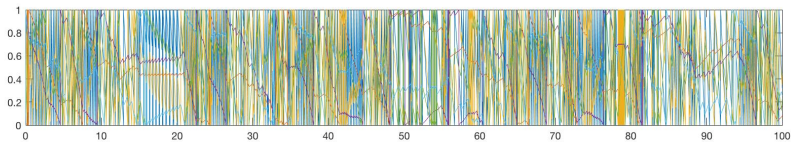

Figure 4.17: A phase plot of the three by two oscillator system. The parameters are $\omega_1 = 2.52$, $\omega_2 = 0.12$, $\omega_3 = 1.8$, $\omega_4 = 0.18$, $\omega_5 = 0.72$, $\omega_6 = 0.24$, $\lambda = 1.5$ and the duration is 100 seconds. The color mapping is the phase of each oscillator, meant to give a sense of long-term structure.

appear parallel to the LOI in regular spacing, separating black clusters (also parallel to the LOI) of different textures. Some of the plots shown have textures with a higher frequency of line structures, while others contain a preponderance of single points. Overall, this shows a deterministic process, which is already know in this case. When RQA is used for analysis of high-frequency radar signals, for instance, this is unknown. The level of statistical determinism is increased when more diagonal line structures are recorded and decreased when more single points are recorded. But since it is known that the generator is a deterministic process the high occurrence of single points reflects greater chaos in the phase space, rather than phase space given by a random generator. The spaced clusters parallel to the *LOI* also reflect an overall quasi-periodic process, the more even the spacing the more periodic and similar at different epochs. While higher laminarity than the 3-COS is present in all the examples recorded, if not concurrent with phase transition structures as a cross of thick horizontal and vertical white bars, abrupt changes between quasi-attractors are not heard. Rather it is slow drifting changes of continuous variations. Abrupt changes between quasi-attractors with strong perceptual salience (as opposed to abrupt changes with lead to meager quantitative differences in texture) are heard in the 3x3-COS, 5-COS and 6-COS.

Figure 4.18 is an example of a statistically deterministic process, where $DET = 71.7$.

The plot exhibits a deterministic drift, with bowed line structures. In some cases these lines are bowed almost to the extent of being orthogonal to the LOI. When lines become orthogonal to the LOI this indicates retrograde motion or reverse time. This property of time and motion existing in a memoryless loop would be an interesting phenomenon. Retrograde sequences are also a classic compositional strategy. But bowed line structures indicate recurrences that contain velocity changes showing a strange continuity of recurrence clusters where velocity-altered recurrences are on a continuum with retrograde motion recurrences. While DIV = 1/114 is relatively fast, the LAM = 50.7 with a TT = 0.19 seconds. The fast divergence seems to disrupt the formation of dense quasi-attraction even with 50 percent laminarity. A sparse quasi-attractor, without much influence on the dynamics is present at approximately 50 seconds, visible on the main diagonal.

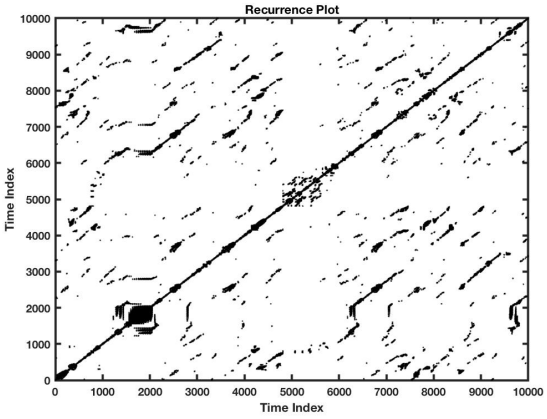

Figure 4.18: A recurrence plot of the three by two oscillator system. The parameters are $\omega_1 = 2.52$, $\omega_2 = 0.12$, $\omega_3 = 1.8$, $\omega_4 = 0.18$, $\omega_5 = 0.72$, $\omega_6 = 0.24$, $\lambda = 1.5$ and the duration is 100 seconds.

Figure 4.19 has nearly identical statistics to Figure 4.18, DET = 67, LAM = 50.6 and TT = 0.2 seconds. However, the DIV = 1/315. The recurrence pattern here shows line-rich clusters with wavy bows. The recurrences have velocity shifts and relatively even spacing showing high-order quasi-periodicity. Note the distribution of square diagonal line clusters. These correspond to convergent hyper-plane searches in the phase space: the blackened hour glass shaped structure near the beginning and the black cube near the end are high frequency entrainment events. The

sparser squares are low-frequency entrainment events. In total there are about 20 of these features in the plot. Between them are descents into chaos, characterized by a higher volume of isolated point and rapid instances of reverse time. When the parameter setting of figure4.19 is altered by making half the parameters negative (with the same absolute value) i.e. $\omega_1 = -0.88$, $\omega_2 = 1.2$, $\omega_3 = -1.95$, $\omega_4 = 0.042$, $\omega_5 = -0.5$, $\omega_6 = 1.26$, the divergence drops significantly to *DIV* = 1/98. The black square structures nearly vanish with only three appearing on the main diagonal with no other recurrences. The introduction of negative intrinsic frequencies for half the values had a significant effect on converging attractor dynamics.

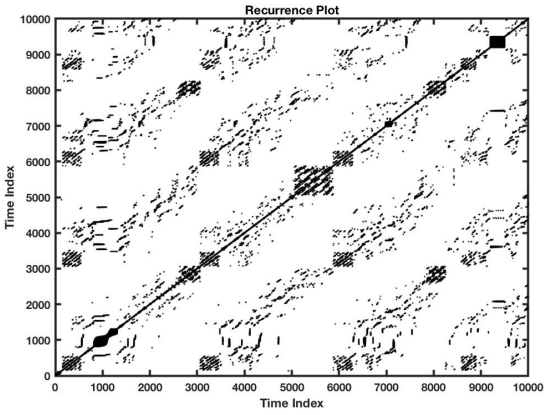

Figure 4.19: A recurrence plot of the three by two oscillator system. The parameters are $\omega_1 = 0.88$, $\omega_2 = 1.2$, $\omega_3 = 1.95$, $\omega_4 = 0.042$, $\omega_5 = 0.5$, $\omega_6 = 1.26$, $\lambda = 1.29$ and the duration is 100 seconds.

Figure 4.20 shows an instance of highly chaotic dynamics generated by the 3x2-COS. The *DET* = 33.5, the *DIV* = 1/182 and the *LAM* = 17.8. The relatively high *DIV* considering the low *DET* is owed to the rare dense events on the main diagonal between 35 and 55 seconds. This event has the features of phase transition without the realization, instead descending again into chaos. The general form of the RP is similar to what has been presented in terms of a series of bowed clusters off of the main diagonal, showing a high-order oscillation. Although, these oscillators contain short line structures and many isolated recurrence points. The significance here is the appearance of chaotic structure with unstable points embedded in a high-order periodicity.

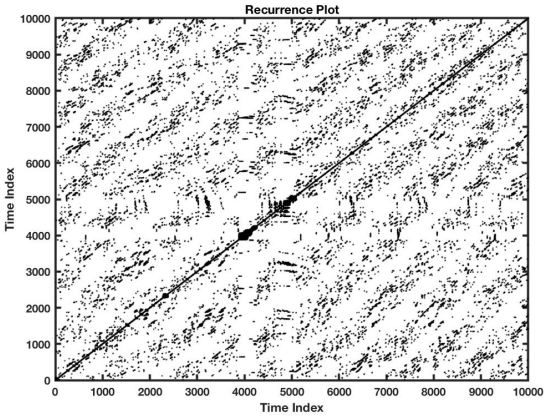

Figure 4.20: A recurrence plot of the three by two oscillator system. The parameters are $\omega_1 = 1.7$, $\omega_2 = 2.9$, $\omega_3 = 1.07$, $\omega_4 = 0.97$, $\omega_5 = 1.5$, $\omega_6 = 3.74$, $\lambda = 1.4$ and the duration is 100 seconds.

4.3 3x3-COS

The three by three oscillator system here contains two concurrent arrangements of subsystems. The first are the subsystems of overlapping pairs of oscillators, that form a node of three oscillators. Then the nodes are organized in overlapping subsystems to form the entire system of nine oscillators. Here we observe another increase in the capacity of the system for long term variation, as well as, an increase in the average speed of the frequency envelopes. Compared to the three oscillator system presented, the intrinsic frequencies, ω_i, are decreased by a factor of ten to hear a similar speed for the envelopes. All nine oscillators can be listened to at once, however it is also interesting to listen to say three selected oscillators at once. Then switch to another three; listening to all the oscillators in a node or an oscillator from each node. This gives a different view or impression of the same regime and can be used to create correlated yet abrupt variations. In another frame of reference, oscillators can be added or subtracted from the mass to create moments of density or sparsity.

Figures 4.21 showing 10 seconds and 4.22 showing 100 seconds, give a depiction of how the long term structure evolves over time. Both figures are of the same point in state-space or rather the same initial parameter setting. Viewing the shorter duration plot, each subsystem of

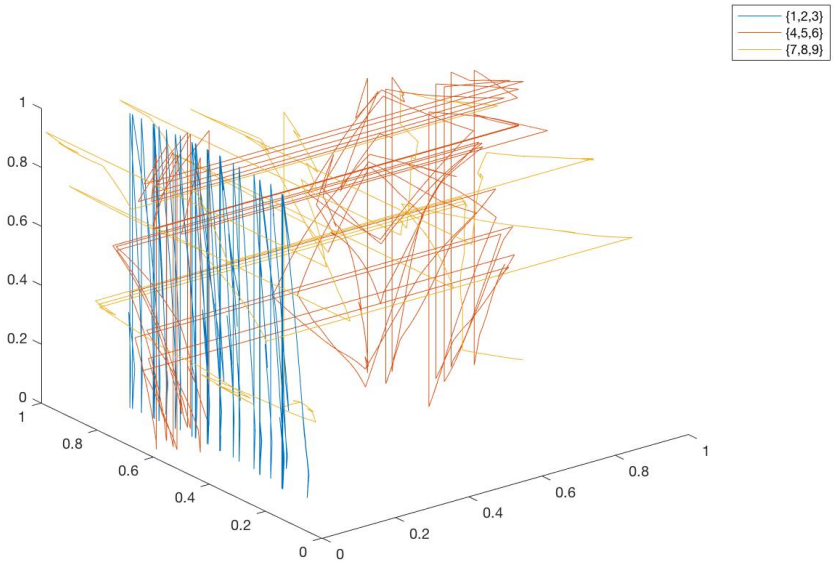

Figure 4.21: A phase plot of the three oscillator system. The parameters are $\omega_1 = 0.32$, $\omega_2 = 0.14$, $\omega_3 = 0.399$, $\omega_4 = 0.261$, $\omega_5 = 0.64$, $\omega_6 = 0.04$, $\omega_7 = 0.305$, $\omega_8 = 0.051$, $\omega_9 = 0.1233$, $\lambda = 2.0$ and the duration is 10 seconds. The color mapping shows a subsystem of 3 oscillators.

three oscillators stays confined within a small region of the phase plot. The regime present here tends to stay within a low volume region for longer, moving through the space taking more of the potential path transitions. In other words, given a limited set of paths, there are a greater number of permutations of those paths. Over longer durations these patterns within low area regions drift toward a different average position, eventually filling the entire area of the phase plot, as seen in 4.22. This is a different result than observed earlier in the simple three oscillator system, where over short durations, the regimes will generate space filling activity with an average phase-position near the center of the plot.

4.3.1 Quantitative Description

In the 3x3-COS recurrence plots start to show more abrupt transitions in the dynamics than previous systems as well as drift that is less periodic than the what was shown in the 3x2-COS. In figure 4.23 a statistically deterministic process is evident with $DET = 70.6$. The $DIV = 1/173$

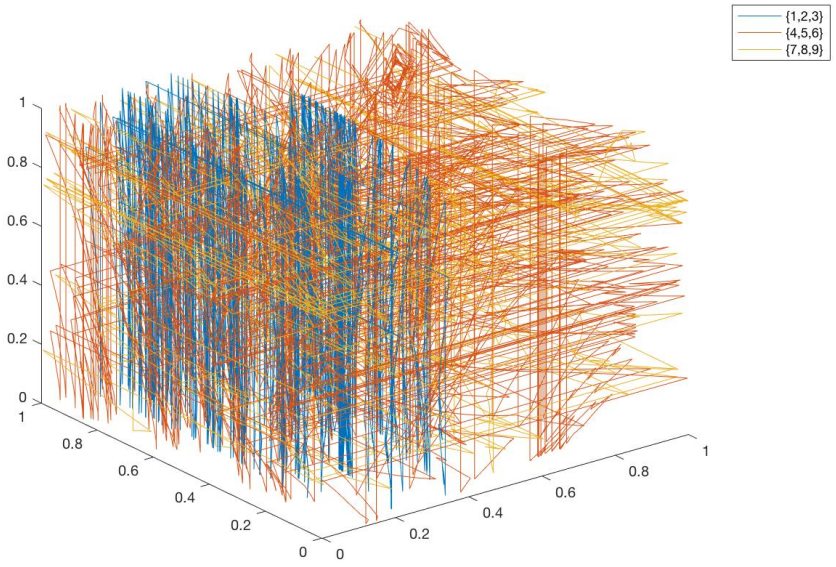

Figure 4.22: A phase plot of the three by three oscillator system. The parameters are $\omega_1 = 0.32$, $\omega_2 = 0.14$, $\omega_3 = 0.399$, $\omega_4 = 0.261$, $\omega_5 = 0.64$, $\omega_6 = 0.04$, $\omega_7 = 0.305$, $\omega_8 = 0.051$, $\omega_9 = 0.1233$, $\lambda = 2.0$ and the duration is 100 seconds. The color mapping shows a subsystem of 3 oscillators.

showing a capacity for convergence when considered in conjunction with a high laminarity rating of $LAM = 80.66$. The $TT = 0.217$ seconds. The clusters on the main diagonal appear with distinct visual differences. Call those clusters A from 0 to 30 seconds, B from 40 to 40 seconds and C from 70 to 100 seconds. Cluster B is unique in structure compared to A and C. A and C share some sparse commonalities as isolated points and vertical lines as see in the bottom right corner of the RP. Generally off diagonal areas of the RP are sparse or all white, reflecting a lack of recurrence between different epochs-here being A,B, and C. A, B and C can be viewed as quasi-attractors in the phase space. In terms of chaotic itinerancy, B, exhibits vertical line structures at its edges at 40 and 70 seconds. This is a key characteristic of chaotic itinerancy: an attractor landscape descends into chaos between quasi-attractors, while at the edge of quasi-attractors there are highly stationary flows with high laminarity. Here may be the beginning of a self-organizing capacity that imitates the perceived intentional organization of sequences of sonic events.

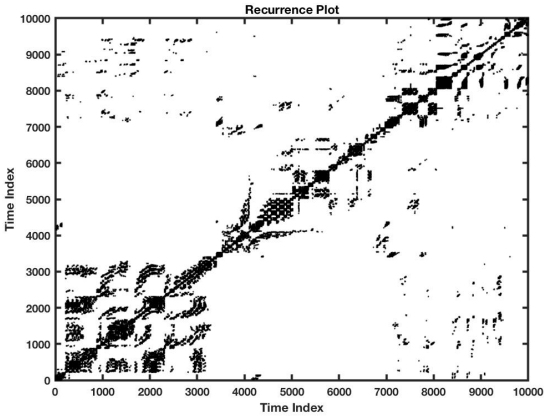

Figure 4.23: A recurrence plot of the three by three oscillator system. The parameters are $\omega_1 = 0.24$, $\omega_2 = 1.68$, $\omega_3 = 0.38$, $\omega_4 = 1.22$, $\omega_5 = 1.88$, $\omega_6 = 0.12$, $\omega_7 = 0.21$, $\omega_8 = 0.62$, $\omega_9 = 0.2466$ $\lambda = 1.3$ and the duration is 100 seconds.

4.4 4-COS

The four oscillator system is constructed differently than the three oscillator systems. While it operates on the same organizing principle of interlinked subsystems, the spatial representation situates phase-positions on a circle rather than a line. As previously stated there isn't a discontinuity in the circular spatial representation in terms of transitions in the magnitude of the phase increment. What happens is the magnitude of the δ^{μ} function is reduced to a range of 0 to 0.5, instead of 0. to 1.. The minimum distance between two points is selected to modify the coupling term. The largest discontinuity in the function then depends on the size of the phase increment over the bound of 0.5. For instance, when the phase increment has a size of 0.2 when starting from 0.49, the next δ^{μ} is 0.31. This is all to say that the phenomenon of the pulsed staircase observed (also seen as black bar formations in RPs) in the three oscillator systems does not occur in the same way in this organization. It is impossible for phase-positions to begin to oscillate over the discontinuity, so there aren't evenly spaced and direct transitions in phase-position from 0. to 1..

A similar feature is observed in the four oscillator organization. The transitions in phase-positions over 0. to 1. occur continuously at an angle significantly less than 90 degrees. The

spacing between these transitions can vary. Meaning the angle of ascent or decent will also vary. This creates a sense of rhythm to pattern pulses as inter-onsets that vary over time. The pattern will also change direction in frequency, leading to a perception of melodic contours. These contours have more complex intermittent timing than the 3-COS and tend to drift from an initially perceived central tendency over periods of time.

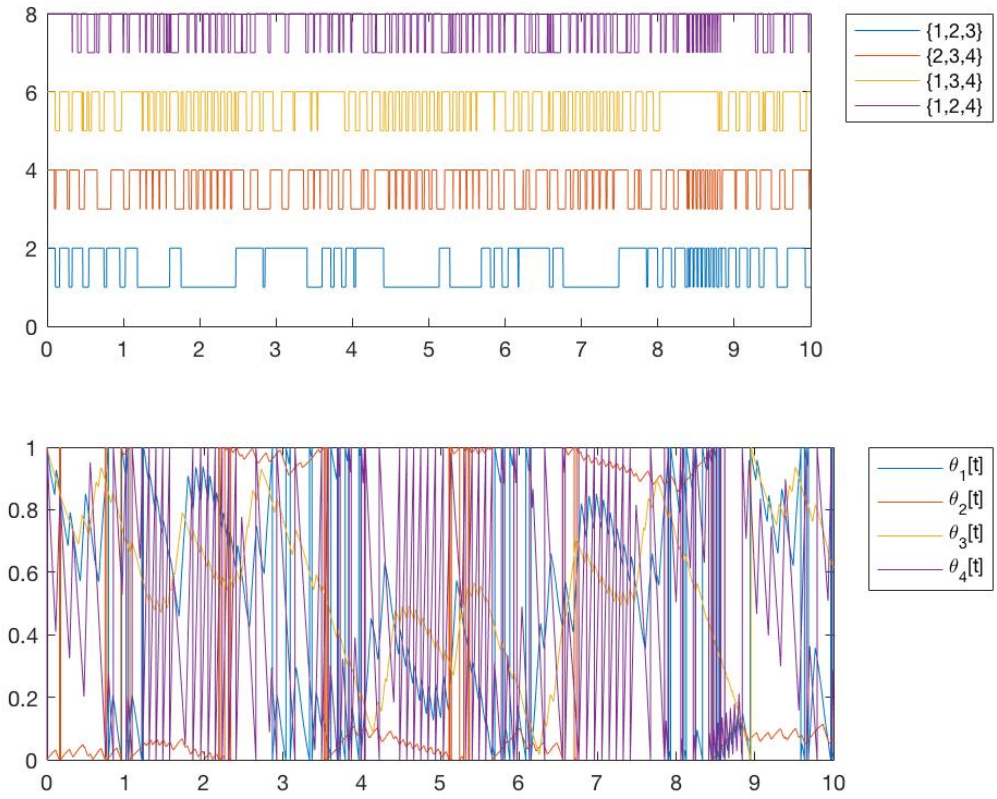

Figure 4.24: A phase ordering plot (top) and a phase plot (bottom) of the four oscillator system. The parameters are $\omega_1 = 2.2$ (blue), $\omega_2 = -0.4$ (orange), $\omega_3 = 1.1$ (yellow), $\omega_4 = 6.1$ (purple), $\lambda = 2$ and the duration is 10 seconds. The phase description plot shows the four subsystems described as having a selected oscillator in the center or not.

Figure 4.24 is shown as a double plot. The top plot shows the state of the description of each subsystem. It is color coded to match the color of the oscillator modified by the subsystem. In the three oscillator system, the reason for the appearance of 2-dimensional hyperplanes

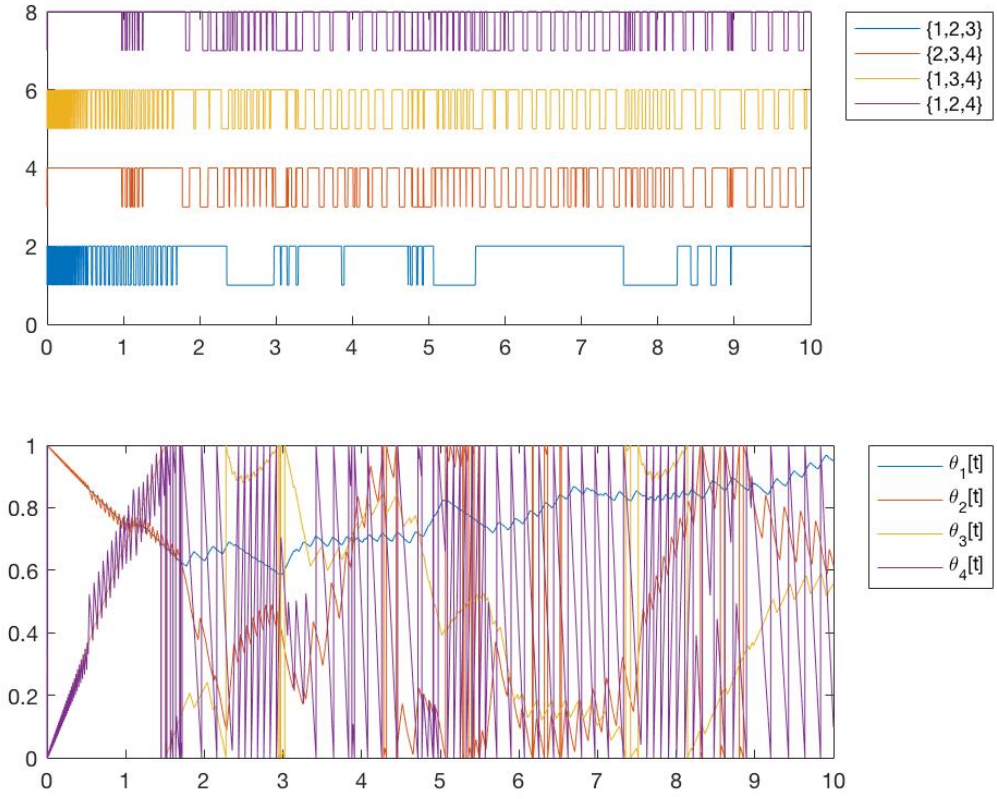

Figure 4.25: A phase ordering plot (top) and a phase plot (bottom) of the four oscillator system. The parameters are $\omega_1 = 0.275$, $\omega_2 = 1.6$, $\omega_3 = -0.7$, $\omega_4 = 6.4$, $\lambda = 2$ and the duration is 10 seconds. The phase description plot shows the four subsystems described as having a selected oscillator in the center or not.

resulting in evenly spaced staircases entrained within the period of an oscillator, switching over the discontinuity, had to do with a subsystem of two phases changing nominal order in rapid succession. Here a rapidly alternating description of a subsystem, whether a selected oscillator is in the center or not, correlates to the appearance of hyperplanes. More specifically, it is the case where three of the descriptions alternate rapidly and one description remains static for the duration of the hyperplane. Many of the hyperplanes in this example have similar features. Here we look more closely at the plane between 1.7 and 2.5 seconds. The purple oscillator has the highest intrinsic frequency, initially set as $\omega_4 = 6.1$. This oscillator keeps a regular tempo switching from

0. to 1. at an angle significantly less than 90 degrees. The other 3 oscillators entrain to this tempo with different orientations, as opposed to unifying into a staircase. The oscillator in blue has the largest average phase-position, ascending then descending in a curve. Its peaks are situated between the valleys of the purple oscillator. The the local minima of the blue oscillator intersects regularly with the purple oscillator as it descends from peak value. The oscillator in yellow also moves in a curve, but in an opposite path direction, starting in descent and then changing to ascent. It is shifted 180 degrees with respect to the oscillator in blue. Having the same low magnitude frequency of the blue oscillator, the local maxima intersects with the blue oscillator's descent from peak value, not the local minima. The orange oscillator with $\omega_4 = -0.4$, has an opposite intrinsic direction relative to the other three oscillators. Here it can be seen to start at a very low average phase-position entrained within the period of $\omega_4 = 6.1$ in purple. Then at about 2.2 seconds the orange oscillator switches at a near 90 degree angle from 0. to 1. in phase and repeats this at few times with irregular spacing before settling at a high average phase close to 1. until about 3.6 seconds. The regime of activity just described can be seen to recur in a few locations, for instance, between 4.4 and and 5.1 seconds, as well as, between 6.7 and 7.4 seconds. In the former, the all the oscillators have similar activity except the yellow and blue oscillators invert roles and are half the size in average phase magnitude. Moving on to a window of time that visually appears to be less regimented, take the section from 2.5 to 4.0 seconds. Again, as in the three oscillator examples we see hyperplanes intermixed with paths in nearly the full dimension of the state space.

Figure 4.25 shows a slightly different parameter setting than the previous plot. Viewing the activity from 0 to 1.4 seconds, two paths are visible. One starting from the phase magnitude of 0.0, where the oscillator in orange oscillates about the relatively smooth path of the oscillator in blue. The other starts from the phase magnitude of 1. with the oscillator in purple oscillating about the oscillator in yellow. In the top plot, the description of the subsystems that modify the yellow and blue oscillators, exhibit relatively high frequency switching between states. After 1.4

seconds, the purple oscillator which has the high intrinsic frequency $\omega_4 = 6.4$ begins to oscillate at a relatively high frequency between 0. and 1. After a few revolutions at nearly 90 degree angles, it slows and concurrently the orange oscillator from the other path diverges from the blue oscillator. This oscillator in blue tends to maintain a smooth path for the entire sample shown.

4.4.1 Quantitative Description

The 4-COS designed here produces similar phenomena to the 3-COS, however the perception of melodic tendency is more complex. The examples to be presented share a feature of relatively low determinism in the range of 20-40 percent. Variable laminarity is also cited across measured instances, at about 3 percent and in some cases as high as 26 percent in others. The high laminarity cases are associated with significant drift in the RP. Other significant details will be illustrated in the following RPs.

Figure 4.26 shows an interesting melodic state. Large square structures are sequenced on the main diagonal, interposed with narrow regions that correspond to hyperplane features. The determinism is low, where DET = 26.28. LAM = 5.2 is also low and the divergence is high at DIV = 1/76. The figure is enlarged to show the narrow clusters orthogonal to the LOI at about 30 seconds. Again this is a significant moment of recurrences of retrograde motion. The previous occurrences are ascending patterns of discreet tones. The retrograde recurrence in this case then creates a descending patterns of tones, although this time with a slight velocity curve and temporal discontinuities. The temporal discontinuities are not silence in this case, rather interruptions in the recurrence pattern shown by the breaks in the orthogonal line-like clusters. With a low laminarity rating it is difficult to claim that there is any form of chaotic itinerancy. While the RP representation does resemble a sequence of quasi-attractors, the high divergence and concurrent low determinism, represent dynamics that may prevent the durability of stationary formations.

Figure 4.27 show a high laminarity case where LAM = 25.76. The divergence is lower at DIV = 1/214, but the determinism is relatively low at DET = 38.66. While an increase in all

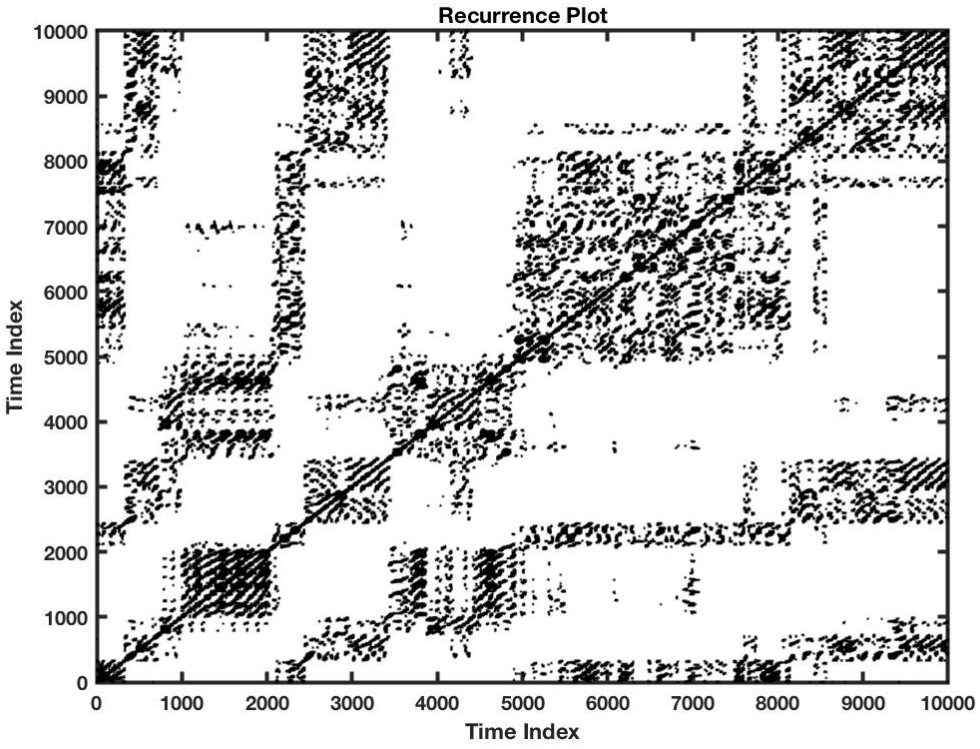

Figure 4.26: A recurrence plot of the four oscillator system. The parameters are $\omega_1 = 2.2$, $\omega_2 = -0.4$, $\omega_3 = 1.1$, $\omega_4 = 6.1$, $\lambda = 1.4$ and the duration is 100 seconds.

three is statistics is positively correlated with respect to the statistics from Figure 4.26, the RP demonstrates drift as opposed to CI. Convergent flows are present, but uncommon due to the low determinism, meaning that straight and diagonal recurrence lines are generally short and in this case distributed widely without much localized self-organization. The *RATIO* measure is low.

4.5 5-COS

As noted in the previous chapter, the combinatorial expansion due to the number of oscillators in the system and also the size of the subsystem, affects the size of the description and results in deeper regimes of activity. The state space is the cartesian product of five lines giving a 5-dimensional cube. The traversal of that space is governed by the number of cases given

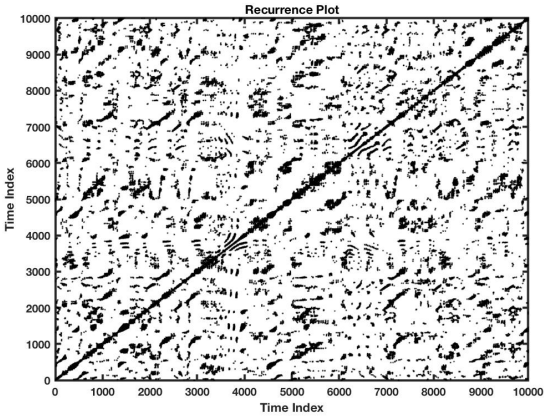

Figure 4.27: A recurrence plot of the four oscillator system. The parameters are $\omega_1 = 1.94$, $\omega_2 = 0.9$, $\omega_3 = 3.2$, $\omega_4 = 1.1$, $\lambda = 1.3$ and the duration is 100 seconds.

by description. Again, there are six cases that effect two oscillators for each subsystem and ten subsystems total. The subsystems overlap, resulting in four coupling terms for each oscillator, updated every sample.

When multiplying the coupling terms as $L_i^*[t] \cdot M_i^*[t] \cdot N_i^*[t] \cdot \emptyset_i^*[t]$, a large and variable range emerges that can switch from low-frequency to high frequency with steep angular frequency envelopes. One potential problem that ensues is the envelopes will lapse into low-frequency inaudible or rather infrasonic regimes for long durations. The problem is a potential problem because in this arrangement the system produces interesting aesthetic material for experimental music and sound art, as infrasonic passages with abrupt transitions to audible notches and unraveling high-frequency envelopes. Figure 4.28 shows a phase plot of the five oscillators, where the product of the coupling terms is not offset by any value. An offset simply means $L_i^*[t] \cdot M_i^*[t] \cdot N_i^*[t] \cdot \emptyset_i^*[t] + \varepsilon$. The θ in this case is some static value between 0. and 1.. In the figure, the characteristic intersections at local peaks and valleys is observed showing a mode of synchronization between oscillators. When one of the oscillators transitions to a high-frequency mode the rest entrain to that period. Solid blocks of color show an oscillator that transitions to a high-frequency mode. Here that is the oscillator in yellow at about 8 and 26 seconds. After the high-frequency transfers abruptly from yellow to purple at this 26 second point. The purple

section at the end of the plot, sounds in the bass register as a quavering, descending line, that decays slowly, but then skips logarithmically back to the infrasonic regime. This point in state space depicts the capability to transition both abruptly and gradually between densities. The infrasonic passages also have moment of abrupt demarcation. One instance appears at about 17 seconds and can be heard as a high note with a percussive envelope. Larger scale proportions are also visible in the plot. The first 10 seconds ending with the dense yellow bar is the same duration as the purple density until the purple starts to unravel. The unraveling in purple is about the same duration as the earlier yellow bar. The low frequency section from 10 to 25 seconds is nearly split in half. The infrasonic event after the purple density continues for 30 seconds doubling the duration of the previous infrasonic event.

Adding coupling terms as $L_i^*[t] + M_i^*[t] + N_i^*[t] + \emptyset_i^*[t]$, produces sonic results similar to what has been observed in the three and four oscillator system. Still intrinsic frequencies need to be reduced by a factor of 10 to hear a similar average frequency to the basic three oscillator system. Figure 4.29 shows the phase plot with same parameters instantiated as figure 4.28.

4.5.1 Quantitative Description

In this 5-COS as observed in the 3x3-COS, we start to see the onset of CI. With distinctly textured formations on the main diagonal, like a sequence of recurrence shapes. Correspondingly, there are high laminarity ratings with long vertical lines located prominently at the edge of these recurrence shapes - or quasi-attractors.

The appearance of quasi-attractor formations, or at least the resemblance of those formations, is not always concurrent with high laminarity, as see in figure 4.32. This at times can be connected to a low coupling strength. The coupling strength in this instance is $\lambda = 0.5$. The stats for this RP are as follows DET = 13.4, DIV = 1/174 and LAM = 8.6. What appears as vertical lines at the edge of the cluster on the main diagonal at approximately 20 seconds are actually a series of short evenly spaced diagonal lines. When the coupling strength of this regime

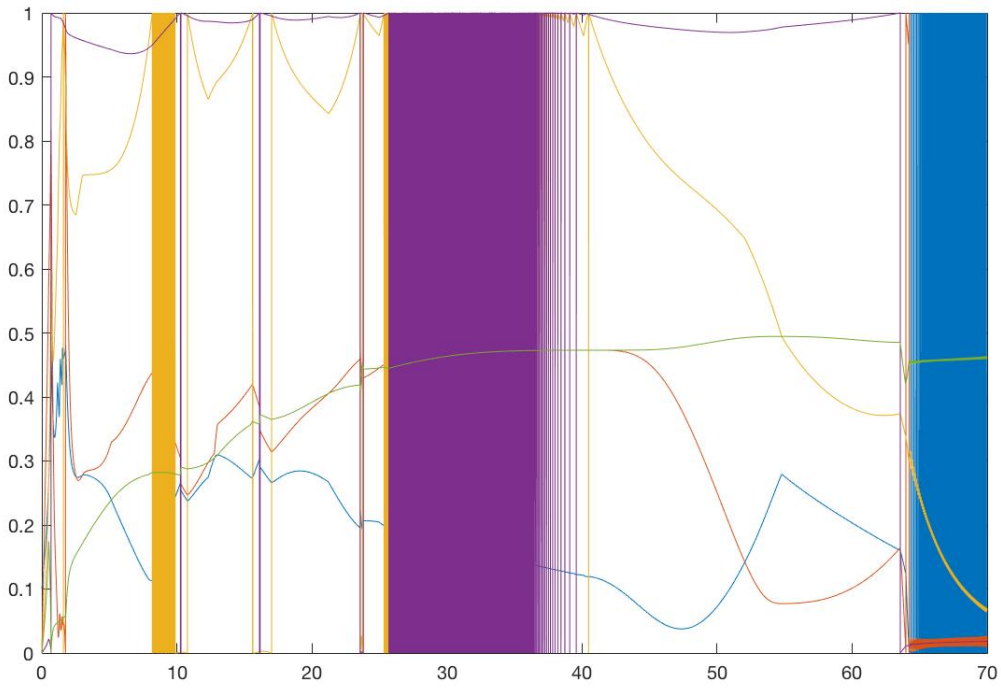

Figure 4.28: A phase plot of the five oscillator system, where the product of the coupling terms are not offset. The parameters are $\omega_1 = 0.22$, $\omega_2 = 0.94$, $\omega_3 = 0.33$, $\omega_4 = 0.03$, $\omega_5 = 0.21$, $\lambda = 1.3$ and the duration is 50 seconds. The phase of oscillator 1 is 0.1 and the rest are 0.0.

is increased to $\lambda = 1.5$, the laminarity (and the determinism) increase as well. Seen in figure 4.33, the *DET* = 28.2, the *DIV* remains nearly the same at 1/171 and the *LAM* = 51.4. Solid vertical lines appear at the edges of quasi-attractors showing stationarity at the edges. Increased coupling strength improved the laminarity ratings, by consolidating evenly spaced short diagonals clustered in vertical organization into minimally broken vertical lines (the long vertical lines in the plot have a few horizontal spaces). CI ranges from perceived wandering sequential organization to intentional sequential organization. The statistical search algorithm for vertical lines is fine grained such that stationarity dynamics that contain minuscule discontinuities in organization are treated as clusters of single points. If stationarity can take forms other than unbroken vertical lines, it may also be inferred that different forms of stationarity can indicate wandering verse intentional activity. These two instances could show a more wandering itinerancy in the former

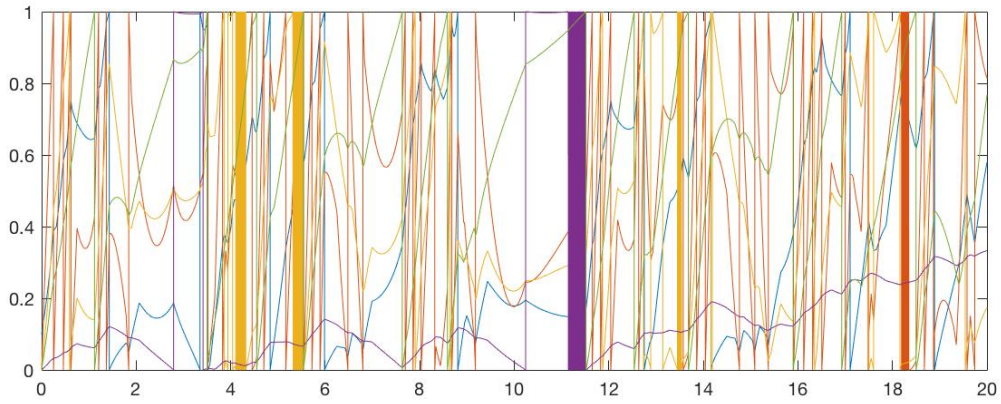

Figure 4.29: A phase plot of the five oscillator system, where coupling terms are added. The parameters are $\omega_1 = 0.22$, $\omega_2 = 0.94$, $\omega_3 = 0.33$, $\omega_4 = 0.03$, $\omega_5 = 0.21$, $\lambda = 1.3$ and the duration is 50 seconds. The phase of oscillator 1 is 0.1 and the rest are 0.0.

and a more intentional itinerancy in the latter. This is because particles are not as easily trapped by the discontinuous laminarity escaping at the gaps. The itinerancy becomes more random, changing to regime dynamics in the mode of brownian noise. Again, black noise is when rare states predominate and is another way of conceptualizing attractor landscapes with multiple basins and continuous laminar trapping flows on horizons of basins.

Conversely, the 5-COS produces drift with high laminarity. The drift contains higher amounts of vertical line structures than diagonal line structures, meaning a mixed regime with stationarity and chaos that results in drifting stationarity. Figure 4.31 shows this case with DET = 35, DIV = 1/132 and LAM = 51. The LAM (and DET) is linked to the coupling strength again in this case, where reducing the coupling strength to 0.2 reduces the laminarity and other statistics: DET = 16.1, DIV = 93 and LAM = 2.25. This reduction in coupling strength also makes the drift more homogeneous. The white bars that indicate phase transitions (descents into chaos that act as a search between attractors) as seen in 4.31 are reduced to impressions of underdeveloped transition dynamics. In this way, the transitions are of minimal impact but do give the vague sensory impression of a change in attractor dynamics. This may be a pre-itinerant state that demonstrates the potentiation of large-scale heterogenous organization breaking down into cells

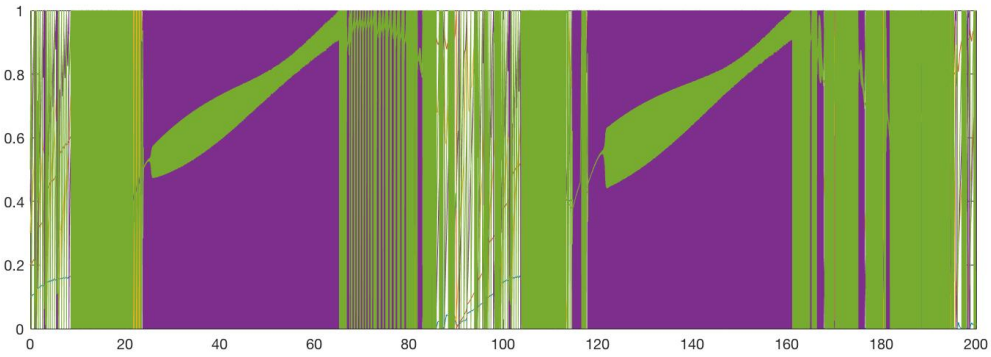

Figure 4.30: A phase plot of the five oscillator system, where the product of the coupling terms are offset, by θ. The parameters are $\omega_1 = 0.04$, $\omega_2 = 0.13$, $\omega_3 = 1.516$, $\omega_4 = 2.6$, $\omega_5 = 5.8$, $\lambda = 1.26$ and the duration is 200 seconds. Initial phases are $\theta_1 = 0.1$, $\theta_2 = 0.2$, $\theta_3 = 0.3$, $\theta_4 = 0.4$ and $\theta_5 = 0.5$.

or domains. Something cannot wander if there is not space to wander in.

Stationarity traps particles (particle is used to name a moving point in a flow) in dynamical flows causing the attraction into basins. Figure 4.34 shows a high laminarity and determinism regime generated with low coupling strength, λ = 0.5. Here *DET* = 52.5, *DIV* = 1/150 and *LAM* = 41.5. Low coupling strength in this system as described in the 3-COS example causes a pulsed signal because the coupling terms allow for changes in signal direction. So the signals are coupled to a certain degree even with a low λ. As we saw with the regime in 4.31, the low λ was concurrent with a low *LAM*. It must be that certain sets of intrinsic frequencies couple better than others. This is certainly true with resonance phenomena depicted in the regime diagram of the circle map [Large and Kolen,1994]. In the regime from 4.31 if λ = 0, the *LAM* = 0.49. In the regime depicted in 4.34 if λ = 0, the *LAM* = 14.4. With every parameter setting and distribution of $L_i^*[t]$ being the same, the intrinsic frequencies are implicated in the *LAM* variability. For the regime diagram of the circle map it is the ratios of intrinsic frequencies that cause placement on the basin of an Arnold Tongue and eventual locking to an integer ratio. These integer ratios are given from the set of numbers generated by the Farey Tree: [0/1 1/9 1/8 1/7 1/6 1/5 2/9 1/4 2/7 1/3 3/8 2/5 3/7 4/9 1/2 5/9 4/7 3/5 5/8 2/3 5/7 3/4 7/9 4/5 5/6 6/7 7/8 8/9 1/1]. The coupling

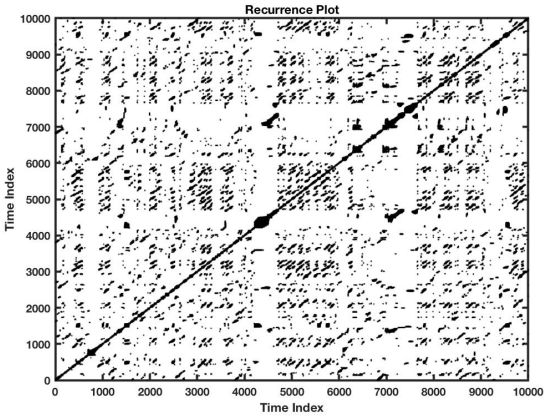

Figure 4.31: A recurrence plot of the five oscillator system, where the product of the coupling terms are offset by ε. $\omega_1 = 1.4$, $\omega_2 = 1.13$, $\omega_3 = 2.516$, $\omega_4 = 1.6$, $\omega_5 = 7.8$, $\lambda = 1.2$ and the duration is 100 seconds.

strength in circle maps is also proportionate to the time until locking. Higher coupling strengths create a faster convergence.

4.6 6-COS

Similar to the 5-COS, the 6-COS represents the possibility for another jump in combinatorial complexity. If the system was designed such that the ordering of four oscillators affects the phase progression of two oscillators the number of $LL_i^*[t]$, or the total number of potential coupling terms in a given system, would be 288. This is an increase from the 5-COS containing 60 conditions. To calculate this number, $LL_i^*[t]$ it is the factorial of the number of oscillators, I, minus the modifier oscillators, I_m, times modified oscillators, times the combinations, I_C.

$$LL_i^*[t] = (I - I_m)! \cdot (I - (I - I_m)) \cdot I_C \tag{4.1}$$

$$I_C = I!/I_m!(I - I_m)! \tag{4.2}$$

So if I = 5, the modifiers = 3 and the modified = 2, the product is 120. The case where I =

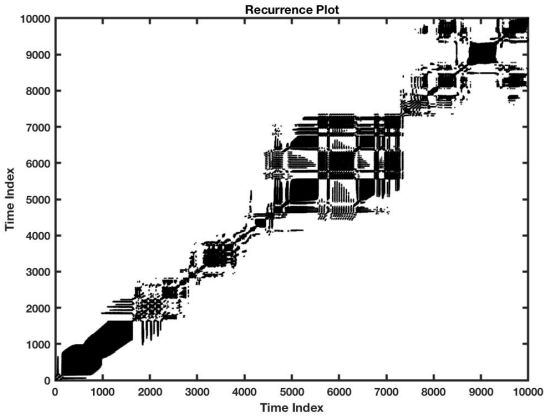

Figure 4.32: A recurrence plot of the five oscillator system, where the product of the coupling terms are offset by ε. $\omega_1 = 0.04$, $\omega_2 = 0.13$, $\omega_3 = 1.516$, $\omega_4 = 2.6$, $\omega_5 = 5.8$, $\lambda = 0.5$ and the duration is 100 seconds.

6, the modifiers = 4 and the modified = 2, gives 720. The case where I = 6, the modifiers = 5 and the modified = 1, also gives 720.

The 6-COS presented here I = 6, the modifiers = 3 and the modified = 3, gives 180. The design is partially about mitigating the effects of combinatorial expansion while preserving a depth of potential regime dynamics. Here with the increase in coupling terms, each oscillator at each timestep is affected by a product of 5 coupling terms, $L_i^*[t] \cdot M_i^*[t] \cdot N_i^*[t] \cdot \emptyset_i^*[t] \cdot P_i^*[t] + \varepsilon$, up from a product of 4 in the 5-COS.

To summarize the combinatorial trajectory (and its management) of the COS designs presented: 3-COS has 6 $LL_i^*[t]$ and 1 $L_i^*[t]$ per oscillator (per timestep), 3x2-COS has 12 $LL_i^*[t]$ and 1 $L_i^*[t]$ per oscillator, 3x3-COS has 36 $LL_i^*[t]$ and a product of 2 $L_i^*[t]$ per oscillator, 4-COS has 8 $LL_i^*[t]$ and 1 $L_i^*[t]$ per oscillator (binary circular representation), 5-COS has 120 $LL_i^*[t]$ and a product of 4 $L_i^*[t]$ per oscillator, 6-COS has 180 $LL_i^*[t]$ and a product of 5 $L_i^*[t]$ per oscillator. The number of $L_i^*[t]$ per target oscillator is given by the frequency of each i in the distribution of modified oscillators. While a higher number of modifiers produces a higher $LL_i^*[t]$, it conversely produces a lower number of $L_i^*[t]$ for the product to affect the phase progression of the target oscillator at each timestep. For instance, in a 6-COS with a mapping of 2 modifiers to 4

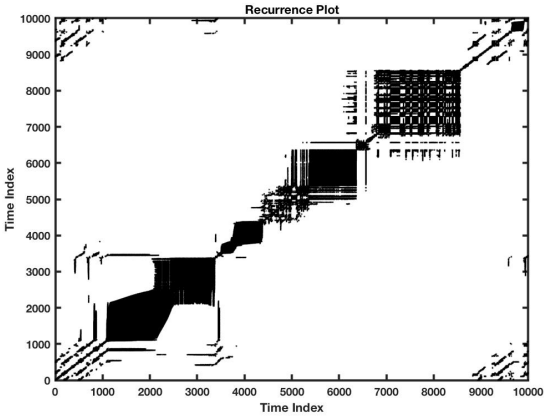

Figure 4.33: A recurrence plot of the five oscillator system, where the product of the coupling terms are offset by ε. $\omega_1 = 0.04$, $\omega_2 = 0.13$, $\omega_3 = 1.516$, $\omega_4 = 2.6$, $\omega_5 = 5.8$, $\lambda = 1.5$ and the duration is 100 seconds.

modified oscillators there are 48 $LL_i^*[t]$ and a product of 10 $L_i^*[t]$ per target oscillator per timestep. Conversely, in a 6-COS with a mapping of 5 modifiers to 1 modified oscillators there are 720 $LL_i^*[t]$ and only 1 $L_i^*[t]$ per target oscillator per timestep. This is all to say that there is a tradeoff between the number of $LL_i^*[t]$ and the number of $L_i^*[t]$ in the target product. Finding a balance between the two sides can preserve complexity while mitigating expansion on either side.

The phase space of the 6-COS is the cartesian product of 6 lines, resulting in a 6-dimensional cube. Figure 4.35 shows the dynamics of the phasors or frequency envelopes over a duration of 100 seconds. The five $L_i^*[t]$ that effect each phasor at each time step are multiplied and the product is offset by 0.2. The sample rate, R is raised to 88200 to help prevent aliasing. Though the oscillators are set at widely different frequency scales any oscillator can jump to a high frequency buzz, ultrasonic in some cases, or a low frequency impression in the infrasonic range. This switching of frequency identity has been observed in the other systems presented, but is especially pronounced when multiple $L_i^*[t]$ are multiplied. In the 4-COS, it was shown in the phase and phase order plots, that when phasors in a subsystem change orderings at high frequency this can cause the target oscillators to jump to a high frequency, even if the intrinsic frequencies are set low. The same is true for the appearance of low frequency oscillation in the sound output. Slow

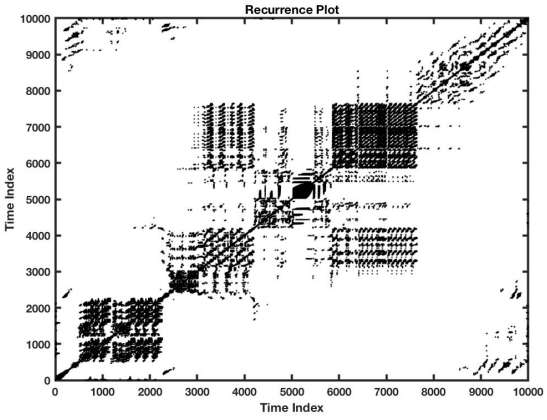

Figure 4.34: A recurrence plot of the five oscillator system, where the product of the coupling terms are offset by ε. $\omega_1 = 3.51$, $\omega_2 = 0.93$, $\omega_3 = 0.68$, $\omega_4 = 0.06$, $\omega_5 = 3.16$, $\lambda = 0.5$ and the duration is 100 seconds.

changing descriptions of phase ordering can drive oscillators with a high intrinsic frequency into infrasound. Figure 4.35 sounds like a series of loops of low frequency pulses. Due to the coupling between oscillators, the velocities of the pulses merge into envelopes with constantly varying slopes. A background low frequency layer vamp pulsates and at times integrates, increasing in frequency and bolstering the primacy of high frequency foreground events. High frequency bursts with noisy spectra demarcate and frame groups of pulses. Ascending buzzes form and at times portend transitions to distinct attractors. These attractors will be looked at more closely in the next section with recurrence plots, showing musically significant changes in the general texture of pulse pattern formation.

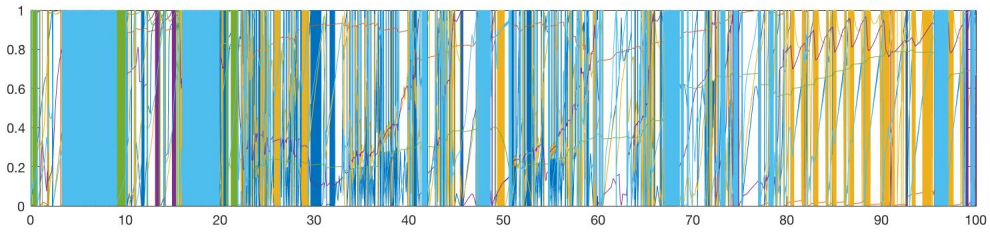

Figure 4.35: A phase plot of the six oscillator system, where the product of the coupling terms are offset by ε. The parameters are $\omega_1 = 2.13$, $\omega_2 = 0.0495$, $\omega_3 = 1.947$, $\omega_4 = 0.2508$, $\omega_5 = 0.018$, $\omega_6 = 1.65$, $\lambda = 1.29$ and the duration is 100 seconds.

4.6.1 Quantitative Description

Like the recurrence analysis of the 5-COS and the 3x3-COS evidence begins to emerge for CI. The 6-COS exhibits orderly CI, or a seemingly deliberate path through an attractor landscape. The basins of attraction cross recur minimally with voluminous white space off the diagonals meaning the basins are informationally distinct. The horizons of the attractors contain continuous laminar flows that trap particles with more impact than attractors with discontinuous laminar horizons.

Figure 4.36 is an example of orderly CI. In terms of RQA statistics, DET = 70.25, DIV = 1/420, LAM = 81.43 and TT = 0.402 seconds. The high determinism and laminarity are an indication of black noise, not only because of the sheer statistical magnitude of both, but because of the location of the features that contribute to the statistics in the plot. Here, laminar structures form at the edges of attractors. The off-diagonal areas of the plot are not completely white as seen in the some of the 5-COS plots. But most of these significant cross-recurrences between attractors in the landscape are the laminar structures located at areas of phase transitions or potential phase transitions. The trapping time seen in most other plots was approximately 0.2 seconds, here the time doubles. With a slow divergence rating in combination with high TT, it can be said that the regime here has a robust capacity for pattern formation and a stabilized, orderly itinerancy.

Figure 4.37 the range of the intrinsic frequencies is reduced along with the coupling strength. With these two changes we see a reduction in RQA statistics and a more homogeneous RP that exhibits drift. In terms of RQA statistics, DET = 50.7, DIV = 1/231, LAM = 66.44 and TT = 0.308 seconds. Laminarity is statistically significant although its location in the RP is distributed throughout as opposed to existing at critical locations. A phase transition of minimal impact occurs at about 50 seconds, shown by imperfect white bars. The two quasi-attractors are demarcated by these bars without laminar edges. The off-diagonal areas also show significant cross-correlation between the two squares on the diagonal. The reduction of intrinsic frequency range and coupling strength led to significant changes in landscape, like an undirected background

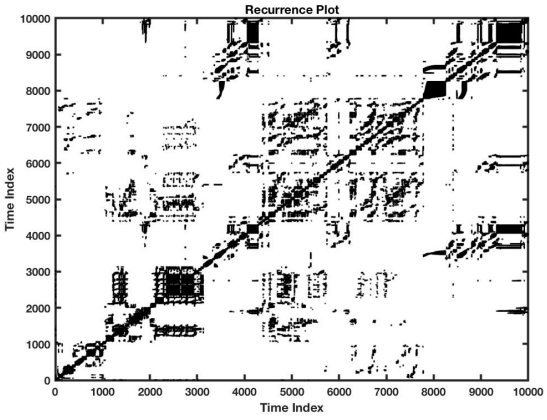

Figure 4.36: A recurrence plot of the six oscillator system, where the product of the coupling terms are offset by ε. The parameters are $\omega_1 = 2.13$, $\omega_2 = 0.0495$, $\omega_3 = 1.947$, $\omega_4 = 0.2508$, $\omega_5 = 0.018$, $\omega_6 = 1.65$, $\lambda = 1.29$ the duration is 100 seconds.

activity related to formalisms of brownian motion with high drift. Of course the systems here are deterministic. Brownian motion is generally a stochastic process that creates a model that resembles the world by statistical proxy. It doesn't say much about the path through the space, which can give a perceived sequence continuity over time. This plot in consequence could be generally considered drifting brown noise, and its recursive determinism and coupled stability gives the sequence perceived, a more robust contiguous organization.

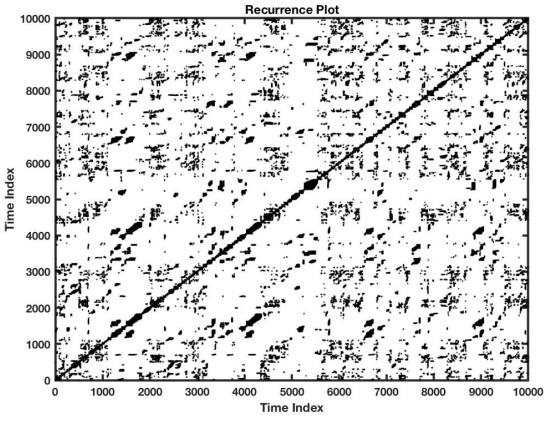

Figure 4.37: A recurrence plot of the six oscillator system, where the product of the coupling terms are offset by ε. The parameters are $\omega_1 = 1.386$, $\omega_2 = 0.7821$, $\omega_3 = 1.485$, $\omega_4 = 1.8546$, $\omega_5 = 0.4521$, $\omega_6 = -0.33$, $\lambda = 0.74$ and the duration is 100 seconds.

4.7 Musical Examples

COS can be used in many different musical modes ranging over valences of heavy and intense to light and ambient. In my personal practice as an experimental electronic musician I have used arrangements of COS as a solo instrument and in collaboration with acoustic musicians. This section will present 4 listening examples of my electro-acoustic improvisations listed in Appendix A. For a more complete catalog of my works you can visit www.davedefilippo.bandcamp.com, where *Scission* and *Business Machines* are the electro-acoustic albums that feature electronic instruments built with COS.

When designing an instrument for musical performance, I tend create 4 or 5 stereo channels (sound sources) that can be mixed together in different combinations. I then map a controller to the parameter space of each sound source. A resulting stereo channel is typically a reduction of a couple COS (in this instance) arranged in a larger recursive loop. Each sound source is horizontally integrated with other sources, in a way that there is subtle correspondence between sources, but each source maintains a certain level of auditory independence. From a networking perspective, this means each source individually is not directly connected to every other source. The sources have degrees of separation achieved when each source only receives input directly from the output of one or two sources (not all). This kind of systematization of sources creates useful instrumental affordances. All the sources will entrain into a regime, usually with rhythmic characteristic. Also, all actions on the parameter space of one source have an effect of varying degree on the all the other sources. Furthermore, when the volume parameter of a source is all the way down, an impression of its activity can be heard across all the other sources that are audible. In this way, the addition of a source to a mix, by raising the source volume, can still be musically surprising (due to the general independence between sources) but also tends to be coherent and perceptually smooth. From a perspective of performing the instrument in real-time, this arrangement also gives me a sense of what the source will sound like before

bringing it into the mix.

Granted that the COS can generate signals with a perceived intention organization, interesting potential opens up in the interaction with other musicians. In theory, the trajectories I synthesize can give an impression of conscious directivity through the quasi-attractor landscape, which can be anticipated by my musical interlocuters. The quasi-attractor landscape sounds like a sequence of short musical ideas, and my co-improvisers can read that sequence to jump ahead of the progression, asserting forms of musical agency that guide the improvisation forward, and give me musical ideas to respond to synthetically.

In the next chapter, the concepts of interaction and intention will be discussed in the context of embedded and extended cognition. My concept of extended intentionality will be described theoretically from the perspective of improvising with a larger system of COS just described. Here it is important to note that with extended intentionality I am able to offload my musical intentions to a sound source. I can then move over to another sound source to work on its parameter space with a purpose of offloading another musical intention.

Below are a few musical examples. When working with acoustic musicians there is a negotiation of sonic languages. The synthesized signal produced by the COS has its own language of sonic gestures (produced without a body) including timbre transformations and morphing envelopes of frequency and amplitude. Each acoustic instrument in conjunction with standard and extended techniques has its own range of sonic qualities. Collectively, we find a common language between the acoustic and the electronic to construct our improvisation.

The first is titled *Absolutist Preoccupation* and was recorded with percussionist Kevin Corcoran. This piece is fast paced with high-energy percussion. Kevin is performing on a 3-piece drum kit and was literally drenched in sweat after this session. If I were to characterize this piece with a genre, I would call it psychedelic math noise. Noise, to me, can range over ambient and harsh and this piece is of the harsher variety. Upon listening it will be evident that Kevin and I, found a common language of deep percussive pulses and patterns of those pulses, rolling,

accelerating and fragmenting into oblivion.

Resistance (part 1) was recorded with cellist T.J. Borden. This piece also is high-energy, a bit less harsh, and is generally maximalist, but interposed with moments of stasis and drone. T.J. employs a range bowing techniques during this recording, varying its weight on the strings, causing gradations of friction. The technique facilitates a range of overtones under envelopes of bowing gestures that interact with the timbral, melodic and bounding rhythmic characteristics of my electronics.

Schismogenesis (part 1) was recorded with percussionist Kevin Corcoran and is more of a ponderous ambient piece. However, it still maintain intensities of affect with the intermittent onset of tones and gestures that pierce to create a doubled and uncertain emotional terrain of calm and urgency. Kevin employs an array of techniques and actions, bowing cymbals and bells and stacking these objects on the floor tom to create arrangements of sympathetic vibration. The undulating resonances of extended percussion find their way into the mix with the slowed down electronic bass pulses and enveloping electronic textures. Other implements are applied to the drum heads as abrading gestures to create the frictive sounds that interact with some of the more tactile sounds of the processed COS signal.

Cyclic/Eclectic was recorded with saxophonist Paul Roth. This piece is an example of a slower and more relaxed actuation between acoustics and electronics. Paul plays deliberately with monotonous melodic cycles. Here interaction has been minimized, as a step into a kind of mutual independence, where the interaction exists in a different register that is away from the momentary demands of our constructed musical environment. It's a liminal interaction where transitions give way to moments of minimal change, only to arrive on the surface of another loop with the electronics sweeping and cascading below it.

Chapter 5

Theory of Interaction and Improvisation

Geared toward a theory of improvisation and interaction with COS, this chapter will start with a summary of important findings from the analysis in the previous chapter to distill a set of descriptors. Descriptions of kinds of dynamics reflect the potentialities of the generated signal and the capacities of the generating system. Furthermore, the descriptions will be presented as a series of cues a musician can perceive and interact with. These cues provide a guiding directivity, where modes of interaction and work can occur. Related to the concept of stigmergy [Dawson, 2014], from the Greek *stigma* meaning sting and *ergon* meaning work, the cues are a local environmental stimulus that cause certain kinds of work that generate the larger structure. The agent doing the work has the agency to change the environment, making work in a sense a closed-loop recursive activity. Without overdetermining the musician interaction, suggestions will be made relating cues to potential performer action. Drawing on the field of embedded and extended cognition, we study the co-creation and extension of intentionality in performances that incorporate parametrizable dynamics systems such as the COS. First, the significant findings of each COS are presented.

5.1 Analysis Summary

The timeseries generated from each system is non-linear and non-monotonic as evidenced by the inability to fit a line to the data at time scales of a third of second or more. Although, at short time scales modeling error of fit and plotting it over time, reveals moments of synchronization between oscillators. These moments of synchronization correspond to the perception of metric pulses in the sound. In these systems there is generally an intermittency between synchronized and desynchronized chaos.

Different initial phase offsets create different deterministic trajectories through the phase space. It appears that the set of intrinsic frequencies and the coupling strength give the attractor landscape, while the initial phase offset will create different sequences of itinerant motion through landscape. There then are multiple trajectories through the same quasi-attractor landscape that can be a form of stabilized CI.

It was also shown that a coupling strength of zero does not create the desynchronized effect of independent sinusoidal motion. Due to the institution of coupling terms that change the direction of one-dimensional motion, the signal shape at a coupling strength of zero is a pulsed signal with coordinated direction changes. If all the coupling terms were of the variety of $L_i[t]$ (for instance), such that the direction of motion of all the oscillators was constant, then a coupling strength of zero results in completely decoupled sinusoidal motion.

The 3-COS is the lowest dimension system presented, so the analysis scrutinized the structure of each system and in particular the distribution of kinds of coupling terms. It was found that an equal distribution of inverse and negative terms, especially $L_i[t]$ and $-1/L_i[t]$, generated the dynamics of phase transitions, as hyperplanes. These where moments of high-frequency entrainment sometimes followed by minimal texture changes, reminiscent of the landscape of quasi-attractors seen later in systems of higher order. Significant laminarity of approximately 30 percent was also observed in these regimes. It is was also important to note that this system

mostly produced regimes with zero laminarity. These systems exhibited drift and variation from a central tendency and features like bowed line structures. Bowed lines structures are recurrences with velocity changes contiguous with retrograde motion.

Even with the appropriate topology, where subsystems target oscillators outside the subsystem, a distribution of $L_i[t]$ and $-L_i[t]$ produced highly repetitive loops for sound with no variation. This shows the impact of the coupling terms on the sound generation independent of the topology. It was also found that undirected coupling terms, $\tilde{L}_i[t]$, that don't compute the absolute value between phasors, have equivalent impact on producing attractor landscapes, just like an equal distribution of inverse and negative terms. Undirected terms and an equal distribution negative and inverse terms are used in the subsequent system designs.

Observed in the 3x2-COS was a complex temporal structure with distinct sections concurrent with more impactful convergent flows and significant laminarity. Brief sections of retrograde motion were also observed, along with more bowed line structures. Recurrent hyperplanes were present in some regimes, where changing half the frequencies to negative values disrupted convergent flows and removed hyperplanes. The vertical and horizontal lines were homogeneously mixed in clusters. Drift was the most common observation. In many cases it was drift embedded in a higher order oscillation, at times with low determinacy.

Evidence for the existence of orderly CI and black noise is seen in the 3x3-COS. The laminarity statistic is high and laminar flows are appropriately situated at the edges of quasi-attractors. The off-diagonal regions show little cross recurrence indicating black noise.

The 4-COS changes its phase representation to a circle without a basepoint, accomplished by a metric representation that has no major discontinuity. Hyperplanes were found not to only be associated with oscillation over the discontinuity of magnitude 1 (as in systems that represent phase-position on a circle with a basepoint), but also with a rapid switching description of a subsystem. More specifically, it was the case where one description becomes static and the other three alternate rapidly. In this case, the description was if a selected oscillator was the center of a

subsystem or not. In other systems, it is the rapid switching of the ordering of phasors on a circle with a basepoint (a line). The melodic structure generated in some regimes stood out as interesting musical material. Retrograde motion was also present. Overall, drift from a central tendency was the most common observation. Correspondingly, metrics of laminarity and determinism were also low.

The 5-COS showed strong evidence for the formation of chaotic itinerancy especially in the formation of black noise. The multiple coupling terms affecting each oscillator are multiplied, giving interesting scaling behavior in the frequency domain. Here abrupt transitions between infrasound and ultrasound can be common occurrences. Like in systems of lower dimension, the system can produce drift with underdeveloped phase transitions. The 5-COS also generates sequences of black noise with laminar flows at the edges of attractors. Coupling strength seemed to be the best was to predict the emergence of chaotic itinerancy from drift. Low coupling strengths tended to induce divergent flows, reduce laminarity and create drift. Although, some sets of intrinsic frequencies especially those nearing harmonic ratios, couple together more robustly than inharmonic sets. In this case we can see attractor formation and high laminarity, even with low coupling strength. The opposite is also true, a high coupling strength over a set of inharmonic frequencies can also induce drift, but usually with high laminarity.

A distinction was made between continuous and discontinuous laminar formations on attractor horizons. The discontinuous formations have gaps where particles can escape and move toward other attractors, leading to a wandering path through the landscape. Continuous formations have more trapping capacity and cause a more intentional sounding sequence through the landscape.

In the 6-COS, considerations about the combinatorial expansion of descriptions were emphasized. Design patterns to manage the expansion were reflected on. Overall, like other systems there was evidence for chaotic itinerancy, this time appearing with highly convergent flows, high laminarity at horizons and a doubling of trapping time.

5.2 Interaction Cues

The analysis yields descriptors of phenomena generated by the capacities of the systems. Here are few of the cues, that can be recognized during an improvised performance in terms of the auditory dynamics. The cues are dynamical descriptors that take on the role of contents, in the sense of both mental imagery and a mental model.

There is an important distinction to make between a mental model and mental imagery. A mental model is a model of what is there. In this case, it is the raw and precise perception of the COS signal. Mental imagery, a kind of imaginative thinking, sometimes called sensory imagery, is imagery about possible changes and manipulations to the environment, as well stimulus independent creative thought. Here, it is a way of thinking about the signal in terms of cues and interpreting the meaning. It is almost a form of questioning the mental model. What do the cues imply about what changes are possible and what motor manipulations would create those changes? In this case of an improvising musician, these are two kinds of contents (i.e. possible futures and corresponding possible actions) attributable to mental states. Both kinds are directed but in different ways. A mental model is directed merely toward what is there to represent, while mental imagery is both directed toward what is there and what could be there (given what is there and how it can be manipulated, as well as, imaginary, absent things).

(1) Intermittency was a general feature as a switching between synchronized and desynchronized chaos, lending to a pulsed rhythmic sound and a sense of meter. Actions of the performer can be synchronized to the pulses, in order to alter the regime at moments of synchronization, as an entrained continuity between musician and synth. The pulses of synchronization have a typical duration of about a third of a second.

(2) Hyperplanes occur as a rare transitory phenomenon, sounding like a buzz, and functionally indicate a search between quasi-attractors; there is also a non-hyperplane search which is a moment of descent into chaos from order. The duration of hyperplanes are on the order of

seconds. Similarity, twisting dials of intrinsic frequencies and coupling strengths is a method of search in order to effectuate musical transitions. Changing values of intrinsic frequencies alters the attractor landscape, while slight modifications to the coupling strength alters the trajectory in the phase space. The system itself can search its phase space via descents or hyperplanes or the parameters can be acted on.

(3) Divergence/ Convergence are like intermittency but are the larger scale temporal trend, where the convergence or not of the frequency envelopes suggest a level of directivity. The envelopes either separate or integrate. While separation leads to polyphony, the integration can lead to timbral fusions or stable limit cycles. Actions can attempt to perturb the system into the effect of interest, where the kind of perturbation as its magnitude, velocity, and direction, are the experience-dependent decisions of the performer about the mapping of action to effect. More specifically, listening for convergence can aid the displacement of a parameter dial in order to achieve a convergent state or reach a quasi-attractor.

(4) Laminarity or the trapping can be heard as stasis. While there may be an inclination to change system parameters, the stasis may be an indication of a self-organizing landscape. The average duration of these is typically around a third of a second.

(5) Stationarity can take the form of laminarity, however can be more generalized referring to stable limit cycles and repetitions on the order of seconds.

(6) Recurrences are consistencies and temporally distributed repetitions. Where the bowed recurrence are recurrences with changes in velocity, perceived as repetition with a variation. Since similar recurrences can reflect stationarity, the variation over recurrences of the same kind indicates non-stationary, that the regime itself is changing. Recurrences can exist on many time scales.

(7) Drift, as with all the cues mentioned, is deterministic. It is the slowly changing dynamics (sometimes over 100s of seconds or more) of the trajectory with temporally widespread and typically granular recurrences as mixtures of unstable points and lines. Drift can at times be

embedded in a pattern of oscillation between recurrence and non-recurrence.

The 7 cues as potential mental contents, with actionable consistences, provide insights into suggested techniques for action or non-action. The actions of the performer are most related to a search of the phase space for states of interest. Human perception is a necessary aid in tuning the dynamics. The intermittent meter of the signal leads to gestural entrainment, so actions that are meant to search, can be synchronized to the dynamics. Parameter shifts can occur at onsets of synchronization or onsets of desynchronization to hide the actions of the hand.

Given that the COS is generating sound and the musician can change the system parameters, there is an interaction taking place where the musician and the COS are cooperating in the production of intentionality. This was referred to earlier as an embedded relation, where directivity of contents and importantly the coherence of transitions between contents are co-created. Since the COS has the capacity to generate directed trajectories through phase space with statistical similarity to intentional organization, the musician perceives the signal as intentional. While the COS is simultaneously what the musician is doing to produce sound and the musician has intentions about how to direct the progression, the province of the intention can be ambiguous. It may have originated in the machine or it may have originated in the musician. Since intentions originating from outside the mind of the musician can be owned as if originating in the mind of the musician, there may be an illusion of interaction. The illusion would be that the musician intended the system to evolve in the way perceived, but really the system directed itself. The interaction and the sense of control could be a mode of self-deception. This notion of the interaction as a mode self-deception will be complicated with extended mind theory (EMT) [Clark and Chalmers, 1998].

EMT says that external devices if meeting certain criteria are not like another mind but are part of YOUR mind. The parity principle is one of these criteria. There is parity if the process done in the mind is functionally isomorphic to the interactive process done with the external object. The functional isomorphism rests on a functionalist theory where the mind is

decomposable into a system of functions. The substrate performing the function is irrelevant. For a functionalist, the operations don't matter unless inefficient. It is only important that the inputs give the outputs, so the mapping from the input to output is essentially a black box. There is some level of parity between the CI in the mind and the CI generated by the COS.

As mentioned earlier in the section Describing Chaotic Itinerancy, CI parity exists among observed electrical phenomena in the brain, including the DMN, a background brain system implicated in many mental functions including mind wandering, creativity and other kinds of imagination and mental imagery. Implicit in these functions, like mind wandering, is a dynamical process of a trajectory through contents. The COS, by parity, could then be considered a functional isomorphism to the DMN, where the mind is extended outside the boundary of the skull into the COS. When the COS is coupled to the DMN bidirectionally in musical interaction, the intentional activity of DMN can be offloaded to the activity of the COS, extending the intentionality.

A stabilized non-stationarity is the case where the signal can be perceived as intentional. A general interaction is stabilizing the musician's default mode network by stabilizing the trajectory through the attractor landscape of the synthesis. Here intentional CI in the mind of the musician is co-created by directing the eventual stabilization of what is heard. The system's dials are manipulated as a search, scanning for indications of stabilization. Once the synthesis is stabilized it may be that both the CI in the mind and the CI in the synthesis share an intention-based stability. An intention originating externally in the COS is owned. The work of stabilizing neural dynamics is accomplished by offloading. Haptic operation of the COS by rotating dials is the interactional component of the offload. The generated signal is altered and fed back to the perceiver.

Interacting with an electrified temporally distributed object (meaning the sound itself) is a negotiation of equilibrium dynamics. Absorbing a tool into the body means increasing its representational space. The tool becomes a state of mind containing action codes and imagery, or contents. Dispositional contents or memories are only accessible at the moments of interaction, evoked in the immanence of certain objectives, given by a state of affairs. Interactions will change

the state of affairs, and alter the sense and representation of disposition, changing the mental imagery of contents. The mental dynamics are coupled to the state of affairs meaning the contents are extensive, pointing at certain recognizable actualities. As mentioned, some of these actualities are present, others depart and become ungrounded, abstract objectives.

While much has been said about intention, attention is an important related concept. Cues need to be attended to and the mental representation of cues of the constative variety are directed by attention to things that are actually there; it is a relation of signifier to signified. External attention relates to stimulus-dependent thought, while internal attention is the focus toward the content of stimulus-independent thought.

With language, a constative sentence directly references things that are actually there in the world, as a descriptive mode. For instance the sentence, "There are four loudspeakers in this room," is constative. Performative sentences involve actions that don't so much describe a situation, but rather modify or make changes to a situation. For instance the sentence, "Turn up the volume of the loudspeaker," is a performative sentence. Philosopher of mind John Searle analyzed these two kinds of sentences in his work on intentionality [Searle, 1979], as varieties of illocutionary acts, that have two directions of fit. The constative sentence is from a viewpoint where words describe the world. The direction of fit is from signifier to signified. The performative sentence has the opposite direction of fit from signified to signifier. The viewpoint is about changing the situation, rather than describing the situation. It is from the world to words.

Varieties of mental language occur when improvising music, whether fully formed as a sentence, or simply the meaning of the sentence, without the sentence, before the sentence has time to form. Cues are the world and constative in direction until an intent emerges in the mind of some origin, that is owned, that wants to change something about the world. Performative mental language, as it could be called, is stimulus-dependent if the attention is externally directed. Still the dark energy in the mind is in play, supporting neural dynamics and generating the default mode mental imagery of stimulus-independent thought. Directing attention inward from mind to

words, is an internally directed performative sentence, as intent to change mental imagery. An estimated 60 to 80 percent of the brain's energy budget is spent on inter-neutral messaging and the supporting cell infrastructure. The momentary demands of the environment are estimated to account for only 0.5 to 1 percent of the budget. The intrinsic activity, such as the DMN based mental imagery of the brain consumes more energy than the evoked activity of momentary external sensory signals [Raichle, 2006]. If the mental imagery is related to modes of imagination, the change of mental imagery can lead to large scale changes to the approach of improvising sequences. In one way, if there are many electronic sound sources of different varieties mixed into a composite, some are silent, some are quiet and others are loud. Here a change to a new composite of sound sources could occur under these conditions by changing the mix of volumes and making sources that were present, absent and visa versa. While there are many combinations of sound sources, for instance with 5 sources there are 120 (binary) combinations, directing attention inward may aid in determining the action of musical transition from the possibilities.

In the COS the act of linear potentiation over a volume parameter, gives consistent and highly predictable results. If a volume dial is turned up, the sound source gets louder proportional to the displacement. If a frequency or coupling strength dial is turned up, the displacement creates a non-linear temporally distributed effect. In the former case, the ability to succeed with an intention directed toward a specific end is guaranteed. The interaction has a linear, monotonic relation and the effect can be known in advance of the action and achieved with careful application of gestures. In the non-linear case the objectives may need to be more abstract, like a cloud possibilities, as opposed to a specific notch. Say the objective is the for the signal to converge to a quasi-attractor. In the case of actions dependent on convergent cues, a dial is displaced while listening for evidence of convergence. The dial is displaced with retraced paths to gain evidence about the local dynamic flows, effectively bringing that information into attention to meet the abstract objective.

While from the perspective of extended mind theory, an objective could to be stabilize

the signal dynamics into a form orderly CI, in order to stabilize a sense of intentionality in the mind of the musician. The opposite could also be an objective, where listening for evidence of divergent flows aids a mental objective of destabilizing a persistent intentional state, in order to explore other possible ideas for musical sequence dynamics. These actions dependent on divergent cues, seek out a more disorderly CI to aid with the formation of imagining potentials and open up space as mind wandering. Moving an auditory landscape, in and out of focus, brings clarity and precision at some moments and fogs of activity at others. The alternation can open up space in an improvisation, and produce a depth of narrative. The out of focus fogs are less demanding in terms of the specificity of the listener interpretation, as an opening to project subjective interpretations onto the musical stimulus.

In the case of operating dials with non-linear, non-monotonic effects, evidence from neural imaging studies of surprise in general suggest changes in brain dynamics as changes in effective connectivity. A certain failing to achieve by people in control. During improvisation there may be switching between modes of mind: the attendance to externalities and the attendance to the default internalities. Investigating the relationship between music and thought [Taruffi, Pehrs, Skouras and Koelsh, 2017] found music can evoke modulation effects between brain systems of meta-awareness and mind wandering. Music labeled as sad and low arousal evoked the DMN, increasing mind wandering and decreased meta-awareness. Happy high arousal music tended to evoke meta-awareness as more acute self-aware attention to the stimulus. Slow tempo in sad music further enhanced the effect to the DMN and self-reports from subjects suggested that while the evoked mood was melancholic, it was also a pleasurable experience. The fMRI imaging also showed mind wandering as a self-referential experience integrating functions of autobiographical memory. A related study [Baird, Smallwood, Schooler, 2011], unrelated to music showed mind-wandering involved in autobiographical planning, as future directed creative thought. Modulations of the orientation of attention occur during conscious episodes: into the internal activity of imagining possible futures and into autobiographies of past, as well as, toward

the external activity of the present.

Externally directed attention occurs when playing non-linear musical objects. Musical instruments contain potential or hidden sensory states activated by sequences of action. The contingencies of the musical environment help influence the development of an action repertoire. Improvising with non-linear systems complicates the linearity of mapping of action to intended sensory effects. In this frame of reference, the non-linear mapping of action to effect, when effects are surprising causes a prediction error in the mind. As discussed in [Posner and Rothbart, 1998] prediction errors evoke brain activity related modes of attention and self-regulation. When a surprise occurs, the Anterior Cingulate Cortex, the most frontal part of the limbic system activates. This region positioned directly behind the prefrontal cortex is considered a supervisory attention system. Typically occurring 80ms after a deviant stimulus the region is central in generating an error related negativity signal (ERN). The signal is a warning sign to the brain as a whole, to focus, alter its performance scheme and to increase the frequency of decisions. The ERN signal in Posner and Rothbart causes painful sensations as negative valences in certain cases. Although, the ERN as demonstrated by [Koelsch, Vuust, and Friston, 2019] can also be evoked by syncopated rhythmic grooves. The syncopation interrupts expectations about the placement of strong and weak beats within a mental model of musical structure. Musical grooves in this case are found to evoke a pleasant interoceptive drive to dance, rather than sensations of discomfort. For the COS, a mixture of prediction and non-prediction is generated. Perceived rhythms in the COS are also shown by analysis to be related to the intermittency of synchronized and desynchronized chaos. These rhythms and also phase transitions modulate attention systems in the mind, evoking a pleasurable drive to move, entrained to the dynamics. Music acts as a stimulus and in some cases a conditioned stimulus that mental activity is directed toward, away from or around.

In [Freeman, 2009] a cinematographic hypothesis of neural dynamics is presented to account for the phenomenological experience of multi-sensory percepts, grouped together across time, as gestalts. Studying the particularities of electrical signal dynamics sourced from 8x8 high

density EEG arrays, Freeman located stable time-based spatialized patterns evoked by external conditioned stimulus. The spatial patterns were of the variety of amplitude modulated aperiodic waveforms; starting local and spatializing via synchronization. The study of timing, texture, duration, spatial extent and magnitudes, lead to the notion of wave packets which support the idea of perceptual grouping into a series of frames, like watching a movie in your mind. Wave packets represent fields of activity and are demarcated by phase transitions. Freeman describes the phase transitions as staccato demarcations, which is effectively similar to the hyperplane searches observed in COS. Moreover, processes of global synchronization create widespread coherence and long range coordination. From this, notions such as whole-brain work [Bacsar, 2006] and a global (cognitive) workspace [Baars, 1997] are useful to describe the dynamics of mental states that represent states of affairs. Collecting many of the terms related to methods and subsequent classifications, much overlap exists between descriptions of synthesized electronic music, like that from a Buchla, and electrical neural dynamics. The moments of wide-scale organization, have features of orderly CI, like the kinds of sequences synthesized with a COS. If the COS produces musical sequences, consistent with neural dynamics, can we say that the electrical dynamics of capacities for mental representations are a musical phenomenon? The brain has never been analogized to a musical synthesizer, so why not now?

Chapter 6

Conclusion

Presented here was a novel digital musical instrument called a Coupled Oscillator System (COS). On the level of algorithm design, the Dissertation presented a new method for coupling any number of oscillators, along with methods for data analysis and description of the signal output. In terms of the systemization of oscillator couplings, oscillators are arranged in subsystems of a size less than the total number in the system. These subsystems modify the trajectory of oscillators not included in the subsystem. Modifier subsystems are described quantitatively at each timestep and those descriptions are used to construct coupling functions that change dynamically based on the descriptions. Only a few of the possible constructions of COS were studied here. Variables in the construction of COS include, the total system size, the size of the modifier subsystems, the mode of description of modifier subsystems and the mathematical design of coupling terms.

The analysis provided a kind of principle for designing dynamical systems for sound synthesis based on recurrence data and the identification of chaotic itinerancy (CI). Namely, the ability to have a range of generated phenomena, from highly chaotic to orderly CI. It is a continuum of dynamics with three poles: (1) from first-order chaos to (2) first-order chaos embedded in a higher-order periodicity to (3) highly stabilized, monotonous quasi-attractor transitions, as an orderly CI. Orderly CI is what can be perceived as an intentionally organized

temporal sequence. The analysis of recurrences also yielded descriptions for other observables, such as, stationarity, drift, divergence, phase-transitions, qualitative-transitions, intermittency of synchronization and desynchronization, and periodicities.

The findings of the analysis in chapter 4 were summarized in chapter 5. In this space, a higher level generalization of the analysis is presented to provide heuristics useful to the design and understanding of such systems. Furthermore, table 6.1 gives a schematic of the findings from each system in terms of categories of dynamical phenomena.

The 3-COS and 4-COS demonstrated the importance of the topological organization (mathematical structure) in COS presented and distribution of kinds of coupling terms in the generation of self-organization and especially the emergence of the staccato demarcations of hyperplane searches indicative of phase transitions or qualitative transitions.

When moving from a 4-COS to a 5-COS design, it is important to note that there was a large jump in the total number of coupling terms, $LL_i^*[t]$, due to combinatorial expansion in modifier subsystems. In this case, if was a jump from 8 to 120, which accounts for, in part, the jump in resulting signal complexity and the observation of higher-level dynamical phenomena. The other part was that smaller modifier subsystems cause more coupling terms to act on each oscillator at each timestep. Correspondingly, a smaller modifier subsystem also reduces the number of $LL_i^*[t]$ creating a tradeoff to negotiate while designing a COS.

The 5-COS and 6-COS, under certain parameterizations show the onset of a quasi-attractor landscape with an itinerant closed-loop trajectory generating temporal sequences of quasi-attractor to quasi-attractor transitions. This kind of behavior was analyzed under the framework of CI from evidence seen in recurrence plots and its quantifications. Each quasi-attractor acts like a short musical idea (on the order of seconds) when heard and the sequence of those as a larger directed sequence of ideas (on the order of minutes). The directivity through that sequence of ideas can be perceived as intentional by a performer allowing for anticipation of the synthesized signal trajectory even if it is changing in a complicated manner. This kind of signal phenomena

was identified as orderly CI occurring with laminarity forming at the edges of quasi-attractors, stabilizing the closed-loop trajectory through the landscape.

Table 6.1: A high-level description of dynamical phenomena found in each COS. Note: laminarity, has additional descriptors *high/low* refer to statistical size, *rare* refers to how likely it is to occur given a particular COS.

SYSTEM	Hyperplanes	Drift	quasi-periodic	Laminarity	Noise burst	CI
3-COS	yes	yes	yes	rare	no	no
3x2-COS	yes	yes	yes	low	no	no
3x3-COS	yes	yes	yes	high	no	yes
4-COS	yes	yes	yes	low	no	no
5-COS	yes	yes	yes	high	yes	yes
6-COS	yes	yes	yes	high	yes	yes

Concerning a theory of musical performance with COS as an embodied activity in the mode of improvisation, extended mind theory was built upon. It was argued that there was an extended intentionality occurring during active states of performance based on parity between CI in neural dynamics and CI in the dynamics of the COS. From a theoretical standpoint, performer intentions are extended and can be offloaded to the COS. The interaction was also viewed from a perspective of stigmergy showing how recurrence-based sonic cues, as local features, play a causal role in the co-creation of larger scale musical dynamics. If features can been seen in recurrence plots, features can also be heard during performance as indications of the signal trajectory. These indications are moments to change parameters of COS (or in some cases to not change parameters) for musical control.

Appendix A

Sound Examples from Selected Figures and Musical Examples

[1] Figure 4.11 : `Fig_4_11_3COS.wav`

[2] Figure 4.12 : `Fig_4_12_3COS.wav`

[3] Figure 4.13 : `Fig_4_13_3COS.wav`

[4] Figure 4.18 : `Fig_4_18_3x2COS.wav`

[5] Figure 4.19 : `Fig_4_19_3x2COS.wav`

[6] Figure 4.20 : `Fig_4_20_3x2COS.wav`

[7] Figure 4.22 : `Fig_4_22_3x3COS.wav`

[8] Figure 4.23 : `Fig_4_23_3x3COS.wav`

[9] Figure 4.26 : `Fig_4_26_4COS.wav`

[10] Figure 4.27 : `Fig_4_27_4COS.wav`

[11] Figure 4.32 : `Fig_4_32_5COS.wav`

[12] Figure 4.33 : `Fig_4_33_5COS.wav`

[13] Figure 4.34 : `Fig_4_34_5COS.wav`

[14] Figure 4.36 : `Fig_4_36_6COS.wav`

[15] Figure 4.37 : `Fig_4_37_6COS.wav`

[16] Musical Example 1: `Absolutist_Preoccuption.wav`

[17] Musical Example 2: `Resistance_(part1).wav`

[18] Musical Example 3: `Schismogenic_(part1).wav`

[19] Musical Example 4: `Cyclic/Eclectic.wav`

Sound and Musical Examples can be downloaded from ProQuest or streamed at soundcloud.com/ddefilip/sets/defilippo-diss-sounds.

Bibliography

[1] JC Alexander, I Kan, and JA Yorke. Riddled basins. *Int. J. Bif. Chaos*, 2:795–813, 1992.

[2] Bernard J Baars. In the theatre of consciousness. global workspace theory, a rigorous scientific theory of consciousness. *Journal of consciousness Studies*, 4(4):292–309, 1997.

[3] Benjamin Baird, Jonathan Smallwood, and Jonathan W Schooler. Back to the future: Autobiographical planning and the functionality of mind-wandering. *Consciousness and cognition*, 20(4):1604–1611, 2011.

[4] Erol Başar. The theory of the whole-brain-work. *International Journal of Psychophysiology*, 60(2):133–138, 2006.

[5] John M Chowning. The synthesis of complex audio spectra by means of frequency modulation. *Journal of the audio engineering society*, 21(7):526–534, 1973.

[6] Andy Clark and David Chalmers. The extended mind. *Analysis*, 58(1):7–19, 1998.

[7] Michael Dawson. Embedded and situated cognition. In *The Routledge handbook of embodied cognition*, pages 59–67. Routledge, 2014.

[8] Diana Deutsch. Grouping mechanisms in music. In *The psychology of music*, pages 299–348. Elsevier, 1999.

[9] Jean-Pierre Eckmann, S Oliffson Kamphorst, David Ruelle, et al. Recurrence plots of dynamical systems. *World Scientific Series on Nonlinear Science Series A*, 16:441–446, 1995.

[10] Rafael Elul. The genesis of the eeg. *International review of neurobiology*, 15:227–272, 1972.

[11] Georg Essl. Circle maps as simple oscillators for complex behavior: I. basics. In *ICMC*. Citeseer, 2006.

[12] James Fei. Real-time prototyping in live electronic music: A modular crackle instrument. *Leonardo Music Journal*, 17(1):38–39, 2007.

[13] Walter J Freeman. A cinematographic hypothesis of cortical dynamics in perception. *International journal of psychophysiology*, 60(2):149–161, 2006.

[14] Walter J Freeman and Jian Zhai. Simulated power spectral density (psd) of background electrocorticogram (ecog). *Cognitive neurodynamics*, 3(1):97–103, 2009.

[15] Albert Glinsky. *Theremin: ether music and espionage*. University of Illinois Press, 2000.

[16] Thom Holmes. *Electronic and experimental music: technology, music, and culture*. Routledge, 2012.

[17] Guan-Chyun Hsieh and James C Hung. Phase-locked loop techniques. a survey. *IEEE Transactions on industrial electronics*, 43(6):609–615, 1996.

[18] Kunihiko Kaneko. Spatiotemporal intermittency in coupled map lattices. *Progress of Theoretical Physics*, 74(5):1033–1044, 1985.

[19] Kunihiko Kaneko. Clustering, coding, switching, hierarchical ordering, and control in a network of chaotic elements. *Physica D: Nonlinear Phenomena*, 41(2):137–172, 1990.

[20] Kunihiko Kaneko. Overview of coupled map lattices. *Chaos: An Interdisciplinary Journal of Nonlinear Science*, 2(3):279–282, 1992.

[21] Tal Kenet, Dmitri Bibitchkov, Misha Tsodyks, Amiram Grinvald, and Amos Arieli. Spontaneously emerging cortical representations of visual attributes. *Nature*, 425(6961):954–956, 2003.

[22] Stefan Koelsch, Peter Vuust, and Karl Friston. Predictive processes and the peculiar case of music. *Trends in cognitive sciences*, 23(1):63–77, 2019.

[23] Edward W Large and John F Kolen. Resonance and the perception of musical meter. *Connection science*, 6(2-3):177–208, 1994.

[24] Nolan Lem. Sound in multiples: Synchrony and interaction design using coupled-oscillator networks. In *Proceedings International Conference Sound and Music Computing. Malaga, Spain*, 2019.

[25] Bill Manaris, Juan Romero, Penousal Machado, Dwight Krehbiel, Timothy Hirzel, Walter Pharr, and Robert B Davis. Zipf's law, music classification, and aesthetics. *Computer Music Journal*, 29(1):55–69, 2005.

[26] Norbert Marwan, M Carmen Romano, Marco Thiel, and Jürgen Kurths. Recurrence plots for the analysis of complex systems. *Physics reports*, 438(5-6):237–329, 2007.

[27] Malia F Mason, Michael I Norton, John D Van Horn, Daniel M Wegner, Scott T Grafton, and C Neil Macrae. Wandering minds: the default network and stimulus-independent thought. *Science*, 315(5810):393–395, 2007.

[28] Marcello Massimini, Fabio Ferrarelli, Reto Huber, Steve K Esser, Harpreet Singh, and Giulio Tononi. Breakdown of cortical effective connectivity during sleep. *Science*, 309(5744):2228–2232, 2005.

[29] Fred Everett Maus. Music as narrative. *Indiana theory review*, 12:1–34, 1991.

[30] J Milnor. On the concept of attractor, 177-195. *Commun. Math. Phys*, 99, 1985.

[31] MI Posner and MK Rothbart. Attention, self–regulation and consciousness. *Philosophical Transactions of the Royal Society of London. Series B: Biological Sciences*, 353(1377):1915–1927, 1998.

[32] Miller Puckette. The oscillator as a dynamical system. *Korean Electro-Acoustic Music Society's*, page 9, 2017.

[33] Marcus E Raichle. The brain's dark energy. *Science*, 314(5803):1249–1250, 2006.

[34] Marcus E Raichle. The brain's dark energy. *Scientific American*, 302(3):44–49, 2010.

[35] Jonathan Reus. Crackle: A dynamic mobile multitouch topology for exploratory sound interaction. In *NIME*, pages 377–380, 2011.

[36] Xavier Rodet. Sound and music from chua's circuit. *Journal of Circuits, Systems, and Computers*, 3(01):49–61, 1993.

[37] Rene RJ Rohr. *Sundials: History, theory, and practice*. Courier Corporation, 2012.

[38] Dan Slater. Chaotic sound synthesis. *Computer Music Journal*, 22(2):12–19, 1998.

[39] Liila Taruffi, Corinna Pehrs, Stavros Skouras, and Stefan Koelsch. Effects of sad and happy music on mind-wandering and the default mode network. *Scientific reports*, 7(1):1–10, 2017.

[40] Giulio Tononi. An information integration theory of consciousness. *BMC neuroscience*, 5(1):1–22, 2004.

[41] Ichiro Tsuda. Chaotic itinerancy as a dynamical basis of hermeneutics in brain and mind. *World Futures: Journal of General Evolution*, 32(2-3):167–184, 1991.

[42] Ichiro Tsuda and Toshiya Umemura. Chaotic itinerancy generated by coupling of milnor attractors. *Chaos: An Interdisciplinary Journal of Nonlinear Science*, 13(3):937–946, 2003.

[43] Benjamin Lee Whorf. The relation of habitual thought and behavior to language. *Sociolinguistics: A reader*, pages 443–463, 1997.

[44] David Wills. The weatherman's booper breakdown. *Youtube*, 2007.